THE SIMULATION AND DESIGN OF BUILDING ATTACHED SUNSPACES

by

BRIAN KEITH PARSONS

A thesis submitted in partial fulfillment of the
requirements for the degree of

MASTER OF SCIENCE
(Engineering)

at the

UNIVERSITY OF WISCONSIN-MADISON

1983

ACKNOWLEDGMENTS

I am indebted to Professors Sanford Klein, William Beckman and John Mitchell for their support, guidance and criticisms. The enthusiasm and energy of these men provided the inspiration for this work.

I am also grateful for the help and friendship of Professor Jack Duffie. The students and staff of the Solar Energy Laboratory and their helpful suggestions and comaraderie will not be forgotten.

To my wife Laurie, without your patience, understanding and love this project never would have been completed. I say thank-you, and more.

I am thankful for the support of the American taxpayer, who helped fund this research through the Solar Heating and Cooling Research and Development Branch, Office of Conservation and Solar Applications, United States Department of Energy. And also a tip of the mortar board to the Graduate School of the University of Wisconsin-Madison for their support during a time of crisis.

ABSTRACT

A detailed computer routine that models the thermal response of building attached sunspaces is described. The routine was developed for use with TRNSYS, a modular transient system analysis program from the University of Wisconsin-Madison Solar Energy Laboratory.

Factorial design studies, using the TRNSYS sunspace model, which quantify the effects of sunspace design parameters and operating strategies are presented.

Finally, a monthly based method for predicting the performance of thermally conductive common wall sunspace systems is developed. First, the solar radiation absorbed by the sunspace wall and floor is calculated for an "average" day of the month. The monthly average heat delivery to the attached building is determined from energy balances using the monthly average ambient, ground, and building temperature. The building auxiliary energy is predicted by using modified base temperature degree-days. Results from the design method agree closely with detailed TRNSYS simulation results.

TABLE OF CONTENTS

Table of Contents (continued)

Table of Contents (continued)

Table of Contents (continued)

LIST OF FIGURES

List of Figures (continued)

LIST OF TABLES

List of Tables (continued)

NOMENCLATURE

This list contains most of the symbols used in the text. It is not totally comprehensive as the meanings of some variables and subscripts are self evident. Others, used only once, are locally defined.

A	area, angle
BL	fraction of beam radiation from the lower glazing
BU	fraction of beam radiation from the upper glazing
C	conductance, centigrade
C_p	specific heat
DD	degree-days
F	view factor
$\hat{F}$	radiation exchange factor (F-hat)
G	instantaneous solar radiation
g	building energy gains
GJ	giga-joules
H	daily radiation intensity
h	heat transfer coefficient
hr	hour
I	hourly radiation intensity
In	input
k	thermal conductivity
Kg	kilograms

Nomenclature (continued)

KJ	kilojoules
K_T	clearness index
L	load
LASL	Los Alamos Scientific Laboratory
LCR	load-collector ratio
m	meter, mass
MJ	megajoules
N	number of nodes
NLC	net load coefficient
NTS	number of internal timesteps per external timestep
Par	parameter
PH	horizontal projection of beam radiation
PV	vertical projection of beam radiation
Q	heat flow
R	resistance, reflectivity, radiation ratio
r_T	ratio of hourly to daily total solar radiation
r_d	ratio of hourly to daily diffuse solar radiation
S	solar radiation
SF	solar radiation absorbed by the floor
SLR	solar load ratio
SSF	solar savings fraction
SW	solar radiation absorbed by the floor

Nomenclature (continued)

T	temperature
t	time
UA	heat loss coefficient
V	wind velocity, volume
W	watt
X_c	dimensionless critical radiation level

Subscripts

a	ambient, adiabatic common wall, absorbed
abs	absorbed
add	added to sunspace air
air	sunspace air
amb	ambient
aux	auxiliary
b	beam radiation, base temperature
d	diffuse radiation
eff	effective
f	floor
gl	glazing
g,gr	ground
i	inside, general node, infinite thermal capacity, incident
in	net energy transferred
insul	insulation

Nomenclature (continued)

j	general node
m	extra thermal mass node
n	noon of the average day
ni	glazing night insulation
o	outside
rm	room or building
s	solar gain
set	thermostat heating set point
ss	sunspace air
str	stored
t	tilted
v	vertical
z	zero thermal capacity

superscripts

-	monthly average value
+	future timestep, only positive values considered
·	rate of instantaneous intensity

Chapter 1: Introduction

1.1 Background

In the last decade, rising energy costs have prompted an examination of traditional building design and construction practices. Residential and commercial sectors use about 21 percent of all the energy consumed in the United States. Nearly all of this is for heating and cooling of buildings (1).

Many different strategies have developed to reduce the heating and cooling energy consumption of buildings. Increasing insulation levels and decreasing infiltration of ambient air can significantly reduce heating requirements. Glass and other glazing materials are used in various applications to increase solar heat gains. These gains can reduce the amount of auxiliary energy required to maintain comfortable building conditions.

Three types of applications are generally categorized as passive solar. The simplest systems are direct gain windows. Direct gain windows are usually multi-paned and oriented for maximum solar exposure (south-facing in the northern hemisphere). Overhangs or other shading devices to reduce summer overheating and moveable insulation to reduce night heat losses may also be employed. The main drawbacks to these systems are large temperature swings in buildings without large heat storage capacities and large nighttime conductive losses. These losses can exceed solar gains for some systems in colder climates. Collector-storage (or Trombe) wall systems partially overcome these difficulties by placing a thermally

massive material, such as masonry or containers filled with water, between the glazing(s) and occupied space. Solar radiation is absorbed by the massive wall and a portion of the energy is conducted through the material and convected or radiated to the building. In addition, some systems include vents in the wall to directly couple the air in the glazing-wall gap with the building air. It has been found that venting of masonry walls does not greatly affect the auxiliary energy use of buildings (2). One problem with widespread use of these systems is that the view is obstructed by the wall. Many homeowners find this aesthetically unacceptable. Sunspaces* are an attempt to at least partially overcome this problem.

1.2 General Sunspace Description

In sunspace systems, the glazing-wall gap of a collector-storage wall system is expanded to allow the space to be used as additional living area. The common wall divides the structure into two zones. The north zone is the main living space and the temperature is kept within normal comfort ranges (typically 18-24° C). The south zone has extensive glazing and the temperature is either uncontrolled or a much larger range is allowed. Removable insulation may be used to reduce nighttime heat losses. The common wall may be thermally massive or of lightweight construction, as in many retrofit applications. Thermally massive common walls may be vented or unvented

---

*Also called solar greenhouses. The term "sunspace" is used in this study because it is concerned primarily with the thermal performance, and not plant production.

as significant amounts of heat are conducted through the wall. Lightweight insulated walls (frame construction), however, are usually vented since little heat travels through the common walls. Additional thermal mass is sometimes added to either type of system to provide additional energy storage and to dampen sunspace air temperature fluctuations.

The space may be used as additional living space or as a greenhouse to extend the local growing season. These uses make the sunspace more than a heating component and additional benefits from these uses must be included in a comprehensive evaluation. Restrictions associated with other uses, however, may have a deleterious effect on thermal performance. Temperatures in uncontrolled sunspaces can exceed the limits of plant tolerance in some cases. Maintaining plant compatible levels during winter months may increase auxiliary heating requirements by a significant amount.

Variables such as temperature bounds, wall material and thickness, glazing properties and additional thermal mass in the sunspace and building have an influence on actual sunspace response to weather conditions at any given location. An analytical method for prediction of these effects is the driving force behind this work.

1.3 Related Previous Work

Building auxiliary energy reduction by passive solar components can be predicted with various levels of sophistication. "Rules of Thumb" for design of these systems abound (3,4,5). "Rules of Thumb" may be the result of specific experiences or they may be average

values from many detailed studies. They are very useful in the conceptualization and preliminary design stage. However, they cannot predict effects of varying final design parameters or differences in performance of identical systems in different locations.

For maximum flexibility and information, detailed computer simulations can be employed. The thermal response is predicted by using basic heat transfer equations, which describe the system with hourly weather data as driving forces. Several computer codes have been developed to simulate passive solar energy systems. A review of many of these programs appears in (6). The two most used publicly-available programs (7,8) for simulation of sunspace solar systems contain many assumptions and limitations which restrict their use. One program which seems to be quite versatile and general is PASOLE (9) from the Los Alamos Scientific Laboratory (LASL). Many passive system configurations have been simulated using the code and results have been checked against experimental tests (18). The program is publicly-available but is not widely used. Documentation is informal (9) and simulation of some systems requires modification of the code.

TRNSYS (10) is a modular simulation program from the University of Wisconsin-Madison. Very general direct gain window, collector-storage wall and shading device components are standard in TRNSYS. The modular structure of the program allows many system configurations to be easily examined.

A sunspace model for TRNSYS has been developed by Schwedler (6). This model breaks the floor and wall into two-dimensional heat transfer networks. These two dimensional conduction and complicated radiation calculations make simulation costs prohibitive. Schwedler found little difference between results of sunspace simulations using one-dimensional and two-dimensional wall and floor heat transfer networks. Several errors were discovered in his code, but they do not affect the overall conclusions of the study. The algorithm for determining the glazing and sunspace air temperature is incorrect and the "rate of energy flow into the sunspace air and glazing" term is ambiguous. The transmission characteristics of the glazings are not included in the model. In addition, no provisions for additional thermal storage devices (such as 55 gallon drums filled with water) are included.

Detailed simulation codes require hourly weather data and access to a main frame computing system. Most designers are unwilling or unable to perform extensive parametric studies to optimize component performance using these codes.

Design methods for passive solar systems attempt to retain generality, yet allow accurate prediction of system thermal performance with a minimum of computational effort. Two methods are generally available at present (11,12,14,15). Both methods require monthly average weather data. This information is readily available for many locations (13). One month is apparently enough time to include significant weather trends, yet only six to ten repetitive calcula-

tions must be done to predict heating season performance. Design methods are derived from detailed hourly simulation results. Design method results generally agree within three percent of detailed simulation results for the range of parameters studied.

The first method to be developed was the SLR/LCR method derived from PASOLE simulations by LASL (4,11,12). Empirical equations are provided which correlate the Solar Saving Fraction (SSF) to Solar Load Ratio (SLR) for various system reference designs. The solar load ratio is defined as:

$$X = \frac{S/DD - LCR_s \cdot H}{LCR \cdot K} \qquad 1.3.1$$

where S is the monthly absorbed solar radiation per unit area projected on a vertical plane, DD is the degree days for the month adjusted to account for building internal gains not including solar gains, and H and K are empirical constants which depend on system type and LCR. LCR_s and LCR are the Load Collector Ratios for the solar component and the building without the solar component respectively. Load Collector Ratio is defined as the heat loss coefficient (UA) divided by the area of the solar component projected on a vertical plane. Building auxiliary energy can be computed from the following equation:

$$Q_{aux} = NLC \cdot DD \cdot (1 - SSF) \qquad 1.3.2$$

NLC (net load coefficient) is the (UA) of the building not including

the solar component. Sensitivity or correction curves are supplied to predict effects of deviating from the reference design for 6 locations. Multiple corrections, however, may introduce non-linearities and interpolation may be difficult. If the reference design is used, a yearly correlation which eliminates the monthly repetition is also available. Ninety-four passive solar reference designs have recently been published (12). Even so, many possible designs, especially for sunspace systems, are not included.

The effects of changing geometry drastically from the reference designs is not well-quantified in the SLR method. This may cause designers to be unnecessarily restricted to passive systems closely approximated by the reference designs. Another drawback of the SLR method is heat storage capacity of the non-solar building is not included as a variable. Interaction between passive solar components and building thermal capacitance can have a significant effect on auxiliary energy requirements. Despite these drawbacks, the ease of application has made the SLR method the most widely-used design tool for passive systems.

The second general design method is the unutilizability method for direct gain windows and collector-storage walls of Monsen, et al. (14,15). Performance of zero thermal capacitance and infinite thermal capacitance buildings can be analytically defined. The equations include the radiation statistic utilizability (16,17). Solar radiation intensity above a system specific critical level overheats the building and must be rejected. Performance of finite

storage capacity systems is correlated to a storage-dump ratio. Generality allows accurate prediction of the effects of changing system parameters, but computational effort is somewhat greater than the SLR method. The advent of relatively inexpensive microcomputers has alleviated this drawback considerably.

The research discussed in this paper includes development of a more cost-effective general sunspace model for TRNSYS and design method for these systems.

1.4 Methodology

The general sunspace model for TRNSYS, described in Chapter 2, was formulated by coupling the basic heat transfer equations which describe the conductive, convective, and radiative heat exchange phenomena of a sunspace. A nodal network was developed and the forcing functions of ambient temperature, solar radiation, and room temperature are inputs to the component. The modular format of TRNSYS enables simulations of many building system configurations and operational modes.

Parametric studies of various sunspace systems were performed in several locations and significant variables were identified.

Simplified methods, based on monthly average weather and building conditions, were then developed for predicting absorbed solar radiation and heat delivery of the sunspace.

Monthly average methods compare closely to detailed TRNSYS simulation results. The limits of building auxiliary heating requirements for sunspace systems are described and problems with

implementing an unutilizability design method are discussed. A monthly method for predicting auxiliary heating requirements of sunspace systems using reduced base temperature degree-day calculations is also presented.

1.5 Organization

Chapter 2 describes the model of the TRNSYS sunspace component. Mathematical equations and assumptions are discussed. Differences between the model developed in this study and the model developed by LASL are included. Results from the model are compared to results from similar models.

Chapter 3 is a summary of many parametric studies of sunspace systems. First, parameters are varied with the sunspace connected to a constant temperature building. Variations in sunspace energy delivery are examined. The second set of simulations takes into account building dynamic behavior. Effects of controls, venting, and wall parameters on building auxiliary energy requirements are examined.

Chapter 4 describes the simplified monthly average method for prediction of absorbed solar radiation, sunspace energy delivery, and building auxiliary heating requirements. Results are compared with detailed TRNSYS simulations.

Chapter 5 contains conclusions of the study and a discussion of both advantages and drawbacks of the design method. Suggestions for future work are included.

The Appendix of computer listings is included for completeness.

Chapter 2: The TRNSYS Sunspace Component

2.1 General Description and Geometry

The detailed hourly TRNSYS model for attached sunspaces determines the various heat flows and temperatures for user-specified sunspace geometry and thermal characteristics using hourly weather data. Solar radiation incident on two arbitrarily sloped glazing planes is either transmitted through the glazings or reflected in proportions determined by optical properties and incidence angles. Transmitted radiation is then absorbed on the wall, floor, and additional thermal mass containers, or reflected back through the glazing. Energy is lost by conduction through the floor to the ground and by both convection and radiation heat transfer from the glazing surface to the environment. Infiltration of ambient air into the sunspace and possible venting of the sunspace provides a direct conductance between the sunspace air and ambient conditions. Heat is transferred to the adjacent building by conduction through the wall and by controlled venting. The remainder of the energy is stored in the massive elements of the sunspace as sensible heat.

The geometry of the sunspace, as shown in Figure 2.1, is specified by user-supplied parameters. The wall height, Par 1; the length of the floor, Par 3; and the horizontal and vertical distances from the intersection of the wall and floor to the intersection of the glazing planes, Par 6 and Par 7 respectively; are used to calculate glazing slopes from horizontal, β and ψ. Three other parameters, the sunspace width, Par 5; the wall thickness,

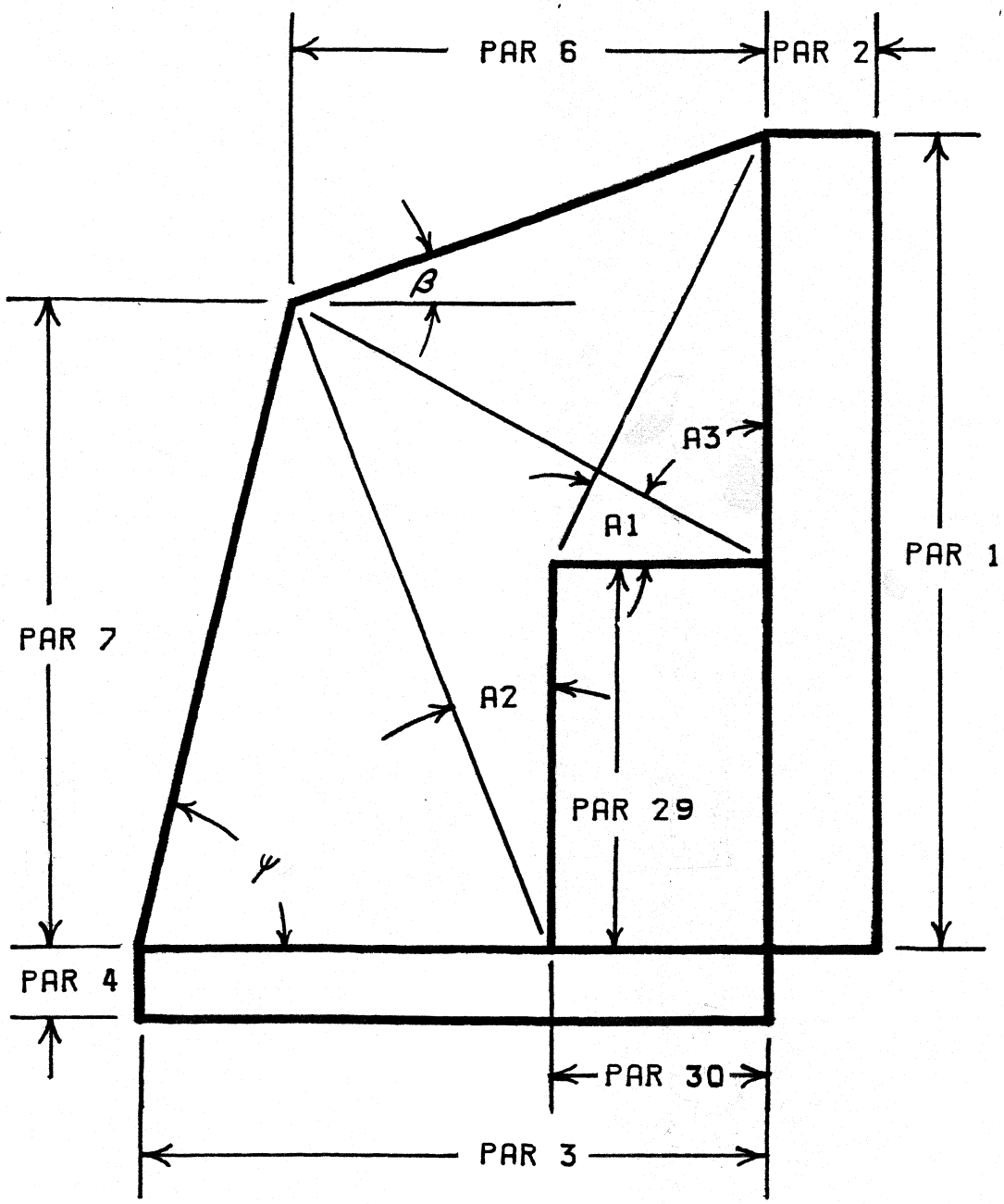

Figure 2.1 Sunspace Geometry

Par 2; and the floor thickness, Par 4; complete the definition of the sunspace geometry. Single plane sunspaces may be simulated by specifying parameters 6 and 7 such that β equals ψ.

Additional thermal storage devices may also be included in the simulation. They are assumed to be placed along the wall and run the entire length of the space. The height, Par 29 and the width, Par 30 of the thermal mass containers define a rectangular cross-section used for radiation exchange calculations. The surface area of the containers, Par 32 is used in convective heat exchange calculations and is specified separately to allow many container geometries to be approximated. If extra thermal storage devices are used, three more angles are computed: A1, A2, and A3. These angles are used in beam radiation calculations described in Section 2.3.3.

2.2 The Thermal Network: Description of Conductances

2.2.1 Introduction

Heat transfer in sunspaces is simulated using the familiar network analogy to electrical circuits. Conductances are defined such that the heat transfer between two temperature nodes is the conductance multiplied by the temperature difference. The thermal network and nodal numbering scheme is illustrated in Figure 2.2. The number of wall and floor nodes can be varied from two to ten. Wall nodes are numbered first, followed by floor nodes and the additional mass node (if used) as shown. Numbers preceded by a "C" represent heat transfer paths, while "T"s represent temperature nodes.

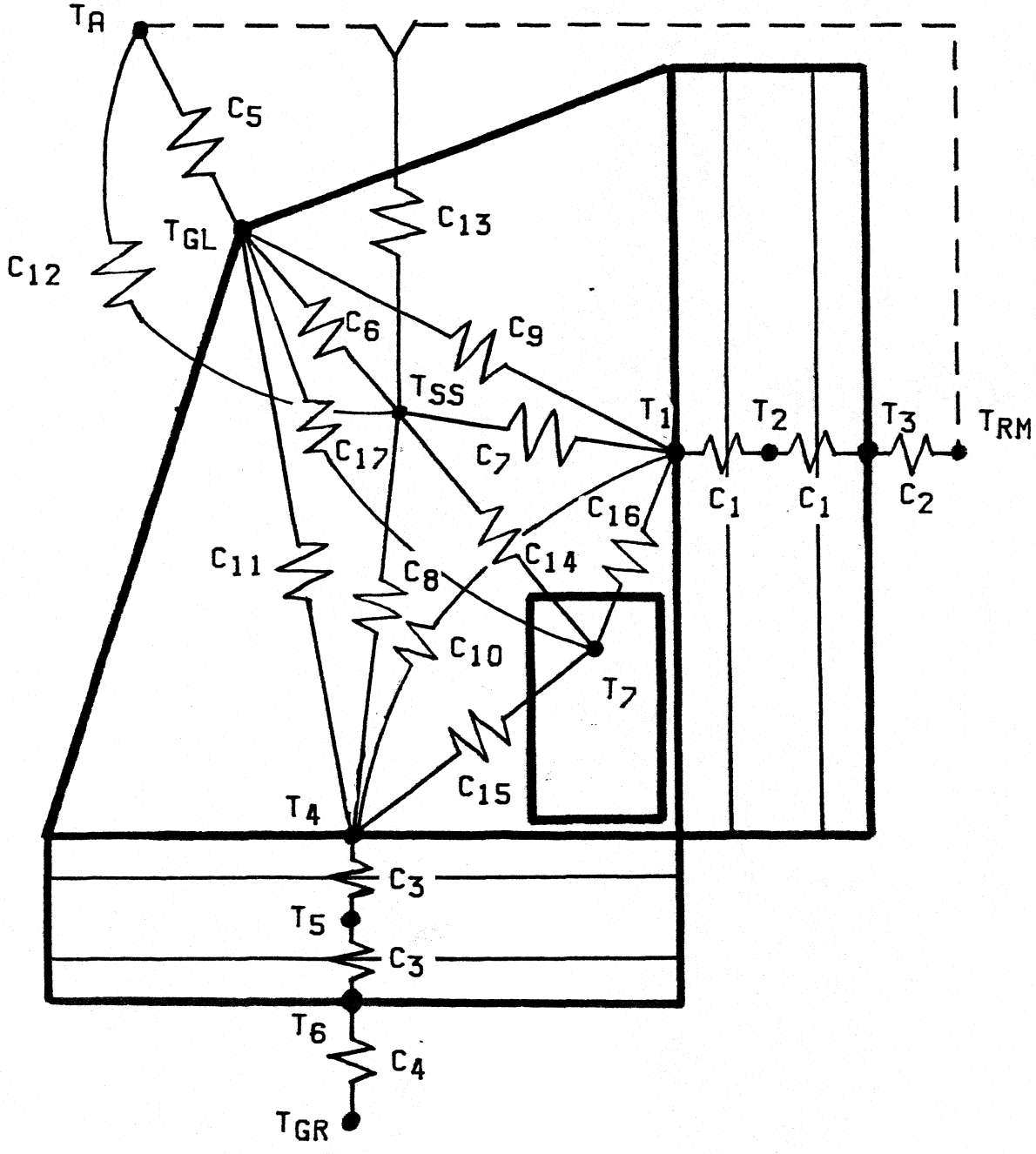

Figure 2.2 Sunspace Thermal Network

2.2.2 Conductive Heat Transfer Paths

Heat transfer through the wall and floor is modeled as one-dimensional. As mentioned in Chapter 1, an earlier study (6) concluded that one-dimensional heat transfer approximations were sufficiently accurate. The conductance between adjacent wall nodes, C_1, is defined as:

$$C_1 = \frac{k_w A_w}{t_w/(N_w-1)} \qquad 2.2.1$$

where k_w is the thermal conductivity of the wall material, A_w is the area of the wall perpendicular to heat flow, t_w is the wall thickness, and N_w is the number of wall nodes. The conductance between adjacent floor nodes, C_3, is similarly defined as:

$$C_3 = \frac{k_f A_f}{t_f/(N_f-1)} \qquad 2.2.2$$

where the subscript "f" refers to floor parameters. The surface nodes of the floor and wall have half the thermal capacitance of interior nodes, as shown in Figure 2.2.

Conduction heat losses to the ground are also modeled as one-dimensional using the cross-sectional area of the floor. ASHRAE (18) suggests a procedure using the slab perimeter area. Ground temperatures can be adjusted to account for the difference in heat loss area if desired. Par 28 is the effective ground resistance, and effects of various values are examined in Section 3.2.2. Optional slab insulation may be added by using parameter 24, the R-value of the insulation, $m^2°C/W$. The total conductance from the bottom floor

node to the ground, C_4 is:

$$C_4 = \frac{A_f}{(\text{Par } 28 + \text{Par } 24)/3.6} \quad \text{kJ/hr°C} \qquad 2.2.3$$

where Par 28 is greater than zero.

The heat transfer between the inner and outer glazing surfaces cannot be truly classified as conduction. The actual mechanism is a combination of convection, radiation and conduction. Conductance values vary with glazing slope, gap distance and temperature difference. The conductance is assumed to be constant throughout the simulation since seasonal variations are small. Parameter 22 is the R-value of the glazing system in $m^2°C/W$.

Numerical values for the resistance of single, double, and triple-pane window systems are given in (19), but many design values include inside and outside air film convection coefficients. R-values from inside glazing surface to outside surface may be computed by subtracting air film R-values from these design values or by assuming the R-value of the glass itself is zero. In the latter case, the R-value of single-glazed windows is zero and that of multiple-paned systems is the R-value of the air gap(s) in parallel with the R-value of the framing. For sunspaces with glazing planes of largely different slopes, an area weighted average value is suggested.

Optional additional window insulation can reduce the window conductance. Input 2 is the insulation control function. A one means

the insulation is in place, while a zero implies no additional glazing insulation. Parameter 23 is the R-value of the additional insulation. If the insulation is in place, no solar radiation is allowed to pass through the glazings. The conductance of the glazings is calculated by the following equation:

$$C_{5c} = \frac{3.6\ A_{gl}}{\text{Par (22)} + \text{Par (23)} \cdot \text{In (2)}}\ \text{kJ/hr°C} \qquad 2.2.4$$

The glazing area, A_{gl}, in the above equation includes both tilted glazing planes and the two end walls.

2.2.3 Convective Heat Transfer Paths

Heat transfers between the solid sunspace surfaces and the various air nodes are computed from user supplied convection coefficients. The coefficients may be correlated to other variables such as temperature, geometry, or air velocity by including TRNSYS type 15 algebraic operators or user-written components in the simulation control statements. Effects of varying convection coefficients are discussed in Chapter 3.

Convection coefficients from the wall, floor, extra mass containers, and glazing to the sunspace air are all separate inputs. Representative values are presented in Chapter 3. This flexibility allows the user to select from the many correlations available in the literature, input actual measured values or select appropriate constants. The surface area of the additional mass, Par 31, should be only the area exposed to the sunspace air. It should not include

the area of contact between the mass containers and floor or wall. It should be noted that the units of the required input convection coefficients are $W/m^2°C$ and the sunspace component converts these values to 'TRNSYS units' of $KJ/hr\text{-}m^2°C$. With these factors in mind, the interior convection conductances are:

$$C_6 = 3.6 \cdot \text{In}\ (10) \cdot A_{gl} \quad KJ/hr°C \qquad 2.2.5$$

$$C_7 = 3.6 \cdot \text{In}\ (9) \cdot A_w \quad KJ/hr°C \qquad 2.2.6$$

$$C_8 = 3.6 \cdot \text{In}\ (8) \cdot A_f \quad KJ/hr°C \qquad 2.2.7$$

$$C_{14} = 3.6 \cdot \text{In}\ (21) \cdot A_m \quad KJ/hr°C \qquad 2.2.8$$

Convective heat transfer from the outside glazing surface to the environment is defined by a similar conductance:

$$C_{5b} = 3.6 \cdot \text{In}\ (6) \cdot A_{gl} \quad KJ/hr°C \qquad 2.2.9$$

Several correlations or values for outside film heat transfer coefficients are in general use (16,19). Some of these values include radiative heat transfer. Care should be taken in choosing a value for input 6 since radiation losses from the glazing to ambient are calculated separately (see section 2.2.4). The following correlation is suggested (27):

$$h = 2.8 + 3.V \quad W/m^2C \qquad 2.2.10$$

where V is the wind speed in m/s.

The convection coefficient between the inside surface node of the common wall and the building temperature node, however, should include radiative heat transfer. Radiation is included in input 7 because radiative heat exchange coefficients vary with building interior geometry and surface properties. ASHRAE (19) recommends using a combined coefficient of 8.3 $W/m^2°C$ in lieu of more detailed analysis. The combined convection and radiation conductance is computed as follows:

$$C_2 = 3.6 \cdot \text{In (7)} \cdot A_w \quad \text{KJ/hr°C} \qquad 2.2.11$$

2.2.4 Thermal Radiation Heat Transfer Paths

Infrared radiation from the outside glazing surface to the surroundings is described by conductance C_{5a}. View factors from the glazing surfaces to the ground and sky vary with sunspace configuration. The ranges are zero to one-half for the view factor from glazing to ground and one-half to one for the view factor from glazing to sky. Clear sky radiation temperatures are somewhat lower than ambient temperatures (16), but values for cloudy conditions are not well defined. Ground temperatures are usually higher than ambient during the building heating season. In view of these considerations, radiative losses from the sunspace glazings are approximated by assuming a combined ground-sky temperature equal to ambient temperature and a view factor of one. Surroundings are treated as a black surface. The radiative heat transfer from outside glazing surface to the surroundings is then:

$$Q = \sigma\varepsilon_{gl}A_{gl}\ (T_{gl,o}^{\ 4} - T_a^{\ 4}) \qquad 2.2.12$$

where σ is the Stephan-Boltzman constant (5.67×10^{-8} $W/m^2\text{-}°K^4$), ε_{gl} is the infrared emittance of the glazing (.88 for glass), and $T_{gl,o}$ and T_a are the absolute outside glazing and ambient temperatures respectively. A heat transfer coefficient can be defined to linearize the equation:

$$h = \sigma\varepsilon_{gl}\ (T_{gl,o}^{\ 2} + T_a^{\ 2})\ (T_{gl,o} + T_a) \qquad 2.2.13$$

and C_{5a} becomes:

$$C_{5a} = h\ A_{gl} \qquad 2.2.14$$

An overall combined conductance from the inside glazing surface to ambient can now be computed:

$$C_5 = \frac{C_{5a}\ (C_{5b} + C_{5c})}{C_{5a} + C_{5b} + C_{5c}} \qquad 2.2.15$$

The infrared radiative heat exchange between the sunspace interior surfaces is not so easily described. Since the wall, floor, glazing, and additional mass containers are not black with respect to thermal radiation, multiple radiation reflections must be included in the calculation of conductances. These reflections are modeled using $\hat{F}$ (F-hat) equations (20). $\hat{F}_{i,j}$ is defined as the radiation leaving node i that is incident on node j, including all possible reflections, divided by the total radiation leaving node i.

The heat exchange between node i and node j is then:

$$Q = \sigma A_i \hat{F}_{ij} \varepsilon_j (T_i^4 - T_j^4) \qquad 2.2.16$$

where T's are absolute temperatures of the nodes. These equations can be linearized and infrared conductances can then be defined as follows:

$$C_9 = \sigma A_w \hat{F}_{w,gl} \varepsilon_{gl} (T_w^2 + T_{gl,i}^2) (T_w + T_{gl,i}) \qquad 2.2.17$$

$$C_{10} = \sigma A_w \hat{F}_{w,f} \varepsilon_f (T_w^2 + T_f^2) (T_w + T_f) \qquad 2.2.18$$

$$C_{11} = \sigma A_f \hat{F}_{f,gl} \varepsilon_{gl} (T_f^2 + T_{gl,i}^2) (T_f + T_{gl,i}) \qquad 2.2.19$$

If additional mass containers are present, the above wall and floor areas must be the areas not covered by the containers. In this case the following additional conductances are also defined:

$$C_{15} = \sigma A_f \hat{F}_{f,m} \varepsilon_m (T_f^2 + T_m^2) (T_f + T_m) \qquad 2.2.20$$

$$C_{16} = \sigma A_w \hat{F}_{w,m} \varepsilon_m (T_w^2 + T_m^2) (T_w + T_m) \qquad 2.2.21$$

$$C_{17} = \sigma A_{gl} \hat{F}_{gl,m} \varepsilon_m (T_{gl,i}^2 + T_m^2) (T_{gl,i} + T_m) \qquad 2.2.22$$

F-hats are computed by inverting a reflectivity matrix whose elements, R_{ij}, are defined as follows:

$$R_{ij} = \delta_{ij} - (1 - \varepsilon_j) F_{ij} \qquad 2.2.23$$

δ_{ij} is the Kronecker delta function where δ_{ij} equals one if i equals j and δ_{ij} equals 0 if i does not equal j. F_{ij} is the view factor

from node i to node j. View factors are calculated using Hottel's crossed string method (21) and by assuming the additional mass node can be represented by an equivalent rectangle which runs the full width of the sunspace, as shown in Figure 2.1. View factors calculated by this method are strictly correct only for infinitely long planes. Thus, the glazing area in equation 2.2.22 should be that of the two glazing planes and not include the end wall areas. The F-hat matrix is computed from the following equation:

$$[\hat{F}_{ij}] = [R_{ij}]^{-1} [F_{ij}] \qquad 2.2.24$$

Computation of exact, finite length view factors is complex (21,22). Table 2.1 compares view factors and F-hats computed by infinite length and finite length methods for the geometry of Figure 2.3. Exact view factors for this geometry can be obtained from tables, interpolation and view factor geometry (21,22). The magnitude of the differences between the two computation methods is not representative since the sunspace length is relatively small. The errors of Table 2.1 represent an upper bound. The infinite length view factors ignore the effect of the glazed end walls. Predictably, the largest errors are for the glazing node view factors. These errors are reflected in the F-hat values calculated by Equations 2.2.23 and 2.2.24. Heat flux equations include an area factor (Equation 2.15). The total glazing area for the example is 31.11. This value is used for exact view factor calculations. The crossed-string method, however, ignores the end wall effects so that the

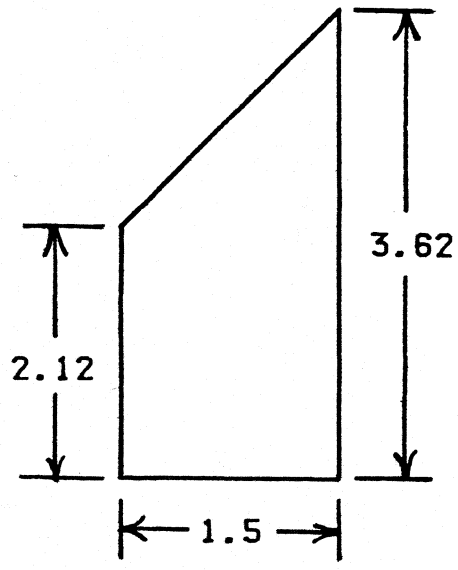

Width of sunspace 5.30
glazing emittance 0.88
wall and floor emittance 0.9

Figure 2.3 Geometry and Surface Properties for View Factor Comparison

Table 2.1a

Comparison of View Factors Computed by Hottel's Crossed String Method and Exact Methods (Hottel's/Exact)

	wall	floor	glazing
wall	0.0/0.0	.16591/.14074	.83409/.85926
floor	.40054/.33978	0.0/0.0	.59946/.66022
glazing	.71194/.53075	.21194/.16880	.07612/.30083

Table 2.1b

Comparison of F-hats Computed from
Crossed-String and Exact View Factor
(Hottel's/Exact)

	wall	floor	glazing
wall	.08105/.06323	.18913/.16002	.86004/.90804
floor	.45660/.38633	.02398/.02004	.64487/.72076
glazing	.73409/.56048	.22799/.18428	.15241/.37468

Table 2.1c

Comparison of Area- F-hat Products
Computed from Crossed-String and Exact View Factors
(Hottel's/Exact)

	wall	floor	glazing
wall	1.5566/1.2143	3.6322/3.0732	16.517/17.439
floor	3.6323/3.0733	.19076/.15942	5.1299/5.7336
glazing	16.517/17.439	5.1298/5.7337	3.4292/11.658

example glazing area becomes 22.5. Including this correction improves simplified cross-string values considerably as shown in Table 2.1c where $A_i \hat{F}_{ij}$ values are compared. A major discrepancy exists between exact and approximate values in the $A_{gl} \hat{F}_{gl-gl}$ term. However, this does not affect temperature or heat flux calculations since the temperature difference of Equation 2.15 is zero. For wider sunspaces, the approximate Hottel's crossed-string view factor calculations are much closer to the exact values.

The utility of the sunspace simulation results is in evaluating differences in performance due to variations in parameters and inputs. Interaction between the view factor calculations and these differences in performance should be small. In lieu of these considerations and in order to maintain geometric generality and computational simplicity, the use of Hottel's crossed-string method to compute view factors is recommended.

Infrared conductances are dependent on nodal temperatures. The model uses mass node temperatures from the previous timestep to calculate conductance values. The glazing temperature is determined by an iteration scheme as described in section 2.5.

2.2.5 Direct Conductances Between Air Nodes

The only conductances left to be defined are C_{12} and C_{13}. C_{12} accounts for the infiltration of ambient air into the sunspace. Construction tightness of sunspaces varies widely and heat loss through infiltration can be significant. Parameter 25 is the infiltration air change rate in changes per hour. Values vary from 0.25 changes

per hour for very tight construction to two changes per hour for very loose construction with 0.5 to 1.0 being typical. The conductance becomes:

$$C_{12} = V \cdot \rho \cdot C_p \cdot \text{Par (25)} \qquad 2.2.25$$

where V is the sunspace volume, ρ is the density of air and C_p is the specific heat of air. Air density and specific heat are assumed to be constant with values of 1.204 kg/m^3 and 1.012 KJ/kg°C.

Venting of the sunspace air is included in the model through C_{13}. Input 1 provides control of the air flow and Input 19 is the mass flow rate of the vented air in kg/hr. If Input 1 equals one, sunspace air is vented to the adjacent building while a value of -1 vents to the environment. No venting occurs if the input value is zero. The air mass flow rate may correspond to the output of a fan or be the result of natural convection. Flow rates for natural convection may be computed by another TRNSYS component using sunspace and building or ambient air temperatures to calculate density differences and Bernoulli's equation to calculate flow rates. This is not included in the sunspace component since friction losses vary with sunspace geometry and vent configuration. The conductance, C_{13}, if Input 1 is not zero, is:

$$C_{13} = C_p \cdot \text{In (19)} \qquad 2.2.26$$

All the conductances in Figure 2.2 have been defined. An additional assumption of the model is that no conductance occurs

between the extra mass containers and the floor or wall. The conductances, with the exception of C_1, C_3, and C_4, are calculated every timestep in the simulation since the user may wish to vary convection coefficients, and infrared conductances vary with temperature.

2.3 Solar Radiation

2.3.1 Introduction and Transmitted Radiation

This section describes how the sunspace model determines the amount of solar radiation absorbed by the floor, wall, and additional mass nodes of the sunspace.

Inputs 11-14 are the incident beam and diffuse solar radiation intensities on the two glazing planes. The angles of incidence (in degrees) of beam radiation for the two surfaces are inputs 15 and 16. All of these inputs are standard outputs of the TRNSYS radiation processor. The amount of radiation transmitted through the glazings depends on glazing optical properties and radiation incidence angle. The function TALF uses the number of covers (Par 18), the extinction coefficient of each cover (Par 20), and the glazing refractive index (Par 21) along with the beam radiation incidence angles to compute the transmitted fraction of beam radiation for both glazing planes. Similarly, the transmitted diffuse fraction is computed using an angle of incidence of sixty degrees (16).

Radiation incident on the end walls of the sunspace is not considered. If both end walls are glazed, and the sunspace faces the

equator, the amount of radiation incident on one end wall that strikes the mass nodes of the sunspace is nearly equal to the radiation incident on the tilted glazing planes which then passes through the other end wall. Thus, the radiation incident on the sloped glazing surfaces is all that must be considered. Only slight errors due to incorrect transmitted fractions in morning and evening hours and inaccuracies in radiation reflection are introduced by this assumption.

2.3.2 Diffuse Radiation Distribution

The diffuse solar radiation transmitted through a glazing plane is distributed to the sunspace floor, wall, mass containers or other glazing plane by multiplying by crossed string view factors. An implicit assumption of this treatment is that the diffuse radiation has a uniform intensity in all directions. Diffuse sky radiation is typically 0.2 to 0.3 of the total sky radiation and is assumed to be isotropic. Diffuse ground reflectances in the same range are generally assumed. Thus, even for vertically-sloped glazing planes, the diffuse radiation can be assumed to have a nearly uniform distribution.

2.3.3 Beam Radiation Distribution

Beam radiation is distributed by projecting solar angles through various locations in the sunspace and calculating the actual fractions from each glazing plane striking each surface. PASOLE (9) distributes all radiation with view factors similar to the diffuse treatment of section 2.3.2. The more correct approach used in this

work leads to larger values of absorbed radiation on the wall in winter and smaller values in summer than are obtained by using view factor distribution.

The projection of the beam radiation through a north-south vertical plane can be described by the angle δ as illustrated in Figures 2.4a and 2.4b. δ is computed from equation 2.3.1:

$$\delta = \tan^{-1} (-\tan \theta_z \cos \gamma_s) \qquad 2.3.1$$

In this equation, θ_z is the solar zenith angle (Input 17) and γ_s is the solar azimuth angle (Input 18). Both values are readily available from the TRNSYS radiation processor. Use of this simple equation, the glazed sidewall assumption discussed in 2.3.2, and the following beam radiation distribution scheme limit the component to south facing sunspaces. More complicated equations for beam projections onto non-south facing surfaces exist (23,24) and could be substituted for existing computations if deviations from south are significant.

Sequential checks of solar and sunspace geometry beginning with a choice between δ greater than zero (Figure 2.4a) or δ less than zero (Figure 2.4b) apportion beam radiation between the sunspace surfaces. An example for the particular situation shown in Fig. 2.4a will illustrate the method.

Since δ is between A2 and A3, some of the beam radiation from each glazing surface strikes the extra mass surfaces. The total projected height of the beam radiation from the upper glazing sur-

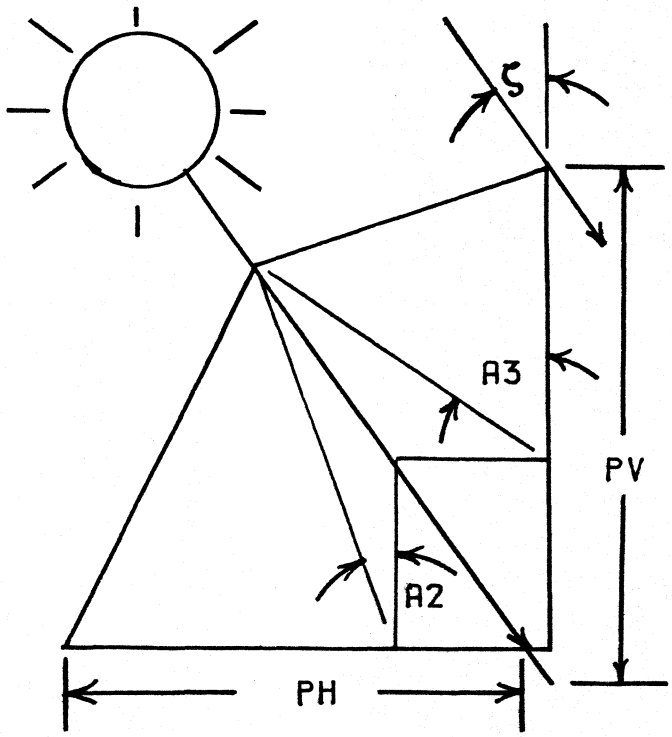

Figure 2.4a Beam Radiation Projection: $\delta > 0$

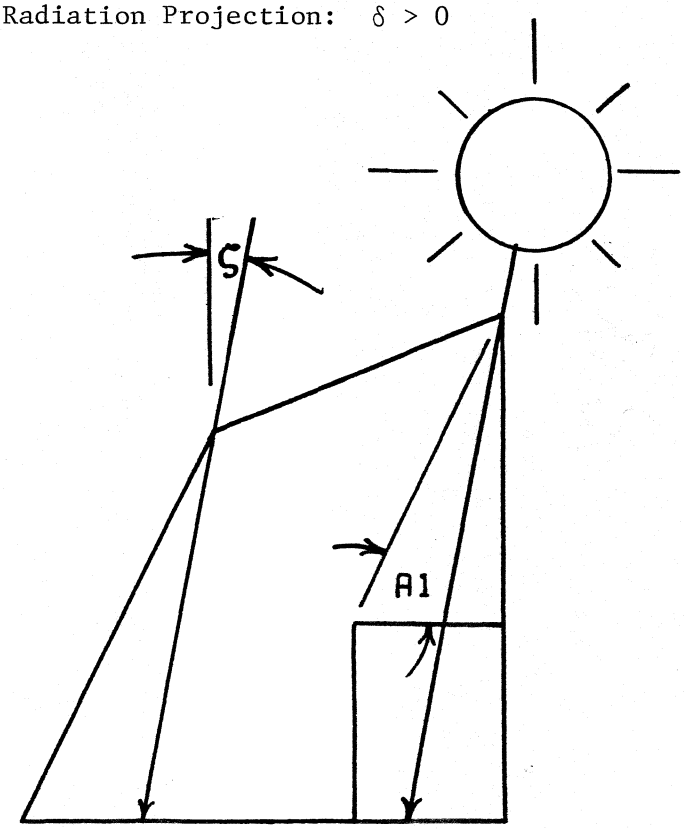

Figure 2.4b Beam Radiation Projection: $\delta < 0$

face is:

$$PV = \frac{\text{Par } 6}{\tan \delta} + \text{Par } 1 - \text{Par } 7 \qquad 2.3.2$$

The fraction of beam radiation from the upper glazing striking the wall and extra mass are respectively:

$$BU_w = \frac{\text{Par } 1 - \text{Par } 28}{PV} \qquad 2.3.3$$

$$BU_m = \frac{PV - \text{Par } 1 + \text{Par } 28}{PV} \qquad 2.3.4$$

Similarly, the total horizontal projection of the beam radiation striking the lower glazing is:

$$PH = \text{Par } 7 \cdot \tan \delta + \text{Par } 3 - \text{Par } 6 \qquad 2.3.5$$

and the fractions striking the floor and mass are:

$$BL_f = \frac{\text{Par } 3 - \text{Par } 29}{PH} \qquad 2.3.6$$

$$BL_m = \frac{PH - \text{Par } 3 + \text{Par } 29}{PH} \qquad 2.3.7$$

Beam radiation distribution is defined in a similar manner for all possible situations for two glazing plane sunspaces with or without extra mass containers. If thermal mass containers are included, the calculations assume the width of the containers (Par 29) is less than the horizontal distance from the wall to the intersection of the glazing planes (Par 6) and the height of the containers (Par 28) is less than the vertical distance from the floor to the inter-

section of the glazing planes (Par 7).

2.3.4 Absorbed Solar Radiation

The results of the calculations described in sections 2.3.1 through 2.3.3 are used to calculate the total incident solar radiation on the wall, floor, glazing and extra mass. The total incident radiation is then reduced by a factor to account for the area of the glazing planes that is opaque to solar radiation. Glazing framing may block a significant portion of the solar radiation in some designs. Parameter 26 is the fraction of glazing plane area which is opaque to solar radiation. The incident solar radiation on node i, $Q_{s,i}(i)$ is computed from equation 2.3.4.1:

$$Q_{s,i}(i) = \{BU_i\ \tau_{b,u}\ I_{b,u}\ A_{gl,u} + BL_i\ \tau_{b,l}\ I_{b,l}\ A_{gl,l} + \tau_d[DU_i\ I_{d,u}\ A_{gl,u} + DL_i\ I_{d,l}\ A_{gl,l}]\}\ (1 - \text{Par } 26) \qquad 2.3.4.1$$

BU_i and DU_i are the fractions of beam and diffuse radiation from the upper glazing incident on node i, while BL_i and DL_i refer to fractions from the lower glazing. $I_{b,u}$ and $I_{b,l}$ are the beam radiation intensities incident on the upper and lower glazings. $A_{gl,u}$ and $A_{gl,l}$ are the areas of the upper and lower glazing planes, respectively.

Reflection of solar radiation is modeled using an F-hat formulation similar to the approach used in Section 2.2.4 for infrared radiation. All reflections are assumed to be diffuse and incident radiation is assumed to be uniform. These assumptions also apply to

the infrared radiation modeling, but they are more suspect for the case of solar radiation. The solar radiation is not uniform since transmittances for the beam components are not the same for each glazing sheet and, at times, only part of the floor or extra mass containers may be illuminated by beam radiation. As previously mentioned, breaking the wall and floor into many surface nodes has been found to have little effect on sunspace performance (6).

The total radiation absorbed by node i is:

$$Q_{s,a}(i) = \alpha_i \left[Q_{s,i}(i) + \sum_j \rho_j \, Q_{s,i}(j) \, \hat{F}_{ji}\right] \qquad 2.3.9$$

where α_i is the solar absorbtance of node i and ρ_j is the solar reflectance of node j. For the wall, floor, and extra mass nodes, $\rho_i = 1 - \alpha_i$. The glazing is assumed to have an absorbtance of zero, and $\rho_g = 1 - \tau_d$. That is, whatever is not reflected is transmitted back to the environment.

Solar F-hats are computed by inverting the solar reflectivity matrix whose elements are:

$$R_{ij} = \delta_{ij} - \rho_j \, F_{ij} \qquad 2.3.10$$

then applying equation 2.2.24. The view factors, F_{ij}, are identical to the view factors used in computing the infrared reflectivity matrix, but the F-hats are different since, in general, optical properties are not the same for solar and infrared radiation.

2.4 Numerical Integration and Internal Timestep

With the computation of heat transfer conductances and absorbed solar radiation complete, evaluation of temperatures and heat flows may proceed. The differential equation which describes the behavior of the sunspace temperature nodes is:

$$(mC_p)_i \frac{dT_i}{dt} = \sum_j C_{ij} (T_j - T_i) + Q_{s,a}(i) \qquad 2.4.1$$

where $(mC_p)_i$ is the mass-specific heat product of node i and C_{ij} is the conductance between node i and j. TRNSYS has a built-in modified-Euler integration routine. Euler integration may be unstable if the timestep is larger than a critical timestep (25). The critical timestep, based on the second law of thermodynamics, is the minimum over all mass nodes i of:

$$\frac{(mC_p)_i}{\sum_j C_{ij}} \qquad 2.4.2$$

For the sunspace, the maximum timestep for guaranteed stability is the minimum of the following five expressions:

$$\frac{(mC_p)_w/2\ (N_w - 1)}{C_1 + C_7 + C_9 + C_{11} + C_{16}} \qquad 2.4.3a$$

$$\frac{(mC_p)_w/2\ (N_w - 1)}{C_1 + C_2} \qquad 2.4.3b$$

$$\frac{(mC_p)_f/2\ (N_f - 1)}{C_3 + C_8 + C_{10} + C_{11} + C_{15}} \qquad 2.4.3c$$

$$\frac{(mC_p)_f/2\ (N_f - 1)}{C_3 + C_4} \qquad 2.4.3d$$

$$\frac{(mC_p)_m}{C_{14} + C_{15} + C_{16} + C_{17}} \qquad 2.4.3e$$

For most sunspace simulations, the critical timestep varies from one-sixteenth to one-half hour. Stability requirements of other components in a TRNSYS simulation may be substantially larger than the sunspace requirement. Simulation computing time and cost is directly related to the timestep. In order to allow a simulation timestep greater than the sunspace critical timestep, an internal simple Euler integration is built into the sunspace component. If the sunspace critical timestep is less than the simulation timestep, the internal timestep is defined as:

$$\text{internal} = \frac{\text{external}}{\text{integer}\left\{\frac{\text{external}}{\text{critical}} + 1\right\}} \qquad 2.4.4$$

Euler integration computes energy flows based on previous timestep temperatures. By discretizing the differential, equation 2.4.1 can be rearranged to equation 2.4.5:

$$T_i^+ = T_i + \frac{\Delta t}{(mC_p)_i}\left\{\sum_j C_{ij}\ (T_j - T_i) + Q_{s,a}(i)\right\} \qquad 2.4.5$$

The mC_p product of an interior wall node is:

$$(mC_p)_w = \frac{V_w\ (\rho C_p)_w}{N_w - 1} \qquad 2.4.6a$$

Similarly for an interior floor node:

$$(mC_p)_f = \frac{V_f(\rho C_p)_f}{N_f - 1} \qquad 2.4.6b$$

Applying equation 2.4.5 to the wall nodes yields:

$$T_1^+ = T_1 + \frac{\Delta t}{(mC_p)_{w/2}} \{ C_1(T_2 - T_1) + C_7 (T_{ss} - T_1) + C_9 (T_{gl,i} - T_1) + C_{10} (T_f - T_1) + C_{16} (T_m - T_1)\} \qquad 2.4.7a$$

for the sunspace surface node,

$$T_n^+ = T_n + \frac{\Delta t}{(mC_p)_w} \{ C_1 (T_{n-1} - T_{n+1} - 2 T_n)\} \qquad 2.4.7b$$

for interior nodes, and

$$T_w^+ = T_w + \frac{\Delta t}{(mC_p)_{w/2}} \{C_1 (T_{w-1} - T_w) + C_2 (T_r - T_w)\} \qquad 2.4.7c$$

for the building side surface node.

The floor node equations are:

$$T_f^+ = T_f + \frac{\Delta t}{(mC_p)_{f/2}} \{C_3 (T_{f+1} - T_f) + C_8 (T_{ss} - T_f) + C_{10} (T_1 - T_f) + C_{11} (T_{gl,i} - T_f) + C_{15} (T_m - T_f)\} \qquad 2.4.8a$$

for the top node,

$$T_n^+ = T_n + \frac{\Delta t}{(mC_p)_f} \{C_3 (T_{n+1} + T_{n-1} - 2T_n)\} \qquad 2.4.8b$$

for interior nodes and,

$$T_L^+ = T_L + \frac{\Delta t}{(mC_p)_f/2} C_3 (T_{L-1} - T_L) + C_4 (T_{gr} - T_L) \qquad 2.4.8c$$

for the bottom node. For the extra mass node equation 2.4.5 becomes:

$$T_m^+ = T_m + \frac{\Delta t}{(mC_p)_m} \{ C_{14} (T_{ss} - T_m) + C_{15} (T_f - T_m) + C_{16} (T_w - T_m) + C_{17} (T_{gl,i} - T_m) \} \qquad 2.4.9$$

The only sunspace nodes not yet described are the glazing and sunspace air nodes.

2.5 Massless Node Temperatures

The heat storage capacities of the sunspace air and glazings are much smaller than other sunspace node storage capacities. The TRNSYS model completely neglects the storage capacity of the glazings and air. Since neither node absorbs solar radiation, equation 2.4.5 for these "massless" nodes becomes:

$$\sum_j C_{ij} (T_j - T_i) = 0 \qquad 2.5.1$$

External control of sunspace temperature can be provided by including an additional term in the equation for the sunspace air node. Input 20 is the rate of external heat addition to the sunspace air, Q_{add}. A negative value is the rate of heat removal. The sunspace air is assumed to be fully mixed. Substitution of actual conductances and nodal temperatures leads to two equations with two unknowns:

$$C_5 (T_a - T_{gl,i}) + C_6 (T_{ss} - T_{gl,i}) + C_9 (T_w - T_{gl,i}) + C_{11} (T_f - T_{gl,i}) + C_{17} (T_m - T_{gl,i}) = 0 \quad 2.5.2$$

$$C_6 (T_{gl,i} - T_{ss}) + C_7 (T_w - T_{ss}) + C_8 (T_f - T_{ss}) + C_{12} (T_a - T_{ss}) + C_{13} (T_s - T_{ss}) + C_{14} (T_m - T_{ss}) + Q_{add} = 0 \quad 2.5.3$$

T_s in equation 2.5.3 depends on the destination of the vented sunspace air. If the sunspace air is vented to the adjacent building, T_s equals the building temperature. Venting to ambient sets T_s equal to the ambient temperature. If no venting occurs, T_s is the sunspace air temperature and C_{13} is multiplied by zero. Successive substitution leads to the following equations for the inside glazing temperature $T_{gl,i}$ and the sunspace air temperature, T_{ss}:

$$T_{gl,i} = - (T_a F_4 + T_w F_5 + T_f F_6 + T_m F_7 + T_s C_{13} + Q_{add})/F_3 \quad 2.5.4$$

$$T_{ss} = (T_{gl,i} F_2 - C_5 T_a - C_9 T_w - C_{11} T_f - C_{17} T_m)/C_6 \quad 2.5.5$$

where F_1 through F_7 are:

$$F_1 = (C_6 + C_7 + C_8 + C_{12} + C_{13} + C_{14})/C_6$$

$$F_2 = C_5 + C_6 + C_9 + C_{11} + C_{17} \quad 2.5.6$$

$$F_3 = C_6 - F_1 F_2$$

$$F_4 = C_{12} + C_5 F_1 \qquad \text{2.5.6 (continued)}$$

$$F_5 = C_7 + C_9 F_1$$

$$F_6 = C_8 + C_{11} F_1$$

$$F_7 = C_{14} + C_{17} F_1$$

The values of C_9, C_{11}, and C_{17} depend on the temperature of the inside glazing surface and C_5 depends on the temperature of the outside surface. The program iterates for correct temperatures until the change in sunspace air temperature from one iteration to the next is less than 0.01 C. Temperatures from the previous timestep are used to calculate initial values of the variable conductances. Sunspace air and inside glazing temperatures are calculated from equations 2.5.4 and 2.5.5. The convergence check is performed. If the criterion is not satisfied, new conductances are calculated based on the most recent glazing and air temperatures where:

$$T_{gl,o} = T_{gl,i} - \frac{C_5 (T_{gl,i} - T_a)}{C_{5c}} \qquad \text{2.5.7}$$

The sequence is repeated until the convergence criterion is satisfied. Convergence is rapid, as only two or three iterations are usually required. Other heat flows and temperature changes are then calculated. The whole procedure is duplicated until the internal integration has completed a full TRNSYS timestep interval and out-

puts are set.

2.6 Outputs

Output heat flows are computed by averaging internal timestep values over the TRNSYS step. After the completion of each internal timestep, output energy flow values are averaged using equations similar to the generalized Equation 2.6.1:

$$Q = Q + \frac{C_{ij} \ (T_j - T_i)}{NTS} \qquad 2.6.1$$

NTS is the number of internal timesteps per TRNSYS timestep.

Equations used to calculate outputs will now be discussed. The energy flow from the sunspace to the adjacent building is:

$$Q_{rm} = C_2 \ (T_w - T_r) + C_{13} \ (T_{ss} - T_r) \qquad 2.6.2$$

where T_w is the temperature of the last wall node and the second term is included only if venting to the building occurs. The energy stored in the massive nodes of the sunspace is:

$$Q_{str} = \sum_{\substack{\text{mass} \\ \text{nodes}}} [\sum_j C_{ij} \ (T_j - T_i) + Q_{s,a} \ (i)] \qquad 2.6.3$$

Solar energy incident on the sunspace nodes is:

$$Q_{inc} = \sum_i Q_{s,i} \ (i) \qquad 2.6.4$$

where the summation includes the first wall, the top floor, the glazing, and the extra mass nodes. Absorbed solar energy is a similar summation:

$$Q_{abs} = \sum_{i} Q_{s,a}\ (i) \qquad 2.6.5$$

The rate of heat loss to ambient is:

$$Q_{amb} = C_5\ (T_{gl,i} - T_a) + C_{12}\ (T_{ss} - T_a) + C_{13}\ (T_{ss} - T_a) \qquad 2.6.6$$

but the last term is only included if venting to ambient occurs. Ground heat losses are:

$$Q_{gr} = C_4\ (T_f - T_{gr}) \qquad 2.6.7$$

where T_f is the bottom floor node temperature. Temperatures of all the sunspace node temperatures at the end of the timestep are included in the output array. The last two outputs are the internal integration timestep and the vented air mass flow rate (as determined by input 1 and 19).

A list of the sunspace TRNSYS component parameters, inputs and outputs is found in the Appendix. Computer coding of the TRNSYS sunspace is also contained in the Appendix.

2.7 Verification of the Sunspace Model

2.7.1 Introduction

The results of the sunspace computer model should be checked in some fashion. Ideally, the output temperatures could be compared with test results of actual sunspace systems. The time and cost involved with this kind of validation is prohibitive in this study. The second approach, taken herein, is to compare results with that of other simulation codes and design methods which, in turn, have

been compared with experimental data. Similar results do not guarantee validity of the models, but, at least gross errors in assumptions and coding can be identified.

A sunspace with a masonry common wall, collapsed to the limit of a very small floor width, closely approximates a collector-storage wall. TRNSYS contains a collector-storage wall component and comparisons between simulations using the collapsed sunspace and the collector-storage wall models were performed.

A comparison between TRNSYS sunspace simulation results and results from the SLR monthly method of Los Alamos for several SLR reference designs has also been done.

2.7.2 Comparison of TRNSYS Sunspace and Collector-Storage Wall Models

Simulations of a collapsed sunspace system and a collector-storage wall system were performed using Madison, Wisconsin weather data. The characteristics of the system are summarized in Table 2.2. The collector-storage wall model computes the convection coefficient from the wall and glazing to the air internally. The model was modified so the convection coefficient was included in the outputs. This convection coefficient was the input to the sunspace model. Monthly results for various energy quantities are compared in Figure 2.5 for unvented systems. A comparison between vented systems showed differences very slightly larger than those of Figure 2.5. While the vented system differences are not unreasonable, the fact that they were larger than the unvented system

Table 2.2

Characteristics of Collector-Storage Wall
and Sunspace System Comparison

Location: Madison, Wisconsin

Common Wall

Area 30.2m^2

Thickness 0.3m

Density-specific heat product 2012 kJ/m^3

Conductivity 1.70 W/m°C

Solar absorbtance .75

Infrared emittance .9

Glazing - wall gap 0.1m

Glazing

Number of covers 2

Infrared emittance .88

Extinction coefficient .037

Index of refraction 1.526

No night insulation

Venting Control

Minimum sunspace air temperature 24°C

Air mass flow rate 302 Kg/hr

Building

Loss coefficient (non-solar) 158 W/°C

Capacitance (not including the masonry wall) 5000 kJ/°C

Thermostat set points 23.9°C, 18.3°C

Figure 2.5

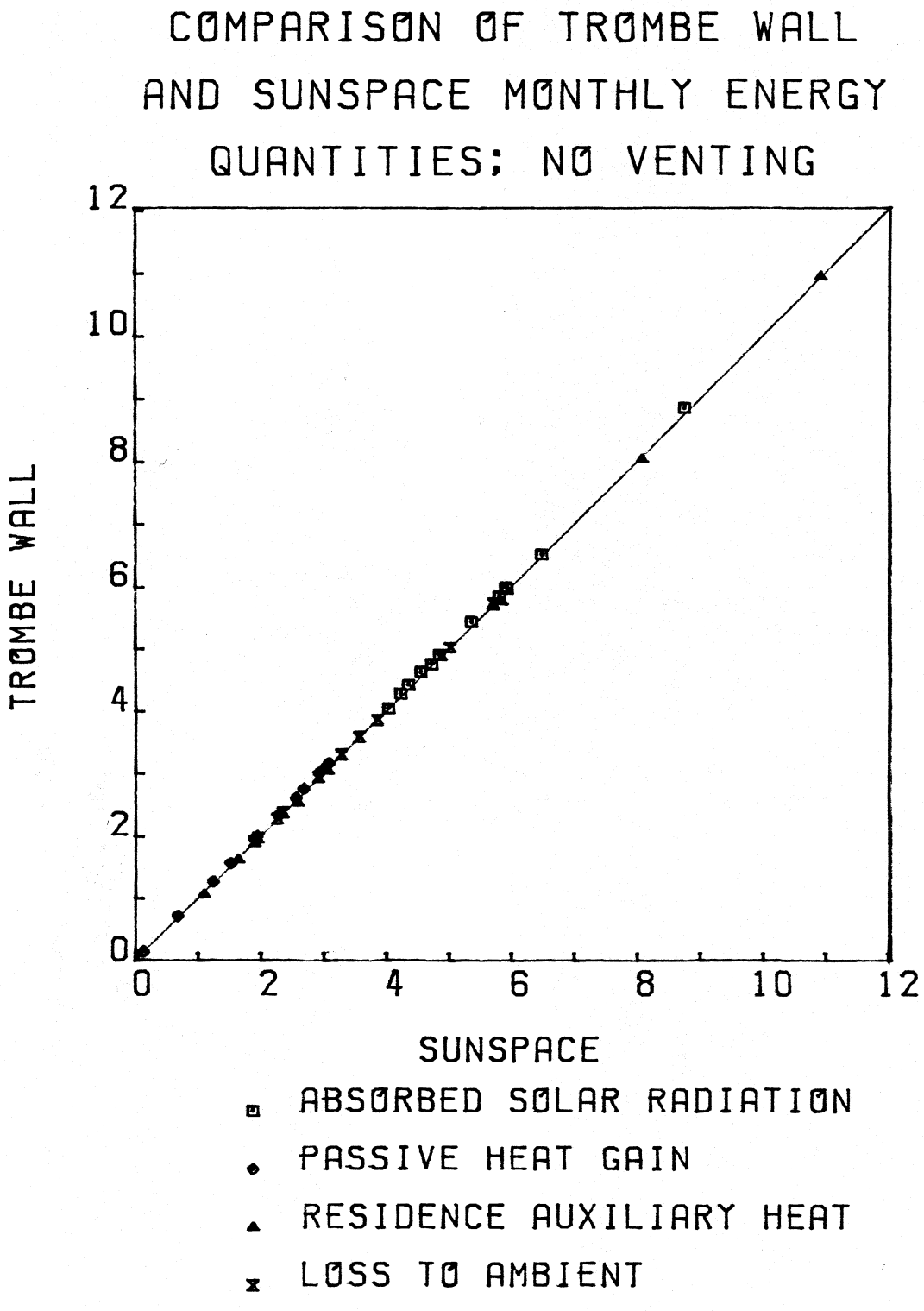
COMPARISON OF TROMBE WALL AND SUNSPACE MONTHLY ENERGY QUANTITIES; NO VENTING
TROMBE WALL
0
2
4
6
8
10
12
SUNSPACE
ABSORBED SOLAR RADIATION
PASSIVE HEAT GAIN
RESIDENCE AUXILIARY HEAT
LOSS TO AMBIENT

differences warrants investigation. The sunspace air is assumed to be fully mixed, that is, no temperature stratification from vent inlet to outlet is computed. The collector-storage wall component, however, does include stratified air temperature in the flow direction since flow geometry is well defined. By temporarily including temperature stratification in the sunspace model, the results of Figure 2.6 were obtained.

The comparisons between the two simulations show very little difference in monthly energy quantities. Temperature and control function histograms are also very similar. The sunspace system has larger ambient heat losses because the sunspace loss area includes the top and side glazings. The sunspace absorbed solar energy is slightly greater than that of the collector-storage wall. Reflections from the side walls, floor and top glazing account for this difference.

2.7.3 Comparison of TRNSYS and Los Alamos Scientific Laboratory Results

Auxiliary energy requirements as predicted by the TRNSYS sunspace model and the SLR design method were compared. The sunspace geometry selected was an attached sunspace with a lower glazing slope of ninety degrees and an upper glazing slope of thirty degrees. The geometry is referred to by LASL as geometry B. Other characteristics of the reference design are found in (11,12,18). The TRNSYS sunspace component geometry and other properties were as close as possible to the reference designs. However, the sunspace

Figure 2.6

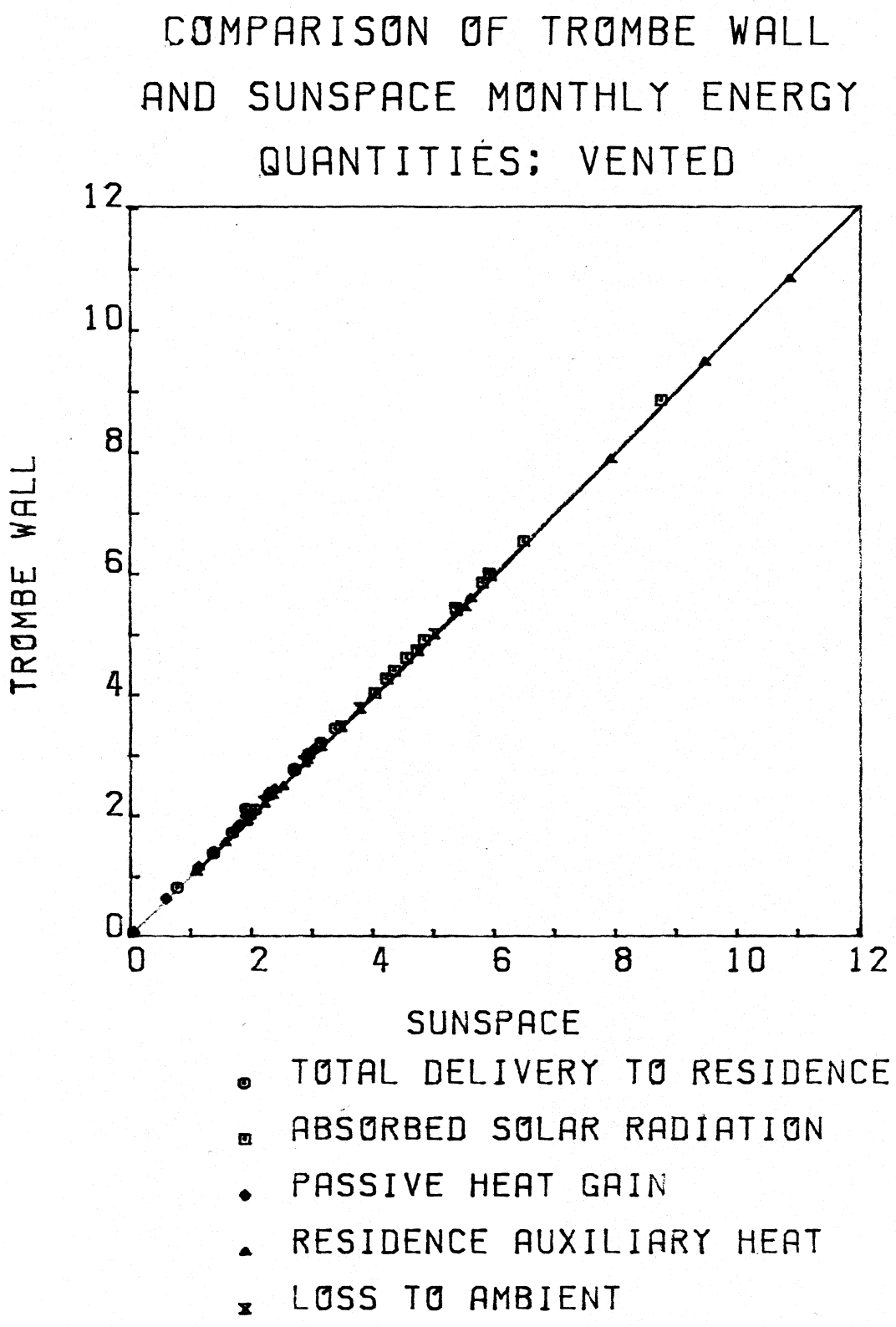
COMPARISON OF TROMBE WALL AND SUNSPACE MONTHLY ENERGY QUANTITIES; VENTED
TROMBE WALL
0
2
4
6
8
10
12
SUNSPACE
TOTAL DELIVERY TO RESIDENCE
ABSORBED SOLAR RADIATION
PASSIVE HEAT GAIN
RESIDENCE AUXILIARY HEAT
LOSS TO AMBIENT

loss coefficient (UA) in the simulations was slightly larger than the SLR default values. The simulation value was used in the SLR equation 1.2.1 to account for this. The Los Alamos reference designs limit the sunspace temperature to 7.2-35.0 C (45-95 F). An auxiliary heater was included in the TRNSYS simulation to maintain these temperatures. This additional auxiliary energy is included in the monthly energy totals.

Table 2.3a lists monthly auxiliary energy predictions for a masonry common wall with no night insulation (reference design B3) in Madison, Wisconsin for a building with a non-solar loss coefficient of 158 W/m^2 C. The TRNSYS simulation predicts 3.25 GJ more auxiliary fuel consumption out of a total load of 48.97 GJ. The monthly trends are comparable. A second simulation of the same system without any solar radiation input was also performed. Table 2.3b compares these results with SLR values computed for monthly absorbed radiation equal to zero. The difference in the non-solar loads is 3.39 GJ. The main difference between the two prediction methods seems to be related to the load calculations. The predicted reduction in auxiliary heat is nearly the same.

A second comparison was done between the methods by including night insulation of the glazing (LASL reference design B4). The results are listed in Table 2.4. The heating season totals are remarkably close. Results for these masonry wall sunspaces in Madison are encouraging.

Table 2.3a

TRNSYS and SLR Predicted Auxiliary Energy
Masonry Wall, No Night Insulation, Madison

Building Auxiliary Heat (GJ)

Month	TRNSYS	SLR
Oct.	1.805	1.483
Nov.	5.758	5.932
Dec.	10.379	9.969
Jan.	12.261	11.602
Feb.	9.324	8.378
Mar.	6.915	6.444
Apr.	2.530	1.912
Total	48.97	45.72

Table 2.3b

Comparison of Building Loads: No Solar Radiation

Building Auxiliary Heat (GJ)

Month	TRNSYS	SLR
Oct.	4.565	4.362
Nov.	8.354	8.493
Dec.	12.888	12.181
Jan.	15.317	14.799
Feb.	13.069	12.150
Mar.	11.816	11.136
Apr.	5.701	5.206
Total	71.71	68.32

Table 2.4

TRNSYS and SLR Predicted Auxiliary Energy
Masonry Wall, Night Insulation, Madison

Building Auxiliary Energy (GJ)

Month	TRNSYS	SLR
Oct.	1.189	0.903
Nov.	4.850	4.878
Dec.	9.261	8.760
Jan.	10.694	10.015
Feb.	8.056	9.168
Mar.	5.323	4.900
Apr.	1.522	1.202
Total	40.90	39.83

Table 2.5

TRNSYS and SLR Predicted Auxiliary Energy
Insulated Wall, No Night Insulation, Madison

Building Auxiliary Energy (GJ)

Month	TRNSYS	SLR
Oct.	2.422	1.832
Nov.	6.342	5.979
Dec.	10.067	9.608
Jan.	12.177	11.317
Feb.	9.469	8.744
Mar.	7.876	6.849
Apr.	2.898	2.310
Total	51.25	46.64

Comparisons of insulated common wall sunspace systems were also performed. The LASL reference design, B7, has a large additional heat storage mass container (7.65 m^3 of water) and venting is driven by natural convection. The TRNSYS venting mass flow rate was set to 250 kg/hr. Results are presented in Table 2.5. The difference in predicted auxiliary energy is greater than in the masonry wall comparisons. The probable cause for this discrepancy is the assumed venting mass flow rate. Delivered energy of insulated common wall sunspace systems is highly dependent on the venting flow rate as discussed in section 3.3.5.

Overall, the comparison of the auxiliary energy prediction shows good agreement. The SLR method results presented in this section are obtained from correlations to detailed simulations. The error between the SLR method and the simulations it was derived from are of the same order of magnitude as the differences in Tables 2.3 through 2.5.

Chapter 3: Parametric Studies of Sunspace Performance

3.1 Introduction

The TRNSYS sunspace component discussed in Chapter 2 can be used to simulate a wide variety of attached sunspace systems. The parameters and inputs to the model, should be chosen to be as close to the true physical characteristics of a sunspace as possible. However, some of the inputs, such as convection coefficients and ground temperature, may not be well-established. In addition, the simulation timestep and the number of nodes in the wall and floor must be chosen. The effects of different values of these variables on sunspace performance is examined in Section 3.2.

The thermal performance of sunspace systems also depends on the attached building characteristics and control strategies. Effects of venting between the sunspace and building, maintenance of sunspace temperature, and the effect of the sunspace on building cooling loads are discussed in this chapter.

The technique of evaluating the effects of changes in the variables employed in these studies is called factorial design. The details of factorial designs are thoroughly discussed by Box, Hunter and Hunter (26). Briefly, values of the variables in question are selected which span the expected range. Multiple computer simulations are performed with all possible combinations of variables, hence the name factorial. The advantage of this method over the traditional approach of changing one variable at a time is that factorial designs provide a measure of the interaction effects

of changing several variables simultaneously.

A large factorial design study of every possible variable that affects sunspace performance would be time consuming and expensive. Instead, smaller factorial design studies of variables that are of interest and that are likely to have significant interactions may be performed. Even though the performance of sunspaces is dependent on sunspace geometry and optical characteristics, interactions of these variables with the factorial designs of this chapter are unlikely. The sunspace geometry and optical properties are the same for all the Chapter 3 studies and are summarized in Figure 3.1.

3.2 Sunspace Model Considerations

3.2.1 Effects of Simulation Timestep and Number of Nodes

The TRNSYS sunspace component has a built-in internal timestep which may be less than the simulation timestep (Section 2.4). This feature, however, only guarantees the stability of the numerical integration, not the accuracy. In addition, the number of nodes representing the temperature gradient in the wall and floor may affect simulation results. The most accurate results are obtained by using a very small timestep and a large number of temperature nodes in the floor and wall. These factors tend to increase simulation computing time and cost. The "best" choice of timestep and number of nodes minimizes computing time and yet increasing the number of nodes, or decreasing the timestep does not change the results significantly. A factorial design in timestep and number of nodes was performed on a sunspace in Madison, Wisconsin. Monthly results

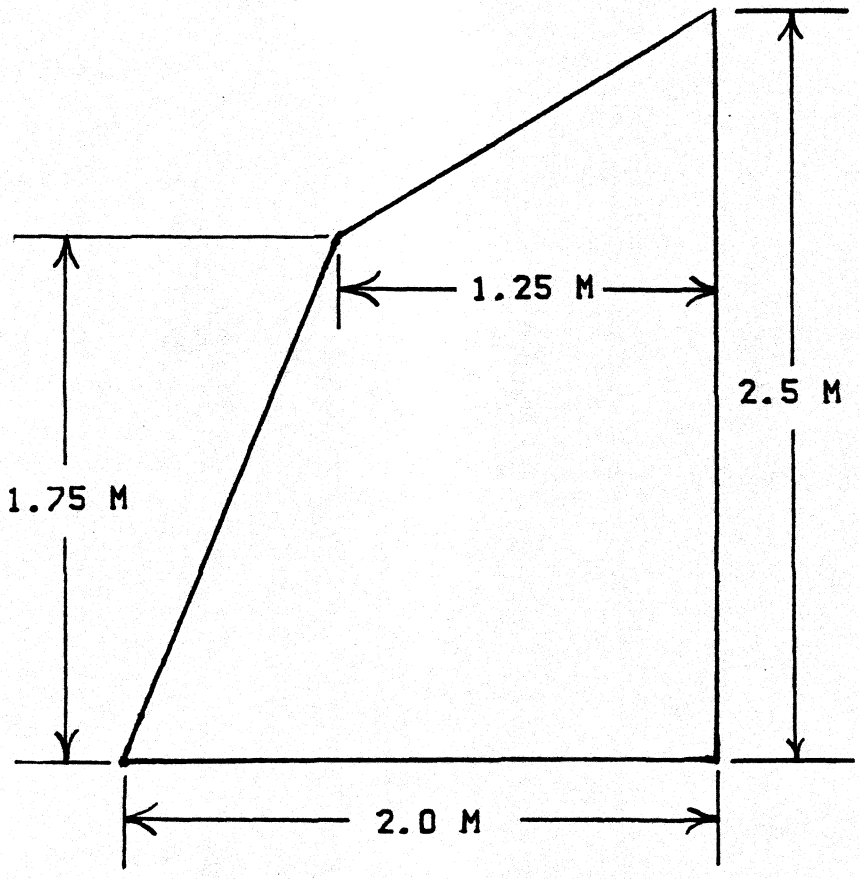

Sunspace width 8.92m
Infrared emittance of the glazings 0.88
Infrared emittance of the floor and wall 0.9
Solar absorbtivity of the floor and wall 0.75
R-value of the double-glazing 0.22 m^2-C/W
Extinction coefficient of the glazing 0.037/sheet
Refractive Index of the glazing 1.526

Figure 3.1 Geometry and Optical Properties of the Sunspaces used in Chapter 3 Parametric Studies

for both January and July were obtained so seasonal interactions could be evaluated. The characteristics of the simulations are summarized in Table 3.1.

Results for January are plotted on Figure 3.2. Energy delivery from the sunspace to the adjacent building is negative in all cases. This means the sunspace monthly energy loss to the environment is somewhat greater than the absorbed solar radiation. The sunspace is still beneficial for heating, since most walls lose more heat than the sunspace. The variation in the number of nodes in the wall does not greatly affect the monthly energy delivery. The timestep, at first glance, seems to have a large effect on the energy delivery, but the scale of the plot magnifies the differences. The total absorbed solar radiation for January is on the order of 5.9 GJ. When taken in this context, the variations of energy delivery are rather small. The numbers in parenthesis are the sunspace internal timestep when it differs from the simulation timestep.

Figure 3.3 shows the computed values of energy delivery for July. No differences between timesteps are observable, and the number of nodes in the wall does not have a large influence on the monthly energy delivery.

The computer execution times for the July simulations on a Univac 1100 are plotted in Figure 3.4. Examination of the figure shows a large increase in computing time when the number of nodes is increased from six to 12 for the simulations with timesteps of one hour and 1/4 hour. Very little difference between monthly energy de-

Table 3.1

Simulation Characteristics for Timestep and Number of Wall Nodes Factorial Design

Location: Madison, WI

Wall and floor thickness: 0.3m

(ρC_p) of wall and floor: 2009 KJ/m^3 C

Conductivity of wall and floor: 1.73 W/m C

Air change rate: 1 change/hr

No night insulation

No venting

Effective ground R-value 7.05 m^2-C/W

No additional floor insulation

No additional thermal storage containers

No sunspace auxiliary heating or cooling

Glazing to ambient convection coefficient: 2.8 + 3.0 V W/m^2 C

where V is the wind speed in m/s (27)

Glazing-to-sunspace air, wall-to-sunspace air, floor-to-sunspace air convection coefficients 4 W/m^2 C

Wall to room heat transfer coefficient 8.3 W/m^2 C

Room temperature: 18.3 C

Ground temperature: -0.6 C (Jan) 14.2 C (July)

Timestep (hr)	Number of Wall Nodes	Months
1	3	Janaury
.25	6	July
.0625	12	

Figure 3.2

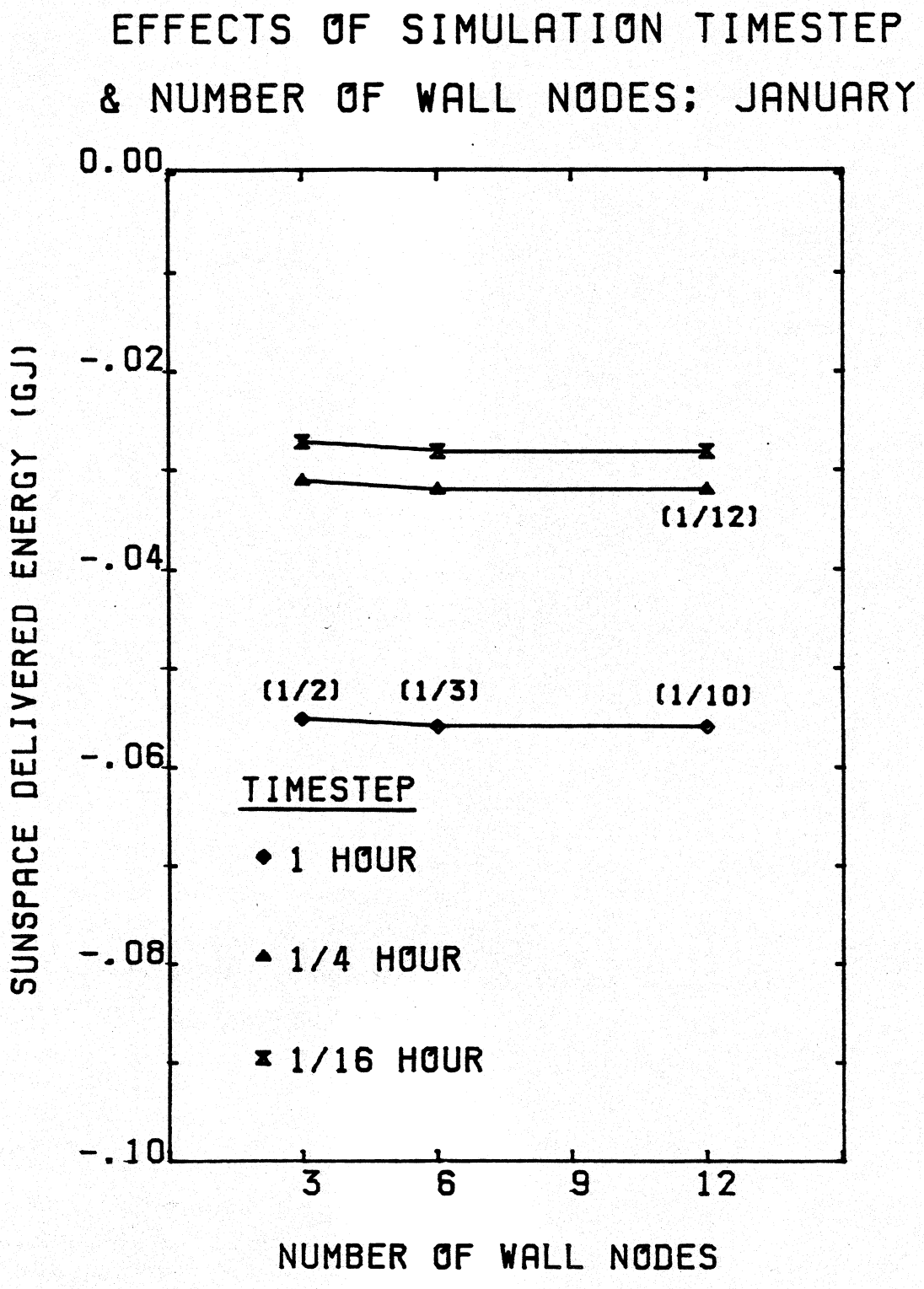
EFFECTS OF SIMULATION TIMESTEP
& NUMBER OF WALL NODES; JANUARY
0.00
-.02
-.04
-.06
-.08
-.10
SUNSPACE DELIVERED ENERGY (GJ)
(1/12)
(1/2)
(1/3)
(1/10)
TIMESTEP
1 HOUR
1/4 HOUR
1/16 HOUR
3
6
9
12
NUMBER OF WALL NODES

Figure 3.3

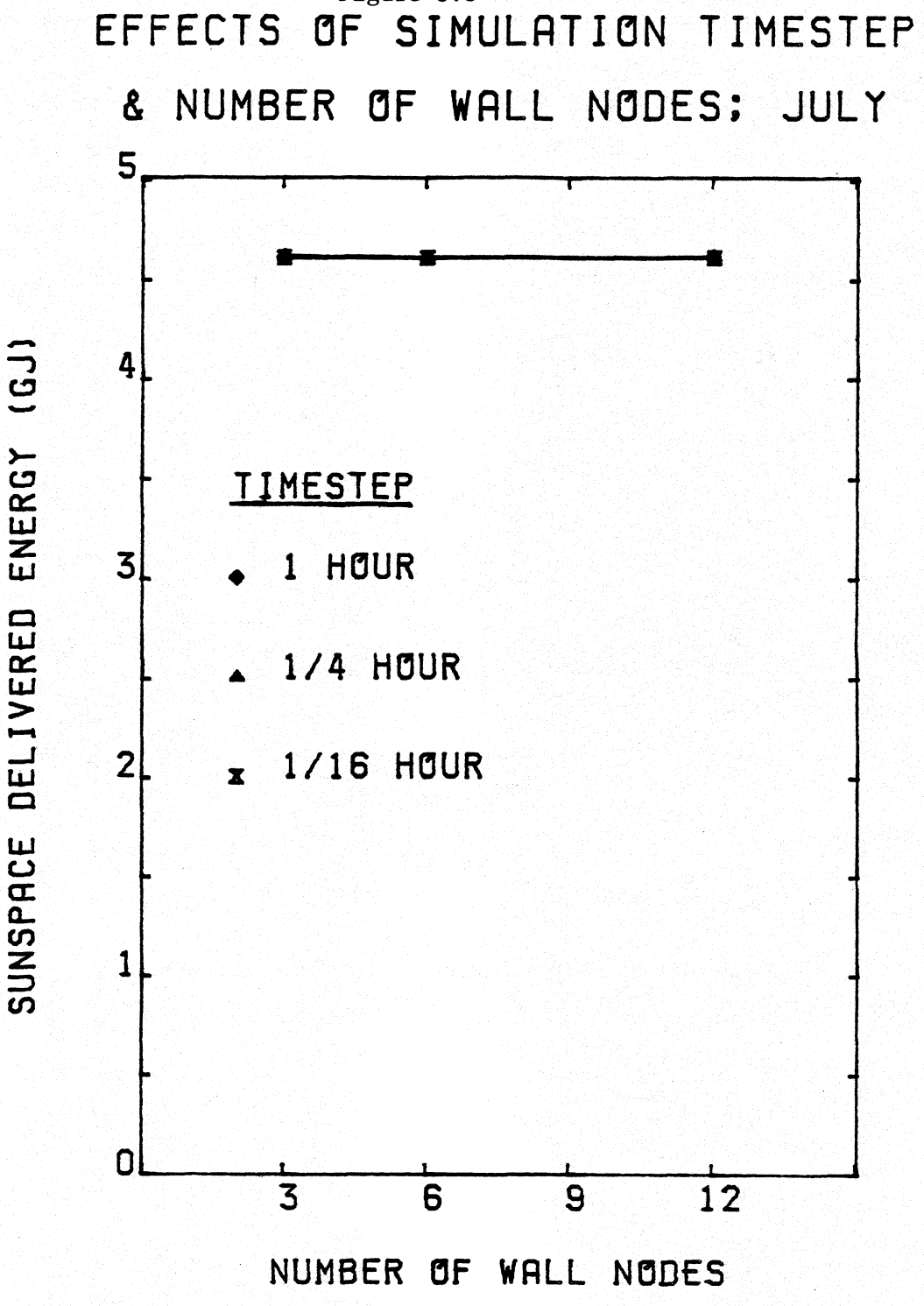
EFFECTS OF SIMULATION TIMESTEP
& NUMBER OF WALL NODES; JULY
SUNSPACE DELIVERED ENERGY (GJ)
5
4
3
2
1
0
TIMESTEP
1 HOUR
1/4 HOUR
1/16 HOUR
3
6
9
12
NUMBER OF WALL NODES

Figure 3.4

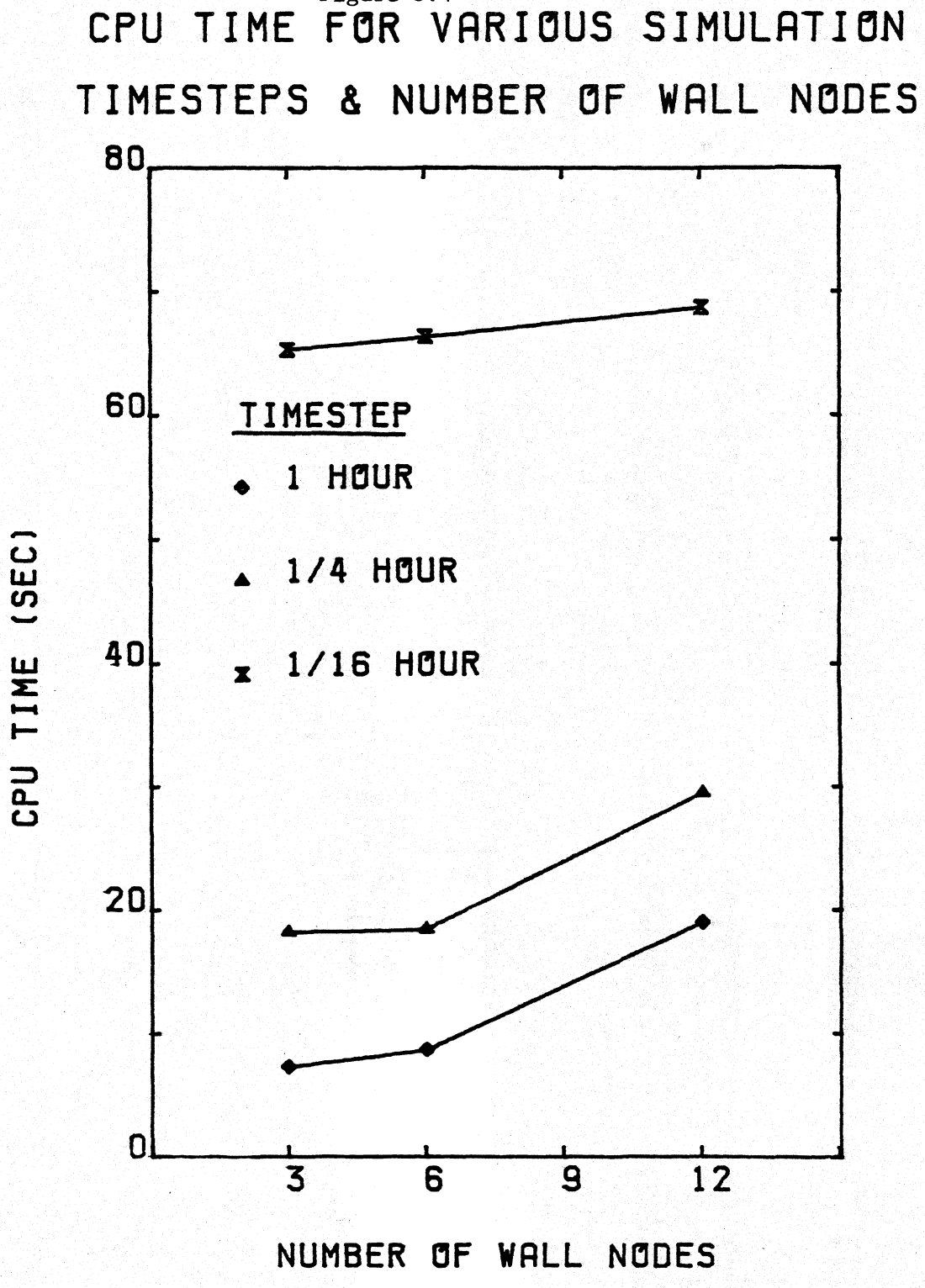
CPU TIME FOR VARIOUS SIMULATION TIMESTEPS & NUMBER OF WALL NODES
80
60
40
20
0
CPU TIME (SEC)
TIMESTEP
1 HOUR
1/4 HOUR
1/16 HOUR
3
6
9
12
NUMBER OF WALL NODES

livery quantities is observed in Figures 3.2 and 3.3 for the same change. Increasing the number of nodes from three to six does not lead to the same kind of change in computing time, and the variation in results is proportionally larger. Changing the simulation timestep from 1/4 to 1/16 hour more than doubles the computing time. The number of iterations per timestep goes down but, of course, four times as many timesteps are required. This change has no effect on the calculated energy delivery. For sunspace simulations with similar wall characteristics, a timestep of one hour is usually sufficient, and a value for the number of wall nodes from 3 to 6 is recommended.

Some simulations of building-integrated systems may require a smaller simulation timestep for overall stability. In addition, simulations with large timesteps may require several iterations before results converge within the specified simulation tolerance. In some cases, decreasing the timestep actually decreases computing time because the number of iterations is reduced. If a large number of simulations are to be performed, examining these factors may result in a significant reduction in computing cost.

3.2.2 Effects of Convection Coefficients

In formulating a sunspace simulation, the inputs to the component having the largest uncertainty are the heat transfer coefficients (Inputs 6-10). This section quantifies the effects on sunspace energy delivery of these variables. A two-level factorial design (26) was performed with the two values of the heat transfer coefficients representing natural convection and the reasonable upper

limit of forced convection. The convection coefficients between the sunspace surfaces (wall, floor and glazing) and the sunspace air are assumed to be identical. The levels of heat transfer coefficients are listed in Table 3.2 where the negative sign indicates the natural convection value and the positive sign designates the forced convection value. The values for the outside convection coefficient are obtained through a correlation (27) to hourly average wind speed taken from the Typical Meteorological Year Weather Data tape (31). The values for the sunspace interior coefficients were computed from heated plate correlations and large aspect-ratio enclosure equations (25). Heat transfer coefficients between the wall and adjaeent building were computed by combining radiation terms and convection values for a vertical plate.

The main effects and two-factor interactions for this factorial design are listed in Table 3.3. The main effects are the changes in sunspace delivery when one variable is changed from its low to high value with all other variables remaining constant. For example, changing the glazing-to-ambient convection coefficient from 3 to 18 W/m^2 C decreases the sunspace energy delivery by 357.9 MJ in January. The two-factor interactions are a measure of the combined effect of variables. For example, when the glazing-to-ambient and wall-to-room coefficients are increased simultaneously, the January energy delivery is reduced by 38.1 MJ in addition to the main effects of the changes. The total change in delivery for this case is -357.9 + 43.2 - 38.1 = -352.8 MJ. A three-factor interaction can

Table 3.2

Heat Transfer Coefficient Values for Factorial Design

Heat Transfer Coefficient (W/m^2 C)	-	+
glazing-ambient	3	18
sunspace air-wall, floor, glazing	1	6
inside wall surface-building	4.5	10

Table 3.3

Effects and Interactions of Heat Transfer Coefficients on Sunspace Energy Delivery

Heat Transfer Coefficients	January	July
glazing-ambient	-357.9 (MJ)	-327.5 (MJ)
wall-building	43.2	925.5
sunspace air-interior surfaces	-466.7	-135.0
glazing-ambient x wall-building	- 38.1	- 13.0
glazing-ambient x ss air-interior	- 49.8	- 22.5
wall-building x ss air-interior	- 48.7	17.5
Average Delivery	162.1	4430.0
Absorbed Solar Radiation	5889.0	10980.0

also be computed, but in this study it was negligible.

To evaluate the significance of these effects, they are compared with the magnitude of other monthly energy quantities. The average overall sunspace energy delivery in January (0.16 GJ) is small when compared with the absorbed solar radiation in the sunspace (5.89 GJ). This means effects which are large compared with the January energy delivery are not necessarily significant.

The glazing-to-ambient convection coefficient has a significant effect on the energy delivery of the sunspace. A large portion of sunspace heat losses to the environment are controlled by its value. Since sunspace temperature is greater than the ambient temperature, increasing the convection coefficient increases heat losses and decreases energy delivery to the building.

The effect of the wall-to-building heat transfer coefficient has a strong seasonal dependence. For unvented sunspaces, the heat transfer coefficient between the common wall and the building controls all of the energy flow between the two. In the summer, the sunspace is warmer than the building. Enlarging the wall-to-building heat transfer coefficient increases the rate of heat delivery to the building. Therefore the effect of raising the wall-to-building heat transfer coefficient is substantial in July. In cold months with lower solar radiation intensities, the sunspace can be either warmer or colder than the adjacent building. Raising the heat transfer coefficient will magnify the heat delivery to the building when the sunspace is warmer than the building. It also augments the heat

loss from the building to the sunspace when the sunspace is colder than the building. The net effect in January is relatively minor. For most well designed sunspaces, the net monthly energy delivery is positive for a majority of the year (see Figures 3.17 and 3.18). In months with significant net sunspace delivery, the effect of the wall-to-building heat transfer coefficient is large. Therefore, for annual or heating season simulations the total effect is substantial.

Increasing the sunspace interior convection coefficients lowers the energy delivery of the sunspace and the effect is somewhat seasonally dependent. Raising the wall-to-sunspace air, floor-to-sunspace air, and glazing-to-sunspace air convection coefficients increases the glazing and sunspace air temperatures. Energy losses to the environment increase and delivery to the building declines. The ambient temperature is lower in winter than in summer so the change in delivery to the building when the interior convection coefficients are raised is greater in January than in July.

All the two-factor interactions, while not completely negligible, are relatively insignificant. The two most important factors are the main effects of the wall-to-building and the glazing-to-ambient convection coefficients.

3.3 Building Integrated Sunspace Studies

3.3.1 Building Load Modeling and System Description

Heat transfer between a building and the environment can be described by a set of partial differential equations, which include

the capacitance of the building skin. Solutions are obtained by numerical integration or, alternatively, by using transfer functions as outlined by ASHRAE (19).

Herein, building loads are calculated by multiplying the heat loss coefficient (UA), which is assumed to be constant, by the building-to-ambient temperature difference. This is the basis of degree-day load calculations (19). This approach is reasonable in the study, since long-term performance is of interest. The building heat storage capacity is modeled as a lumped single-node "effective" capacitance. This assumption implies the building interior has a uniform temperature.

These factors are included in the TRNSYS Type 12 building load model. Mode 4 of the model requires a lumped building capacitance in KJ/C. The building interior temperature is calculated from input heat fluxes, the building loss coefficient and capacitance, and the ambient temperature.

The TRNSYS simulations described in this chapter were performed by using the building temperature to control a Type 8, Three-Stage Thermostat component. The thermostat controls venting between the sunspace and building, and auxiliary heating and cooling of the building. A dead band setting is included in this component to reduce oscillations of the thermostat output control functions. Heating and cooling rates of the building are supplied by Type 6, On-Off Auxiliary Heater components. Cooling is provided by specifying a negative heating rate for that Type 6 component.

3.3.2 Effects of Floor Slab Heat Losses

Most of the sunspace simulations in this chapter assume an effective ground R-value of 7.05 m^2-C/W. A single variable study examining this assumption was performed. Significant interaction effects with other variables are unlikely. The simulation characteristics are similar to earlier studies (Table 3.1). Changes and additions are summarized in Table 3.4. Three heating season simulations were performed using hourly weather data for Madison, Wisconsin (31). The ground temperature was assumed to be the average of the annual and monthly average ambient temperatures (28). Monthly energy quantities for effective ground R-values of 7.05, 1.76, and 0.44 m^2-C/W are plotted in Figure 3.5.

Decreasing the effective ground insulation magnifies the heat transfer from the floor to the ground. Other sunspace heat loss terms shrink as the ground losses rise. This balancing effect causes the energy delivery of the sunspace to vary less dramatically than one would expect on consideration of ground losses alone. The building auxiliary heat is affected by an even lesser amount.

This study shows that the assumed value of effective ground insulation does not have a large effect on the auxiliary energy requirement of the building. However, the effective ground R-value may be important in some cases such as a high ground water table or a study of the utility of additional floor slab insulation.

Table 3.4

Simulation Characteristics for the Effective Ground Insulation Study

Sunspace

wall thickness 0.15m

floor thickness 0.10m

sunspace interior convection coefficients 5.7 W/m^2 C

Thermostat

Heating Set Point 17.2°C

Cooling Set Point 25.5°C

Dead band 1.5°C

Building

UA 158 $W/m^2°C$

Capacitance 5000 KJ/C

Auxiliary heating rate 26000 KJ/hr

Auxiliary cooling rate -12000 KJ/hr

Internal Gains: 24 hr cycle

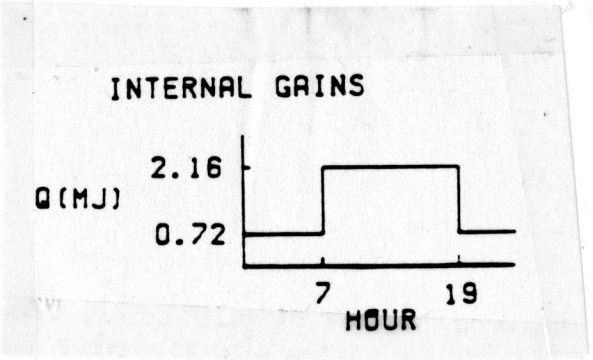

Figure 3.5

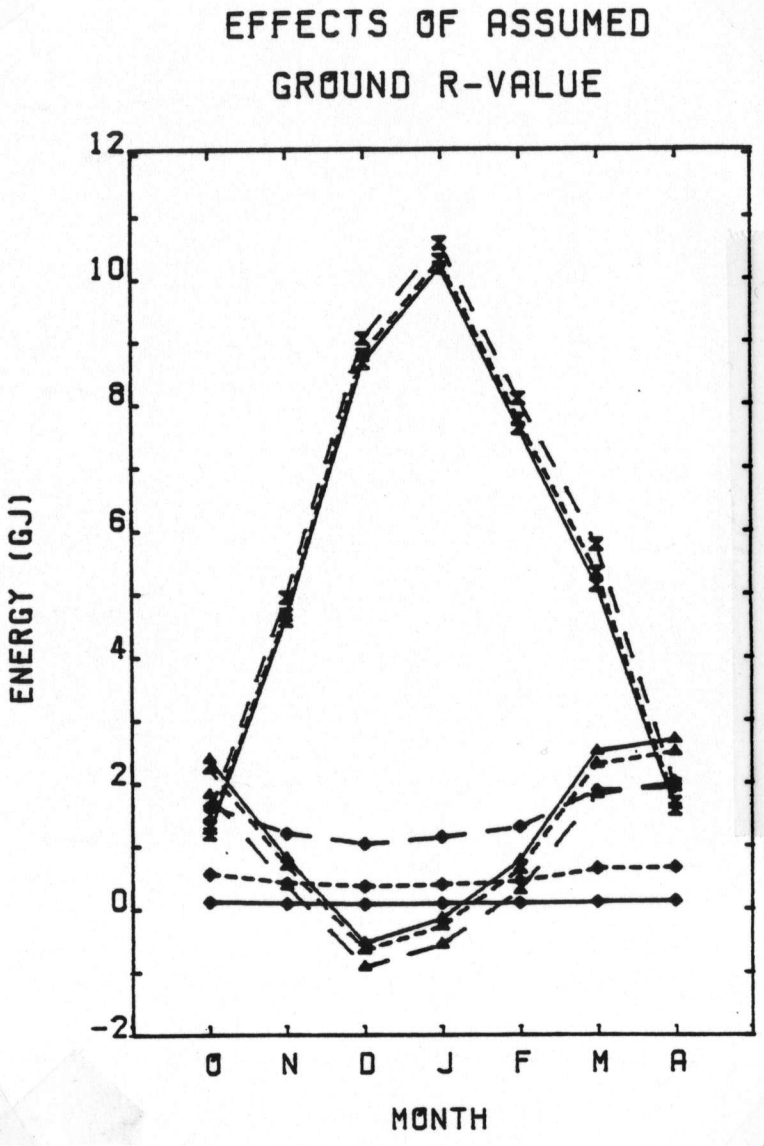

KEY FOR FIGURE 3.5

◆ HEAT LOSS THROUGH THE FLOOR

▲ HEAT DELIVERY OF THE SUNSPACE

⧗ BUILDING AUXILIARY HEAT

——— 7.05 M^2-C/W

----- 1.76

— — 0.44

3.3.3 Effects of Venting Control Strategy

One of the features of many sunspace designs is vents in the sunspace-building common wall. Sections 3.3.3 through 3.3.5 examine the effects of venting the sunspace air to the building.

One possible advantage of venting between the sunspace and the building is the energy flow can be somewhat controlled. If a building heating load exists and the sunspace air is warmer than the building air, dampers can be opened and a fan activated. If no building load exists, the dampers remain closed. This section examines the effects of various control strategies on the sunspace and building energy flows.

Vented sunspace system simulations for both masonry and insulated common walls for March in Madison, Wisconsin were performed for three different venting control strategies. March was selected for study because annual simulations of similar sunspaces show that the vented energy is a large proportion of the total sunspace energy delivery in the month of March. The control strategies are illustrated in Figure 3.6. The building auxiliary heating set point is 17.2 C and the cooling set point is 25.5 C. If the building load is such that the building temperature is outside these limits, the auxiliary heater or cooler is activated. A dead band setting of 1.5 C is used. The dead band limits thermostat control function oscillations by keeping the auxiliary component on until the building temperature is heated to 18.7 C or cooled to 24.0 C. The minimum solar source temperature is set at either 24.0 C or 21.5 C.

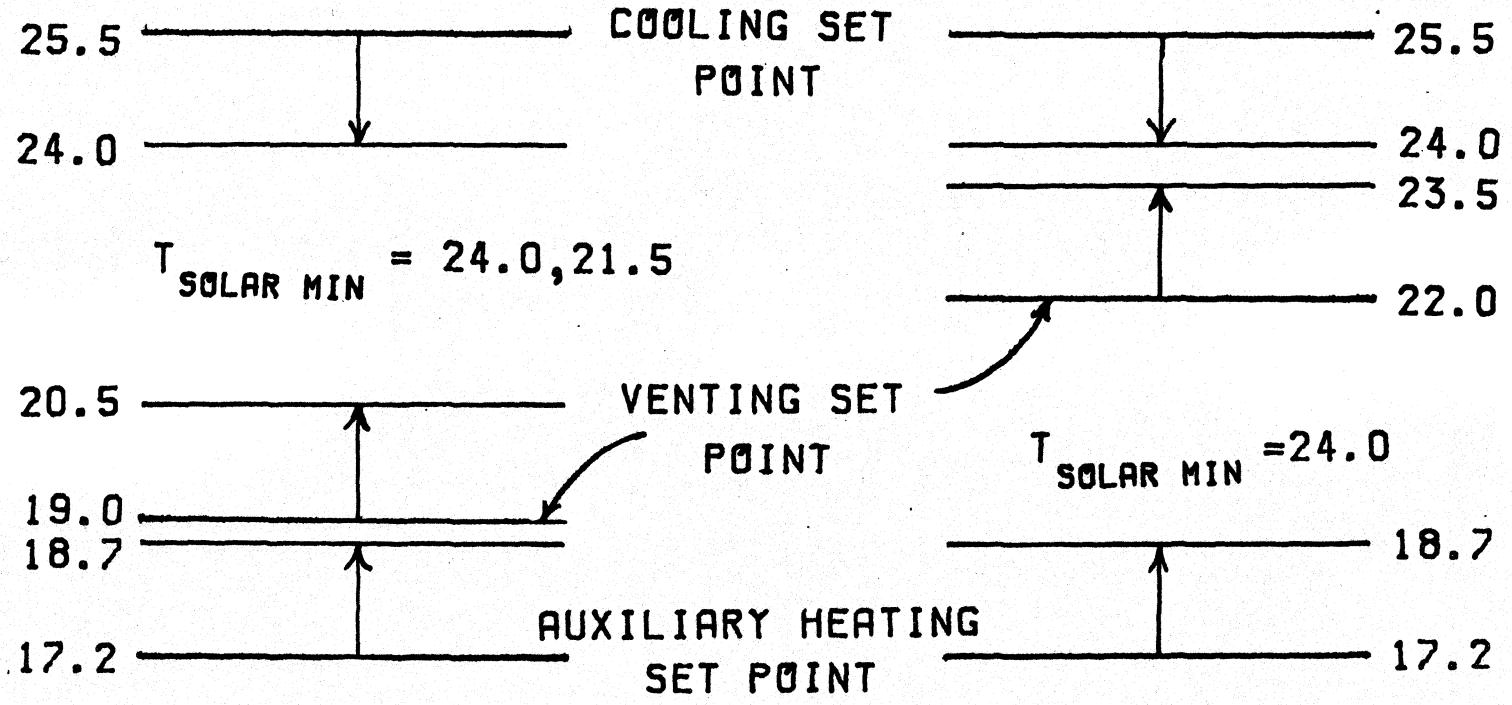

Figure 3.6 Venting Control Strategies

If the sunspace air temperature is below this value, no venting between the sunspace and building is allowed. If the sunspace air temperature is greater than the minimum solar source temperature, the solar set point is the minimum building temperature where the vent dampers remain closed. When the building temperature drops below this point the dampers are opened and the fan is activated. The dead band causes venting to continue (if the sunspace air remains above the minimum solar source temperature) until the building temperature is 1.5 C above the solar set point. Table 3.5 summarizes the other simulation characteristics.

Results from the six simulations are presented in Table 3.6. Lowering the minimum solar source temperature leads to more venting in a given month. The energy convected from the sunspace to the building through the vents increased by 0.161 GJ for the masonry common wall and 0.105 GJ for the insulated common wall. The total sunspace delivery, however, only rose by 0.055 MJ and 0.093 MJ respectively. Increased venting lowers the average wall temperature so less energy is conducted through the wall. This effect is most noticable in masonry walls, as a significant portion of the energy delivery of the sunspace is conducted through the wall. The auxiliary heating requirements of the systems diminished by only about 1 1/2 percent. The reasons that the auxiliary requirement is not reduced by the same amount that the sunspace delivery is increased are discussed in detail in the next section.

Table 3.5

Simulation Characteristics of Venting Control Strategy Study

Location: Madison, Wisconsin Month: March

Heat Transfer Coefficients (W/m^2 C)

glazing-to-ambient 2.8 + 3 V V: wind speed m/s

sunspace interior 17 (venting) 5.7 (not venting)

wall to building 8.3

Ground Temperature $(\overline{T}_{month} + \overline{T}_{year})/2$

Venting Rate 700 kg/hr

Building

Heat Loss Coefficient (UA) 158 W/°C

Capacitance 5000 KJ/°C

Auxiliary heating rate 26000 KJ/hr

Auxiliary cooling rate -12000 KJ/hr

Internal gains (see Table 3.4)

Common Wall

	masonry	frame
thickness	0.15 m	0.15 m
ρC_p	2009 $KJ/m^3°C$	280 $KJ/m^3°C$
Conductivity	1.73 W/m°C	0.045 W/m°C
Sunspace extra thermal mass capacitance	0	4453 KJ/°C

Table 3.6

Effects of Venting Control Strategy

Common Wall	Minimum Solar Source Temperature	Venting Set Temeprature	Vented Sunspace Delivery	Total Sunspace Delivery	Building Aux. Heating Req.
Masonry	24.0 °C	19.0 °C	0.845	2.772 GJ	4.797 GJ
Masonry	21.5	19.0	1.006	2.827	4.732
Masonry	24.0	22.0	1.295	2.916	4.836
Insulated	24.0	19.0	1.595	1.675	6.804
Insulated	21.5	19.0	1.697	1.768	6.706
Insulated	24.0	22.0	1.652	1.726	6.790

Raising the venting set temperature also augmented the vented energy delivery and total energy delivery of both systems. However, the masonry system auxiliary energy requirement rose slightly. Possible reasons for this are discussed in detail in the next section. The auxiliary energy requirement of the insulated wall system did not change by a significant amount.

The effects of changing the sunspace venting control scheme were minor in this study. Effects calculated from annual simulation results would be even less significant.

3.3.4 Effects of Venting for Masonry Common Wall Systems

The results of the previous section suggest that venting of the sunspace only slightly increases the energy delivery of masonry common wall sunspace systems, and the effect on building auxiliary energy is modest. A large heating season factorial design was devised to investigate further. An interaction between the interior convection coefficient and vented energy delivery is possible. If the coefficient is raised, more of the absorbed solar energy is transferred to the air and venting of the air may have a greater effect. Another variable included in the study was building thermal capacitance. For a given amount of energy input, a larger capacitance building will exhibit a smaller temperature change. Venting may continue for a longer period of time and may be more significant. Table 3.7 lists the relevant simulation characteristics and the level of the variables for a study of the effects on a system in Madison, Wisconsin.

Table 3.7

Characteristics of Masonry Wall Venting Study

Common Wall

thickness 0.15 m

ρC_p 2009 KJ/m^3 C

conductivity 1.73 W/m C

area 22.3 m^2

Venting Rate

0, 335, 2230 kg/hr

Interior Convection Coefficient

$\dot{m}$	-	+	
0	1.5	5.7	(W/m^2 C)
>0	5.7	16.0	

Building

Heat loss coefficient 158 W/°C

Internal gains: see Table 3.4

Thermal Capacitance: 5000, 25000 KJ/C

Total heating season energy quantities for the low-level (Table 3.7) sunspace interior convection coefficients are plotted in Figure 3.7. A similar plot for the high level convection coefficients is found in Figure 3.8. For reference, a simulation was performed with low-level convection coefficients and a house capacitance of 5000 KJ/C with no solar radiation input to the sunspace. The auxiliary heating requirement of the no-solar system was 56.6 GJ.

The general behavior of the sunspace is similar to that of vented collector storage walls, as described by Utzinger (2). An energy balance on the sunspace is:

$$Q_{abs} - Q_{env} - Q_{in} - Q_{store} = 0 \qquad 3.3.1$$

Q_{abs} is the absorbed solar energy, Q_{env} is the heat loss to the environment and includes loss to the ground and ambient air, Q_{in} is the energy delivery to the building, and Q_{store} is the energy stored in the massive elements of the sunspace. On an annual basis, Q_{store} is negligible. Venting of the sunspace air increases the sunspace interior convection coefficients by raising the air velocity across the surfaces. This tends to increase the losses to the environment. Venting also causes the wall and floor temperatures to decrease, which diminishes losses to the environment. The net effect is that losses to the environment go down slightly. As the amount of vented energy increases, the amount conducted through the wall declines. The net energy delivery is enhanced with larger air flow rates, especially in the high building capacitance cases.

Figure 3.7

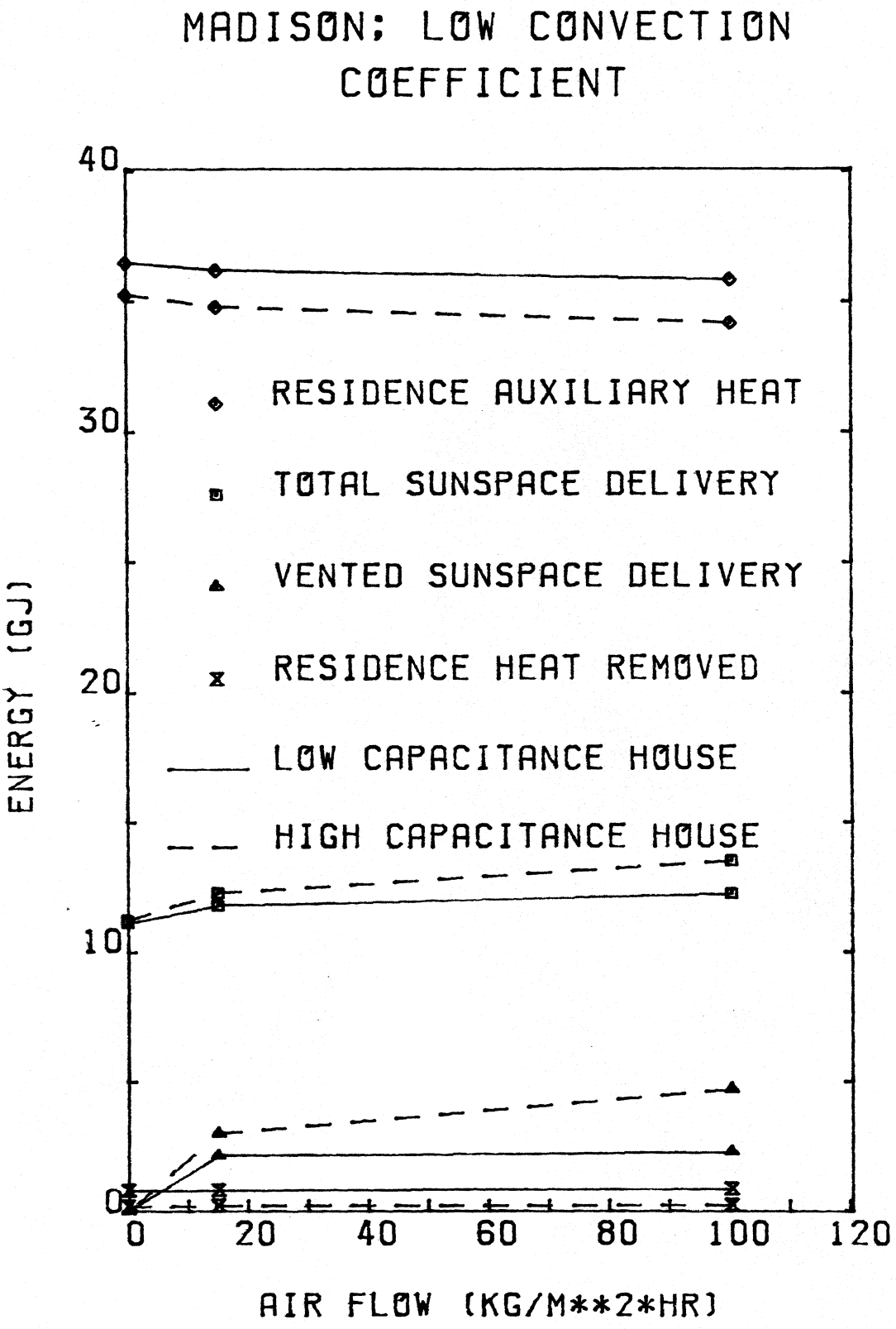
MADISON; LOW CONVECTION COEFFICIENT
ENERGY (GJ)
40
30
20
10
0
0
20
40
60
80
100
120
AIR FLOW (KG/M**2*HR)
RESIDENCE AUXILIARY HEAT
TOTAL SUNSPACE DELIVERY
VENTED SUNSPACE DELIVERY
RESIDENCE HEAT REMOVED
LOW CAPACITANCE HOUSE
HIGH CAPACITANCE HOUSE

Figure 3.8

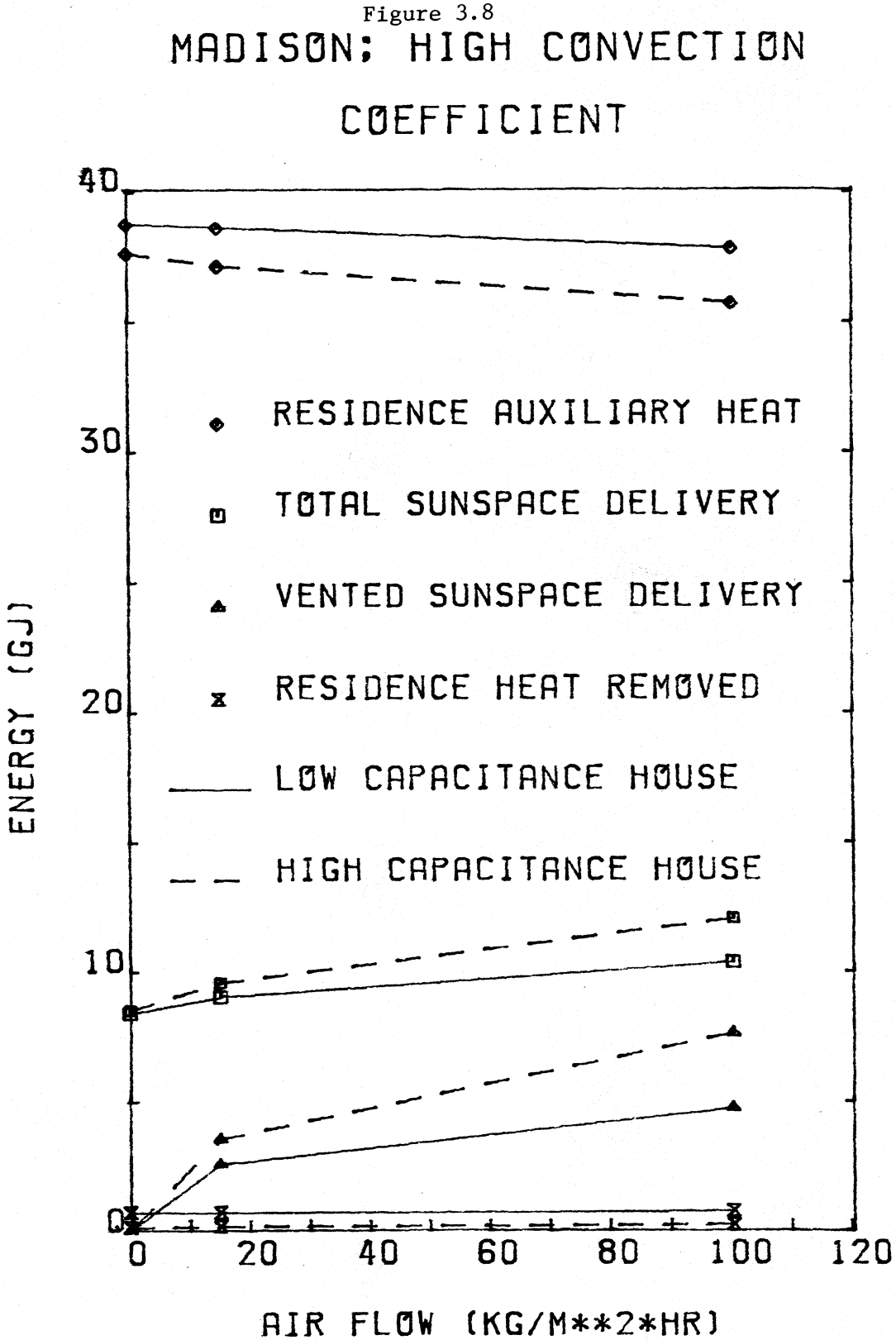
MADISON; HIGH CONVECTION COEFFICIENT
40
30
20
10
0
ENERGY (GJ)
RESIDENCE AUXILIARY HEAT
TOTAL SUNSPACE DELIVERY
VENTED SUNSPACE DELIVERY
RESIDENCE HEAT REMOVED
LOW CAPACITANCE HOUSE
HIGH CAPACITANCE HOUSE
0
20
40
60
80
100
120
AIR FLOW (KG/M**2*HR)

However, the building auxiliary energy is not reduced by the same amount. An energy balance on the building is:

$$Q_{in} + Q_{aux} - Q_{loss} - Q_{store} - Q_{cool} = 0 \qquad 3.3.2$$

Q_{aux} is the auxiliary heat, Q_{loss} is the building heat loss, and Q_{cool} is the heat removed from the building when the temperature rises above the cooling set point of 25.5 C. Q_{store}, the energy stored in the building as sensible heat, is negligible on an annual basis. In Madison, the heat removed from the building is relatively constant as venting air mass flow rate is varied. The energy loss from the building must increase as venting air mass flow rate is raised. Since the loss is directly proportional to the temperature difference, the average building temperature is higher when venting is allowed. On sunny, cold days venting of the sunspace air and auxiliary heat input can occur simultaneously. The building temperature is higher than it would have been if venting were not allowed. Therefore, the change in auxiliary heating requirement does not equal the increase in sunspace energy delivery as venting air mass flow rate is raised.

The different levels of the sunspace interior convection coefficients and the building capacitance have a significant effect on system performance. Higher sunspace interior convection coefficients increase the vented sunspace delivery, but the total delivery is diminished because of losses to the environment. This boosts the building auxiliary heating requirement. As expected, a higher

building thermal capacitance results in more energy delivery and a lower auxiliary heating requirement. Changes in energy quantities with vented air mass flow rate were also greater for the high building capacitance simulations than the low building capacitance simulations.

The above explanation prompted an examination of the effects of venting in other locations. Figure 3.9 is a plot of the results of simulations for a 25,000 KJ/C capacitance building in Albuquerque, New Mexico. A simulation with no solar radiation input, low interior convection coefficients, and a venting mass flow rate of zero had an auxiliary heating requirement of 33.84 GJ. The energy removed from the building to prevent overheating is substantial. Similar simulations with high interior convection coefficients in Nashville, Tennessee are plotted in Figure 3.10. The high coefficient levels were chosen because the effects on the auxiliary energy requirement are the greatest. Even so, the effects are similar to those of the Madison simulations. The venting air mass flow rate does not have a major effect on the building auxiliary energy consumption. This conclusion is similar to that of Utzinger (2) and Ohanessian (29) for collector-storage wall systems.

In the limit of a perfectly-insulated common wall, all the energy delivery of the sunspace must be transferred by convection through the vents. The above studies were of a relatively thin (0.15 m) masonry common wall. Effects of venting for thicker walls and for walls with different thermal characteristics may vary from

Figure 3.9

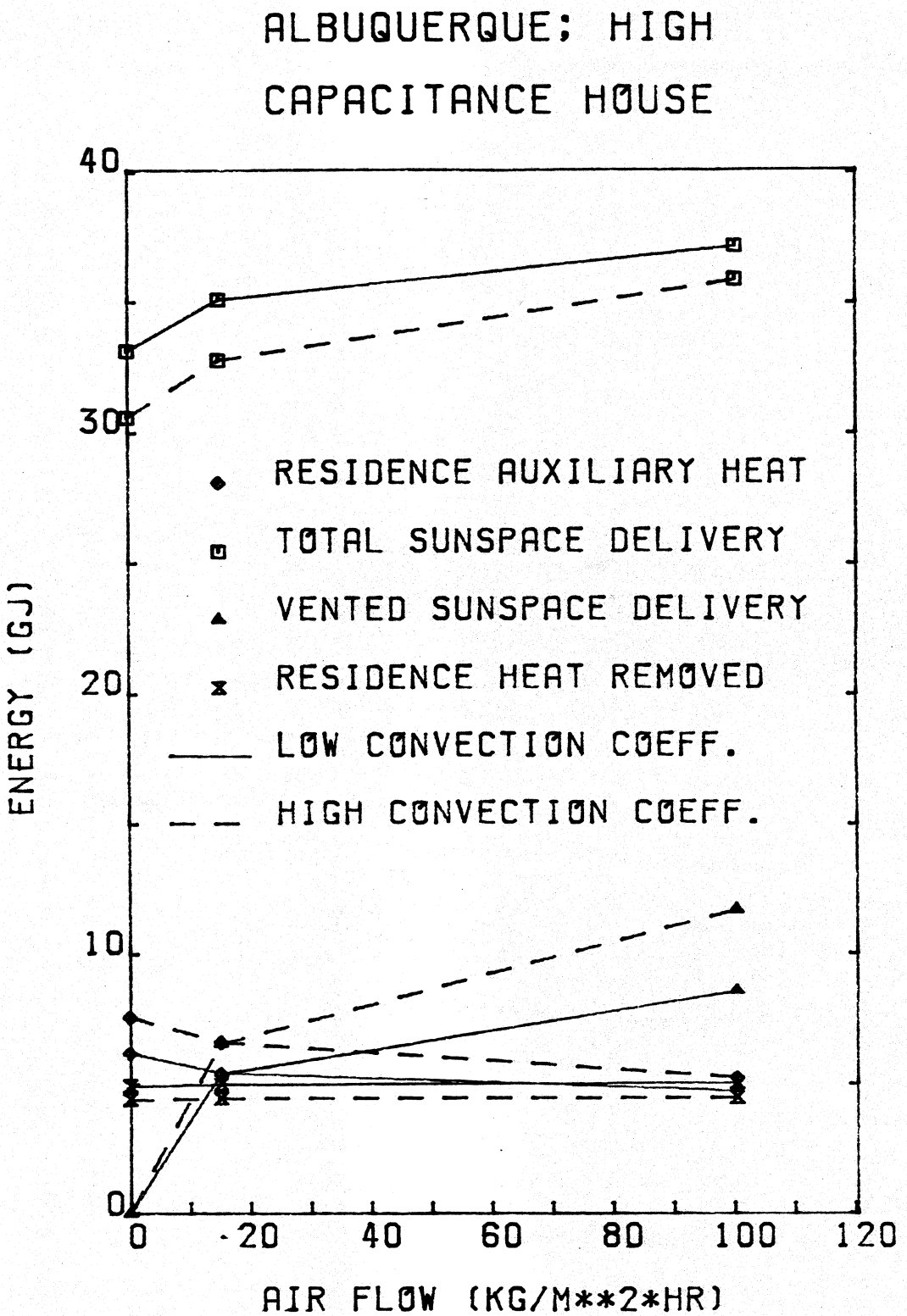
ALBUQUERQUE; HIGH CAPACITANCE HOUSE
ENERGY (GJ)
AIR FLOW (KG/M**2*HR)
RESIDENCE AUXILIARY HEAT
TOTAL SUNSPACE DELIVERY
VENTED SUNSPACE DELIVERY
RESIDENCE HEAT REMOVED
LOW CONVECTION COEFF.
HIGH CONVECTION COEFF.
0
10
20
30
40
0
20
40
60
80
100
120

Figure 3.10

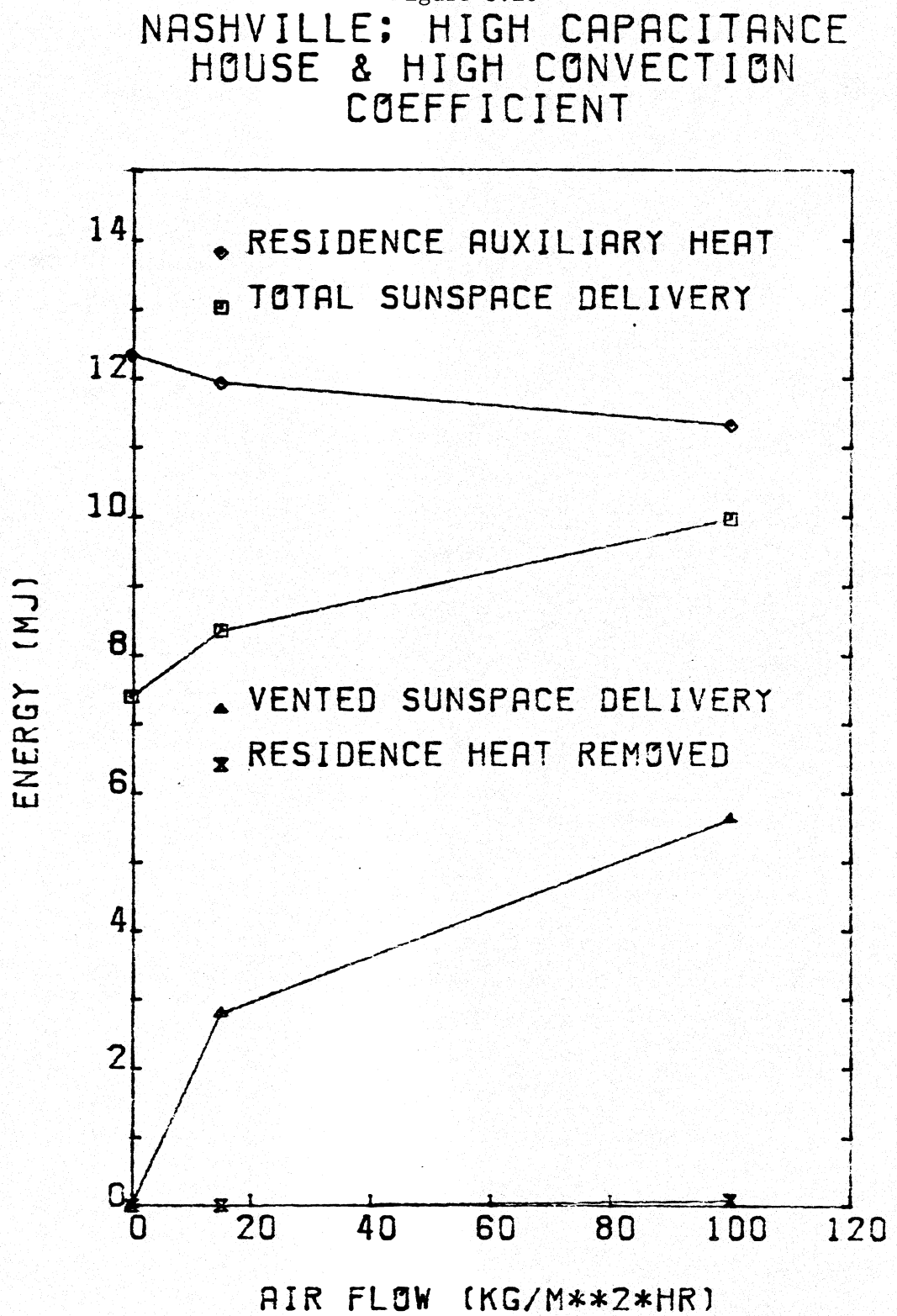
NASHVILLE; HIGH CAPACITANCE HOUSE & HIGH CONVECTION COEFFICIENT
RESIDENCE AUXILIARY HEAT
TOTAL SUNSPACE DELIVERY
VENTED SUNSPACE DELIVERY
RESIDENCE HEAT REMOVED
ENERGY (MJ)
0
2
4
6
8
10
12
14
0
20
40
60
80
100
120
AIR FLOW (KG/M**2*HR)

those discussed above. Typical thermal properties of various massive wall materials are listed in Table 3.8. A factorial design of various wall properties and thicknesses was developed to quantify these effects. Table 3.9 summarizes the simulation variables. The properties of the walls are not typical for masonry and adobe; instead, they represent the extremes.

Figures 3.11 and 3.12 are plots of the results. Venting has less effect on the auxiliary energy requirements of masonry common wall systems because the thermal conductivity of the wall is higher. The auxiliary requirements for unvented walls are less if the walls are thin because the thermal resistance of the wall is lower. However, for vented systems, the auxiliary energy is somewhat greater for thin walls. The useful delivered energy, that is, the total delivered energy minus the heat removed to prevent overheating, for the vented thick wall is larger than that of the thin wall.

3.3.5 Effects of Venting for Insulated Common Wall Systems

The effects of venting the sunspace air to the building for insulated common walls are quite different than the effects of venting for thermally-massive and conductive common walls. For insulated common walls, nearly all of the heat transferred from the sunspace to the building is convected through the vents. As a consequence, the mass flow rate of the air will have a large effect on energy delivery. Since the thermal storage capacity of the wall is low, sunspace temperatures vary over a broader range than masonry common wall systems. Many insulated common wall sunspace designs

Table 3.8

Thermal Properties of Various Massive Wall Materials

Material	Solar Absorbtance	ρC_p (KJ/m^3 C)	k (W/m C)
masonry	0.65 - 0.93	2000 - 2200	1.73
brick	0.6 - 0.9	1500 - 1700	0.935
adobe	~ 0.8	~1600	0.575
water	-	4190	0.60

Table 3.9

Simulation Characteristics for the Study of
Wall Properties and Venting

Location: Albuquerque, NM

Common Wall

Material	ρC_p (KJ/m^3 C)	conductivity (W/m C)
masonry	3000	2.0
adobe	1200	0.5
thickness	0.1 m	1.0 m

Venting mass flow rate (kg/hr) 0, 1800

Interior convection coefficients

$\dot{m}$	0	>0
h (W/m^2 C)	5	15

Building

UA 158 W/°C

Capacitance 5000 KJ/°C

no internal gains

Figure 3.11

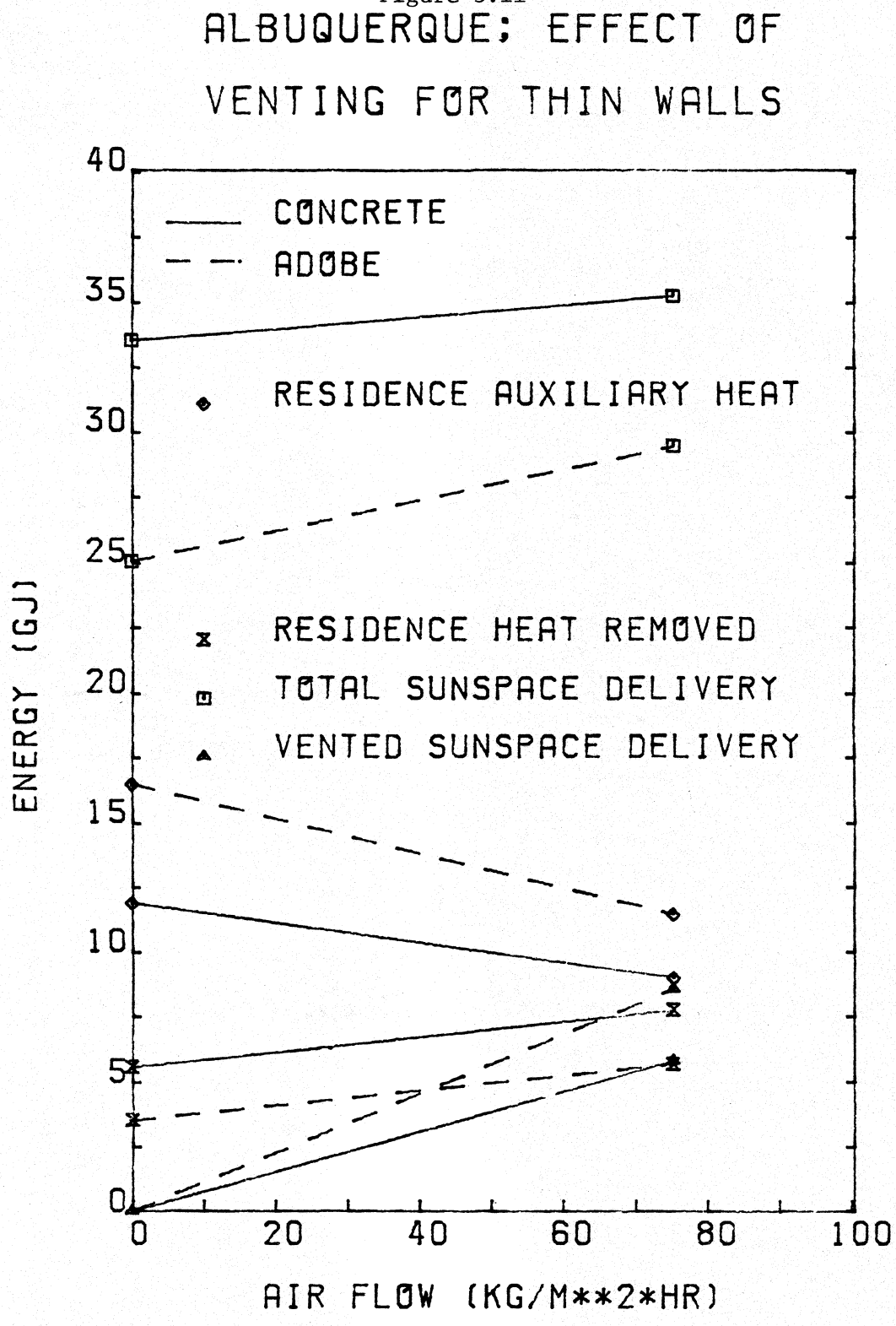
ALBUQUERQUE; EFFECT OF VENTING FOR THIN WALLS
CONCRETE
ADOBE
RESIDENCE AUXILIARY HEAT
RESIDENCE HEAT REMOVED
TOTAL SUNSPACE DELIVERY
VENTED SUNSPACE DELIVERY
ENERGY (GJ)
AIR FLOW (KG/M**2*HR)
0
5
10
15
20
25
30
35
40
0
20
40
60
80
100

Figure 3.12

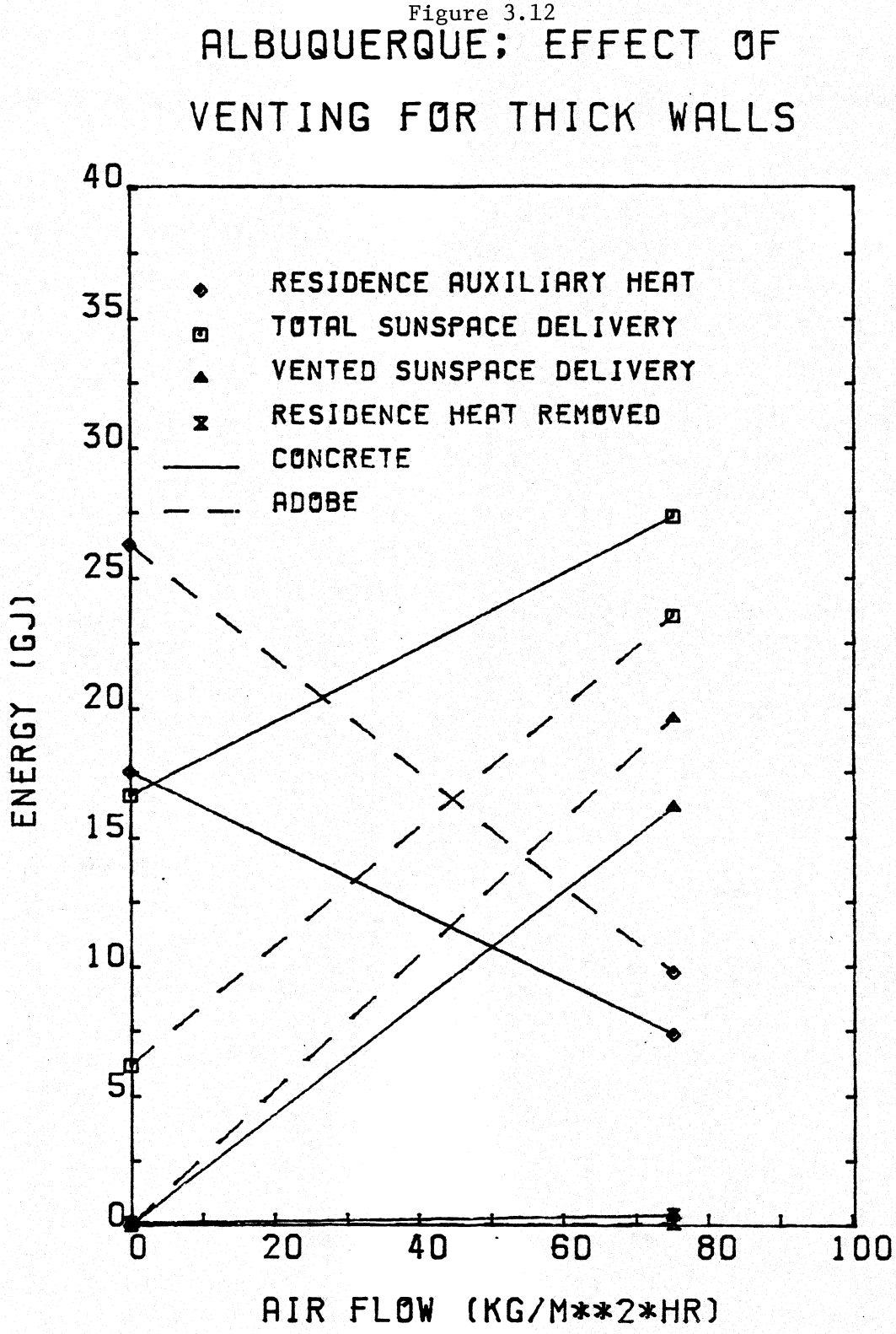
ALBUQUERQUE; EFFECT OF VENTING FOR THICK WALLS
RESIDENCE AUXILIARY HEAT
TOTAL SUNSPACE DELIVERY
VENTED SUNSPACE DELIVERY
RESIDENCE HEAT REMOVED
CONCRETE
ADOBE
ENERGY (GJ)
0
5
10
15
20
25
30
35
40
0
20
40
60
80
100
AIR FLOW (KG/M**2*HR)

include additional thermal storage devices in the sunspace to dampen the air temperature fluctuations. As in the masonry wall studies, the thermal storage capacity of the adjacent building also affects performance. A factorial design was performed for an insulated common wall sunspace system to examine these effects. The variables are the venting air mass flow rate, the capacity of the sunspace extra thermal storage devices, the building thermal storage capacity, and the sunspace interior convection coefficients. The levels of the variables and other simulation characteristics are found in Table 3.10. The high level of the additional sunspace thermal storage capacity corresponds with 55-gallon drums standing on end against the back wall, running the full length of the sunspace.

Results are plotted in Figures 3.13 and 3.14. Comparing the two Figures indicates that the sunspace interior convection coefficient does not greatly affect the sunspace performance. A larger convection coefficient leads to only slightly lower building auxiliary energy requirements. Including extra thermal mass in the sunspace does dampen sunspace temperature fluctuations as shown in Figure 3.15. Here the sunspace air temperature distributions of the low capacitance building with low sunspace interior convection coefficients are compared for the month of March, with a venting air mass flow rate of 1115 kg/hr. However, the increased thermal mass causes a slight decline in the performance of the sunspace system by boosting the nighttime sunspace temperature and increasing losses to the environment. As with masonry common wall systems, the per-

Table 3.10

Simulation Characteristics for the Study of Insulated Common Walls and Venting

	Common wall	floor
ρC_p (KJ/m^3 C)	280	2009
conductivity (W/m C)	0.045	1.73
thickness (m)	0.15	0.15
α	0.75	0.75
ε	0.9	0.9

Venting mass flow rate (kg/hr) 0, 223, 1115, 2230

Sunspace extra thermal mass (KJ/C) 0, 17810

Sunspace interior convection coefficients (W/m^2 C)

$\dot{m}$	-	+
0	1.5	5.7
>0	5.7	17.0

Building

UA 158 W/C

Capacitance (KJ/C) 5000, 25000

Internal gains see Table 3.4.

Figure 3.13

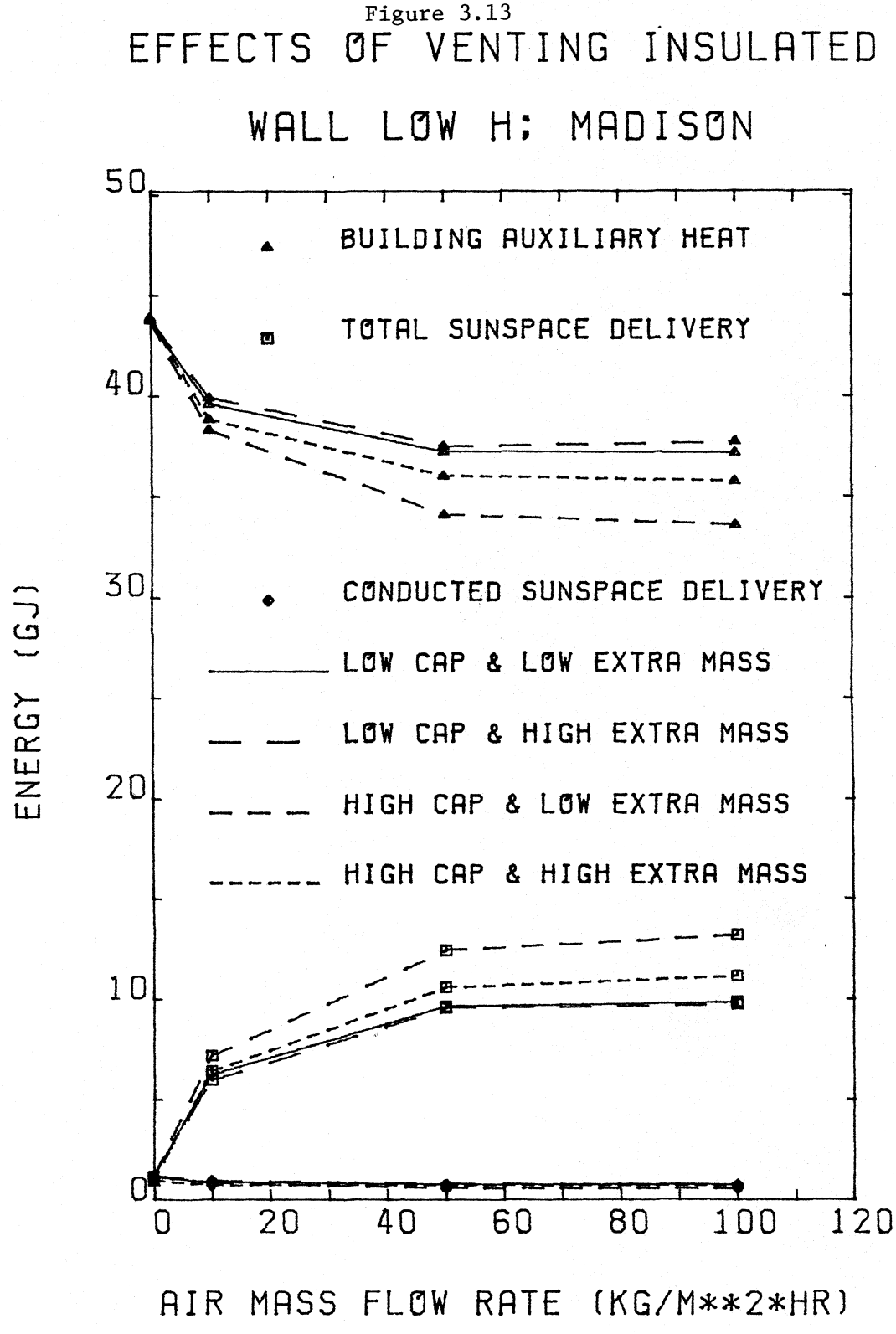
EFFECTS OF VENTING INSULATED
WALL LOW H: MADISON
BUILDING AUXILIARY HEAT
TOTAL SUNSPACE DELIVERY
CONDUCTED SUNSPACE DELIVERY
LOW CAP & LOW EXTRA MASS
LOW CAP & HIGH EXTRA MASS
HIGH CAP & LOW EXTRA MASS
HIGH CAP & HIGH EXTRA MASS
ENERGY (GJ)
0
10
20
30
40
50
0
20
40
60
80
100
120
AIR MASS FLOW RATE (KG/M**2*HR)

Figure 3.14

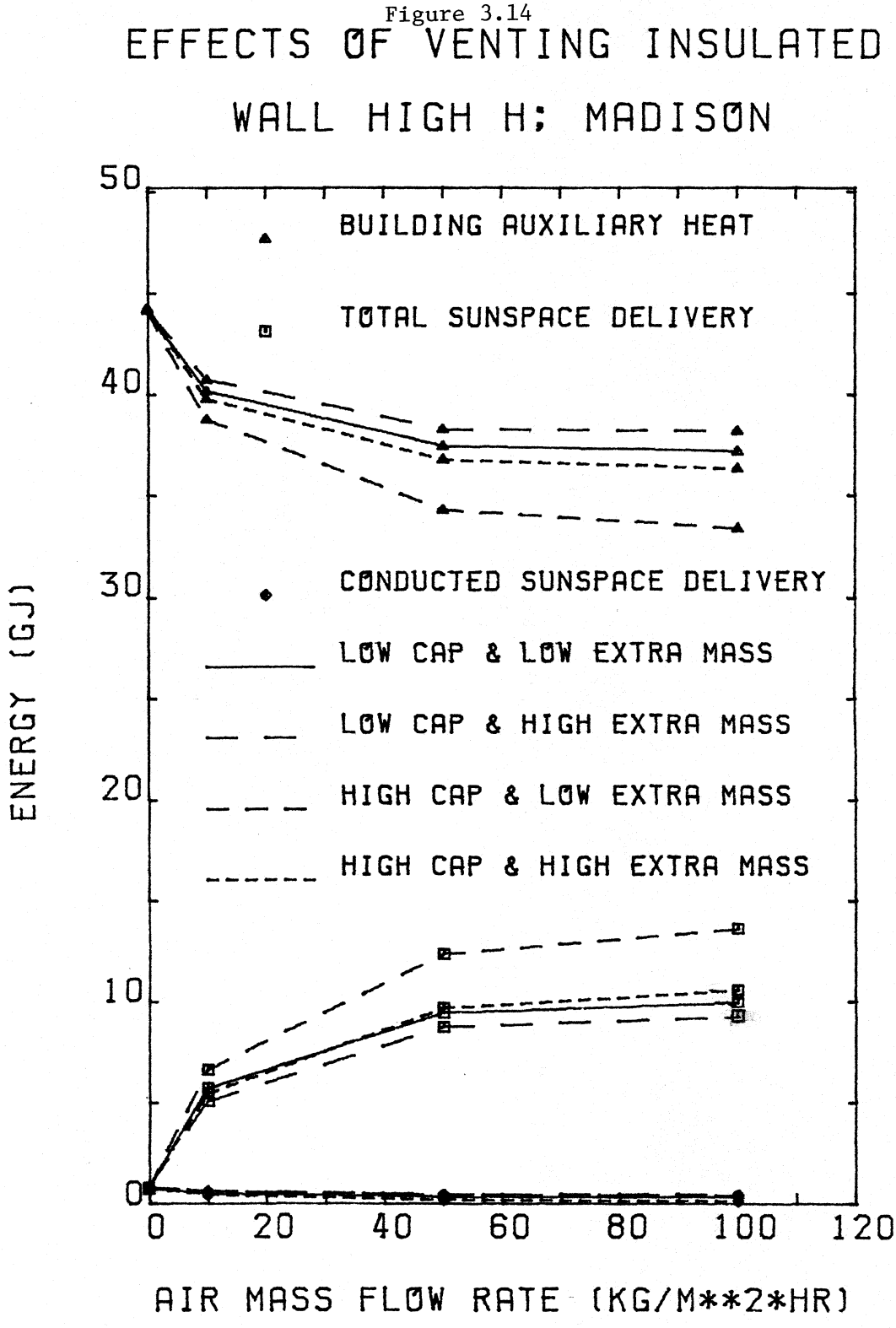
EFFECTS OF VENTING INSULATED WALL HIGH H; MADISON
BUILDING AUXILIARY HEAT
TOTAL SUNSPACE DELIVERY
CONDUCTED SUNSPACE DELIVERY
LOW CAP & LOW EXTRA MASS
LOW CAP & HIGH EXTRA MASS
HIGH CAP & LOW EXTRA MASS
HIGH CAP & HIGH EXTRA MASS
ENERGY (GJ)
0
10
20
30
40
50
0
20
40
60
80
100
120
AIR MASS FLOW RATE (KG/M**2*HR)

Figure 3.15

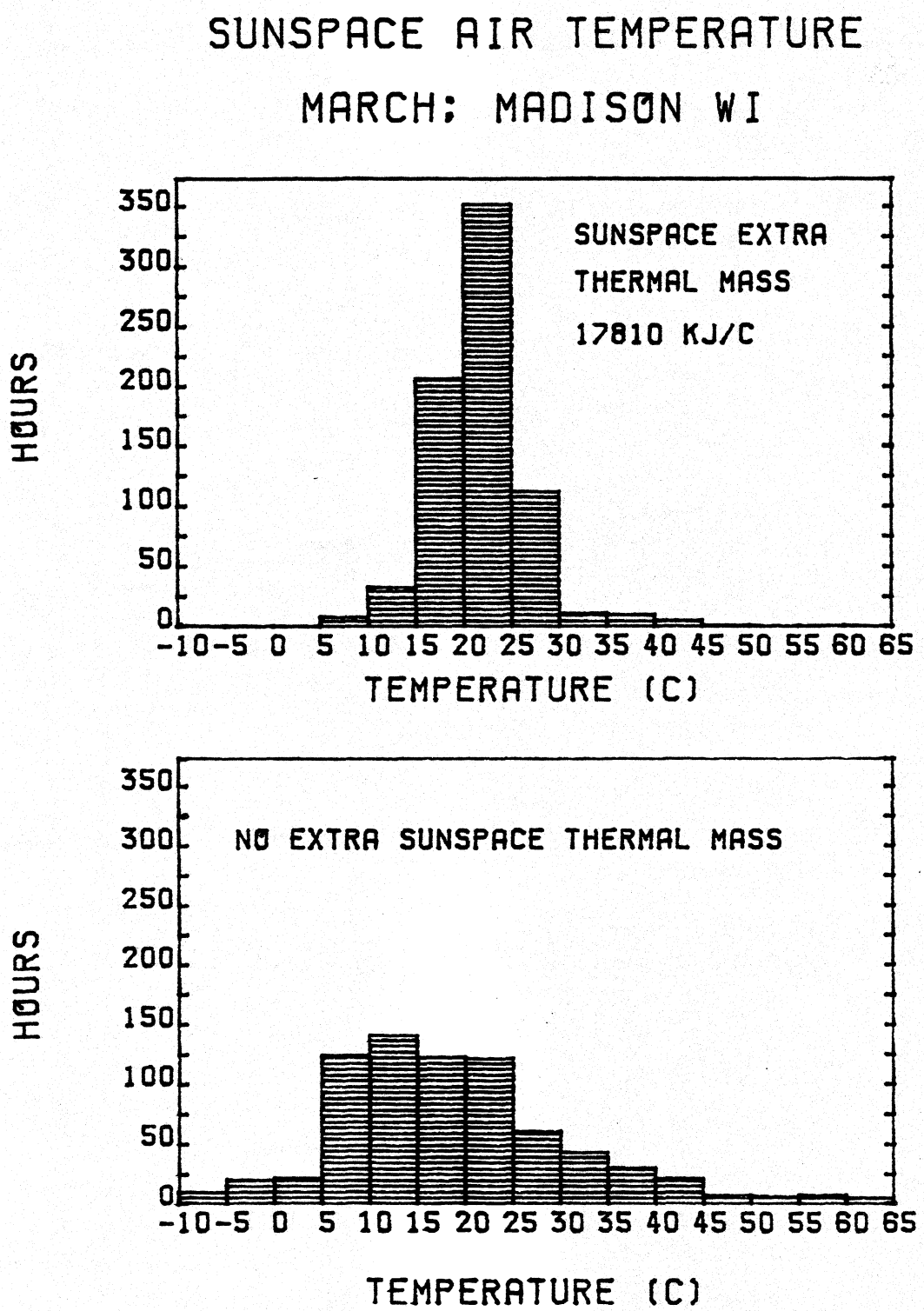
SUNSPACE AIR TEMPERATURE
MARCH: MADISON WI
SUNSPACE EXTRA
THERMAL MASS
17810 KJ/C
HOURS
350
300
250
200
150
100
50
0
-10 -5 0 5 10 15 20 25 30 35 40 45 50 55 60 65
TEMPERATURE (C)
NO EXTRA SUNSPACE THERMAL MASS
HOURS
350
300
250
200
150
100
50
0
-10 -5 0 5 10 15 20 25 30 35 40 45 50 55 60 65
TEMPERATURE (C)

formance of the system is enhanced by increasing the building thermal capacitance. A large interaction effect between building thermal capacitance and the presence of extra thermal storage devices in the sunspace is also apparent. Raising the building capacitance allows more energy to be vented to the adjacent structure, and building energy losses abate due to a lower average building temperature. A low level of thermal storage in the sunspace causes the sunspace air temperature to rise above the minimum solar source temperature frequently. Combining these two effects leads to significant gains in the total time that venting takes place.

Increasing the venting air mass flow rate improves the sunspace performance considerably. The figures also illustrate that very little energy is conducted through the wall since the delivery is very low for a venting mass flow rate of zero. At higher mass flow rates the sunspace delivery begins to level off. At some point the increase in sunspace energy delivery is overshadowed by heightened parasitic power requirements of the venting fan.

Comparing the results of Figures 3.13 and 3.14 for insulated common wall systems with high venting mass flow rates (30 to 60 air changes per hour) to the results of Figures 3.7 and 3.8 for masonry common wall systems shows that the annual auxiliary heating requirements are similar. Masonry common wall systems deliver more energy to the building during daylight hours but nighttime losses are substantial. Insulated common wall systems, however, have lower daytime delivery and very small nighttime losses. It is interesting that, at

least in this case, the net effect produces nearly identical auxiliary heating requirements.

3.3.6 Effects of Limiting the Sunspace Air Temperature

Many manufacturers and installers of sunspaces emphasize benefits other than building auxiliary energy reduction. Extension of the local growing season or use as a sunroom are viable uses of the sunspace. These uses may place restrictions on the sunspace air temperature. Most plants can survive nighttime temperatures near freezing, but vegetable production and growth decline dramatically as the minimum temperature goes down (30). Recommended minimum temperatures for vegetable production range from 4.4 C for cool season vegetables such as broccoli and spinach to 18.3 C for warm season vegetables such as tomatoes and peppers. In addition, maximum daytime temperatures should optimally not exceed 32.2 C.

Sunspace temperatures frequently exceed these bounds. Uncontrolled sunspaces have air temperatures much greater than 32 C during much of the summer. This overheating may also have a large impact on building air-conditioning loads. The ambient temperature is usually less than the sunspace air temperature, so overheating can be reduced by venting the sunspace air to the environment. Summer overheating is examined in Section 3.3.7.

Vegetable production in residential attached sunspaces is usually accomplished during colder months. Maintaining plant compatible temperature levels during the winter requires additional heat input to the sunspace in many cases. The auxiliary heat re-

quired by the sunspace may be provided by an additional heating system, such as a small electrical resistance heater in the sunspace, or by venting warm building air to the solar greenhouse. This addition of auxiliary heat to the sunspace affects the sunspace delivery and adds to heating fuel costs. Use of removable nighttime insulation on the glazing is helpful in reducing the sunspace auxiliary heat requirements and augmenting energy delivery.

Simulation of single and double-glazed sunspaces both with and without nighttime insulation were performed in Madison, Wisconsin for various minimum sunspace temperature requirements. The simulation characteristics are presented in Table 3.11. Total monthly energy quantities are plotted in Figures 3.16a and b for single-glazed systems and Figures 3.17a and b for double-glazed systems.

The use of night insulation decreases both the building auxiliary heat load and the amount of energy required to maintain minimum sunspace temperatures, especially for the single-glazed systems. Adding another glazing sheet to single-glazed systems has the same effect. Significant amounts of energy must be supplied to the single-glazed sunspace with no night insulation, simply to maintain a minimum temperature of 4.4 C. Use of night insulation or double glazing kept the sunspace air temperature above 4.4 C nearly all winter without additional sunspace heat. If additional sunspace heat is required, not all of this heat is lost to the environment. Increasing the sunspace temperature heightens energy delivery to the adjoining building and lessens the building heating requirements.

Table 3.11

Simulation Characteristics for the Study of Minimum Sunspace Temperature

Location: Madison, WI

Common Wall	Building
thickness 0.15	UA 158 W/m C
ρC_p 2009 KJ/m^3 C	capacitance 5000 KJ/C
conductivity 1.73 W/m C	no internal gains

Night insulation 1.59 m^2 C/W (R-9)

glazing R-value: single glazing 0 double glazing 0.22 m^2 C/W

venting air mass flow rate 1115 kg/hr

maximum sunspace temperature 32.2 C

minimum sunspace temperatures

none, 4.4, 11.3, 18.3 C

interior sunspace convection coefficients

$\dot{m}$	0	>0
h (W/m^2 C)	4	10

Minimum solar source venting temperature 24°C

Building venting set point 20°C

Building auxiliary heating set point 17.2°C

KEY FOR MINIMUM SUNSPACE TEMPERATURE PLOTS

▲ BUILDING AUXILIARY HEAT

◆ TOTAL SUNSPACE DELIVERY

■ SUNSPACE AUXILIARY HEAT

⧗ SUNSPACE HEAT REMOVED

Figure 3.16a

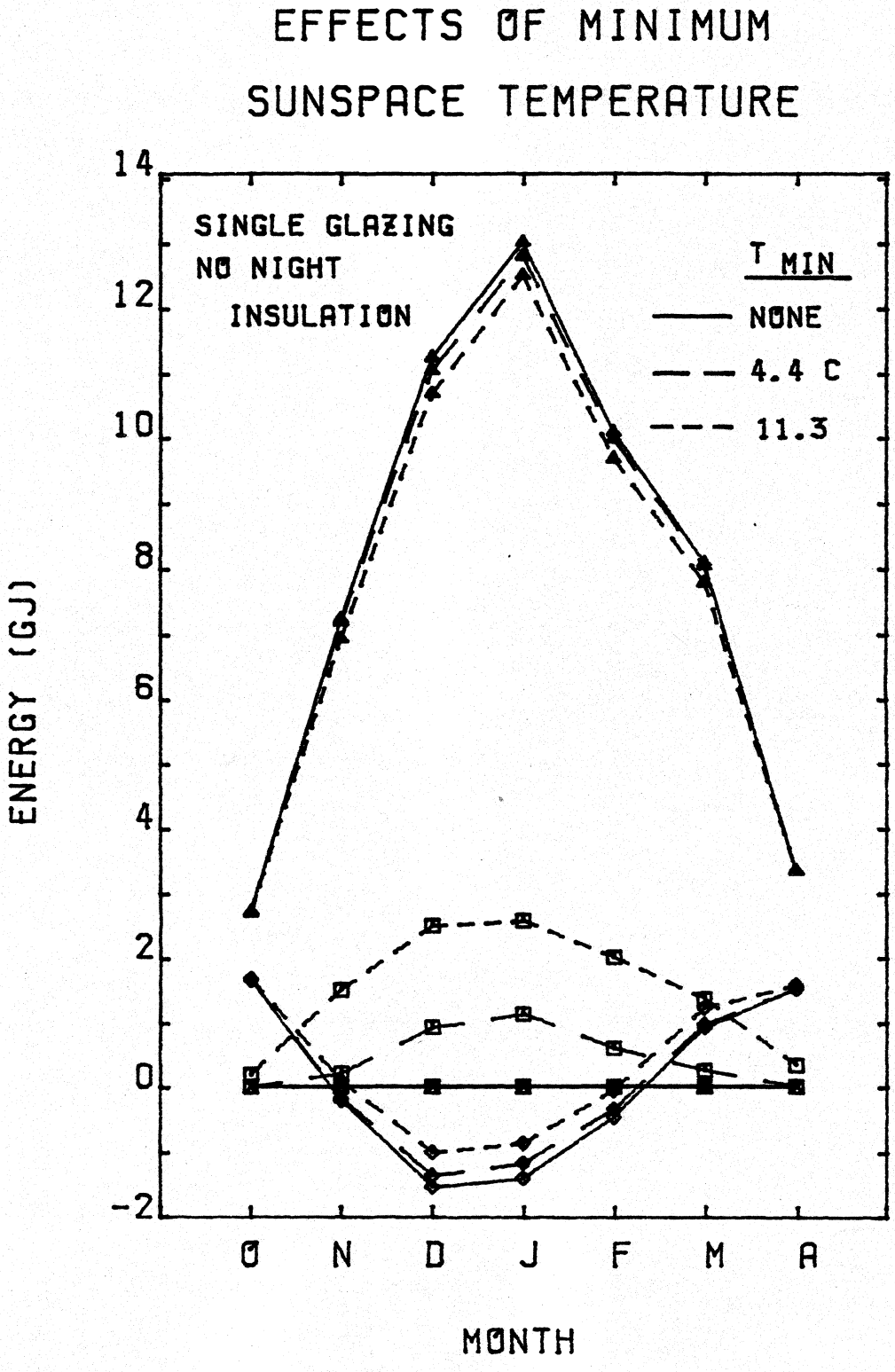
EFFECTS OF MINIMUM
SUNSPACE TEMPERATURE
SINGLE GLAZING
NO NIGHT
INSULATION
T MIN
NONE
4.4 C
11.3
ENERGY (GJ)
14
12
10
8
6
4
2
0
-2
O
N
D
J
F
M
A
MONTH

Figure 3.16b

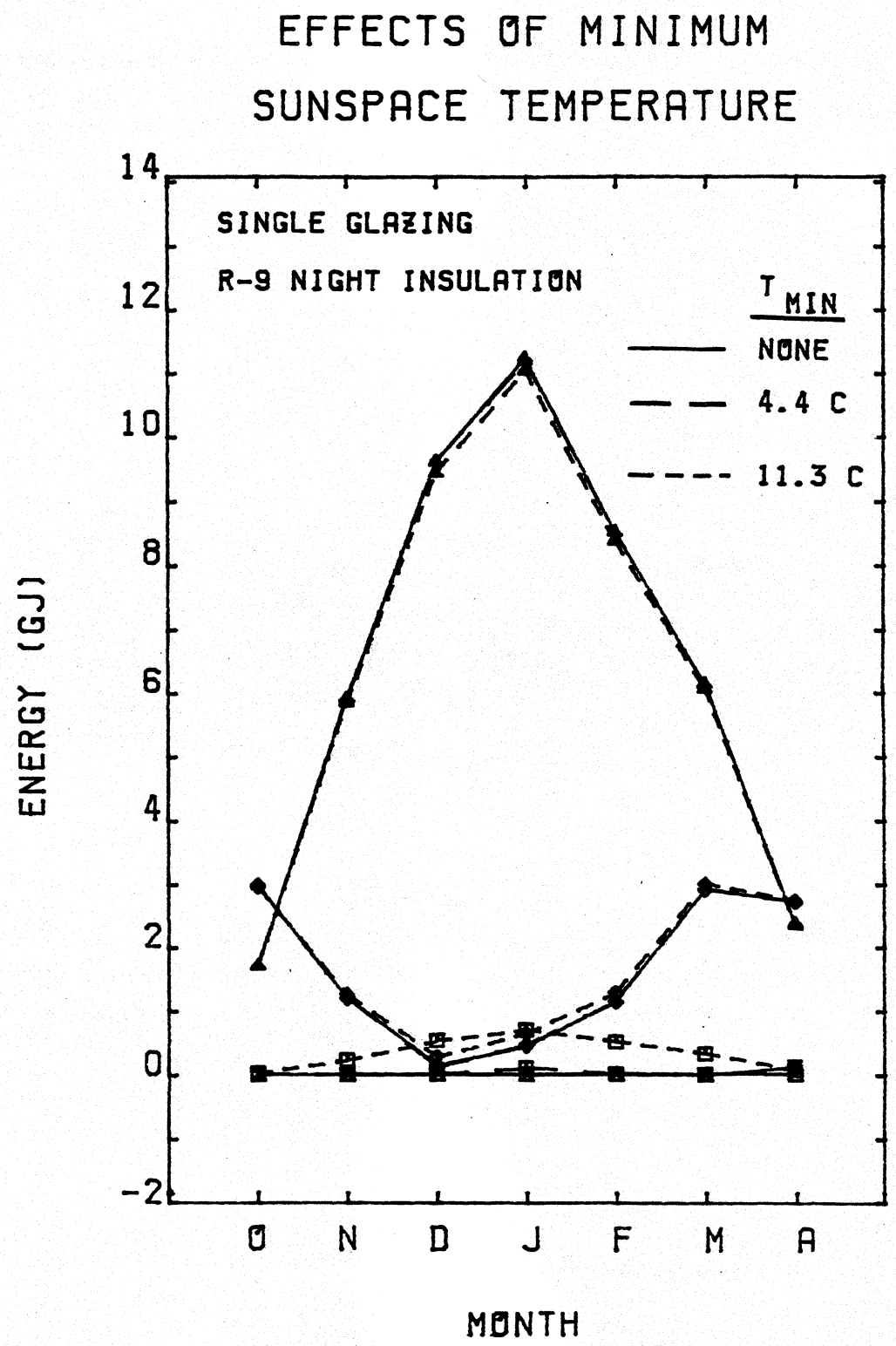
EFFECTS OF MINIMUM
SUNSPACE TEMPERATURE
SINGLE GLAZING
R-9 NIGHT INSULATION
T MIN
NONE
4.4 C
11.3 C
ENERGY (GJ)
14
12
10
8
6
4
2
0
-2
O
N
D
J
F
M
A
MONTH

Figure 3.17a

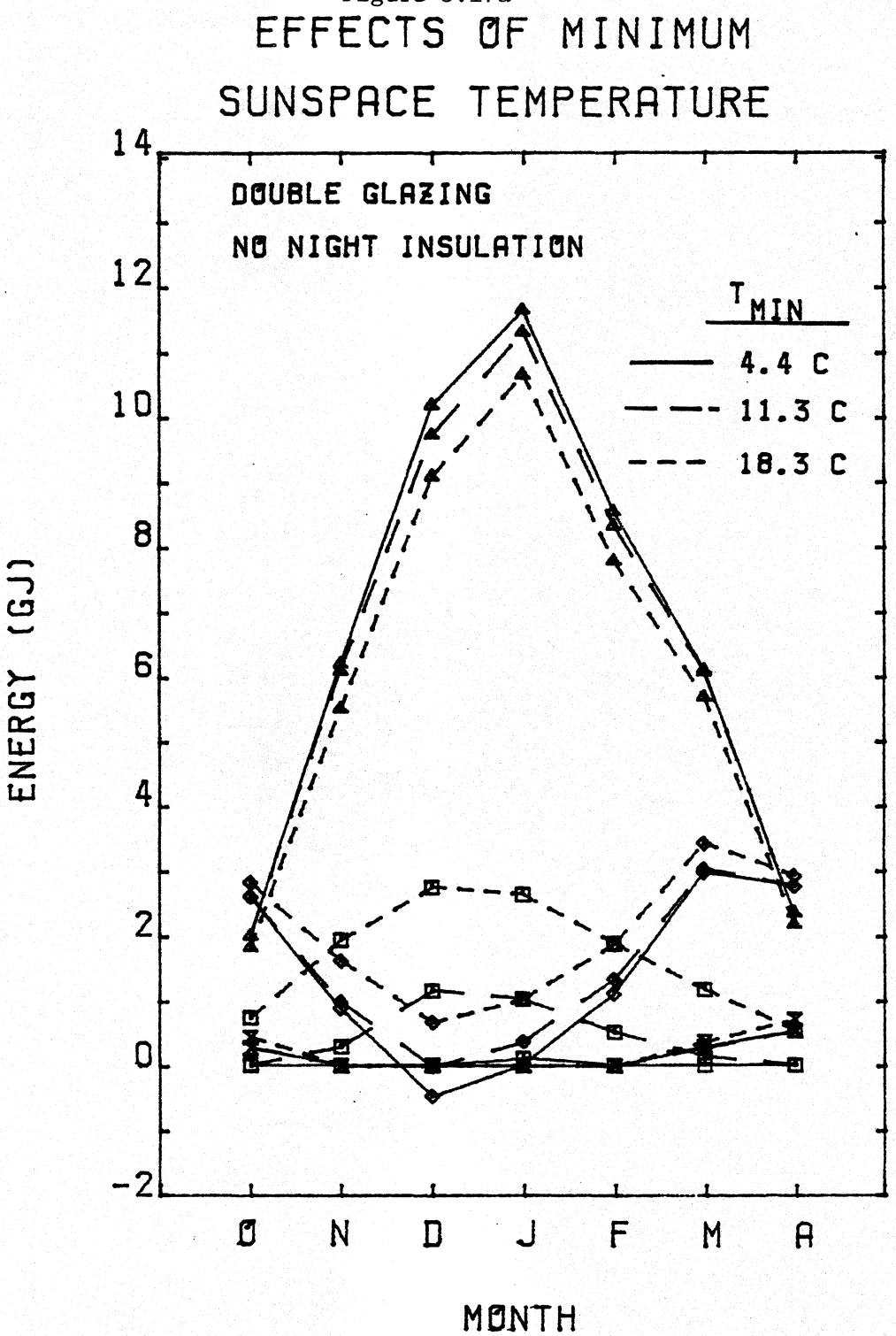
EFFECTS OF MINIMUM
SUNSPACE TEMPERATURE
DOUBLE GLAZING
NO NIGHT INSULATION
T MIN
4.4 C
11.3 C
18.3 C
ENERGY (GJ)
14
12
10
8
6
4
2
0
-2
O
N
D
J
F
M
A
MONTH

Figure 3.17b

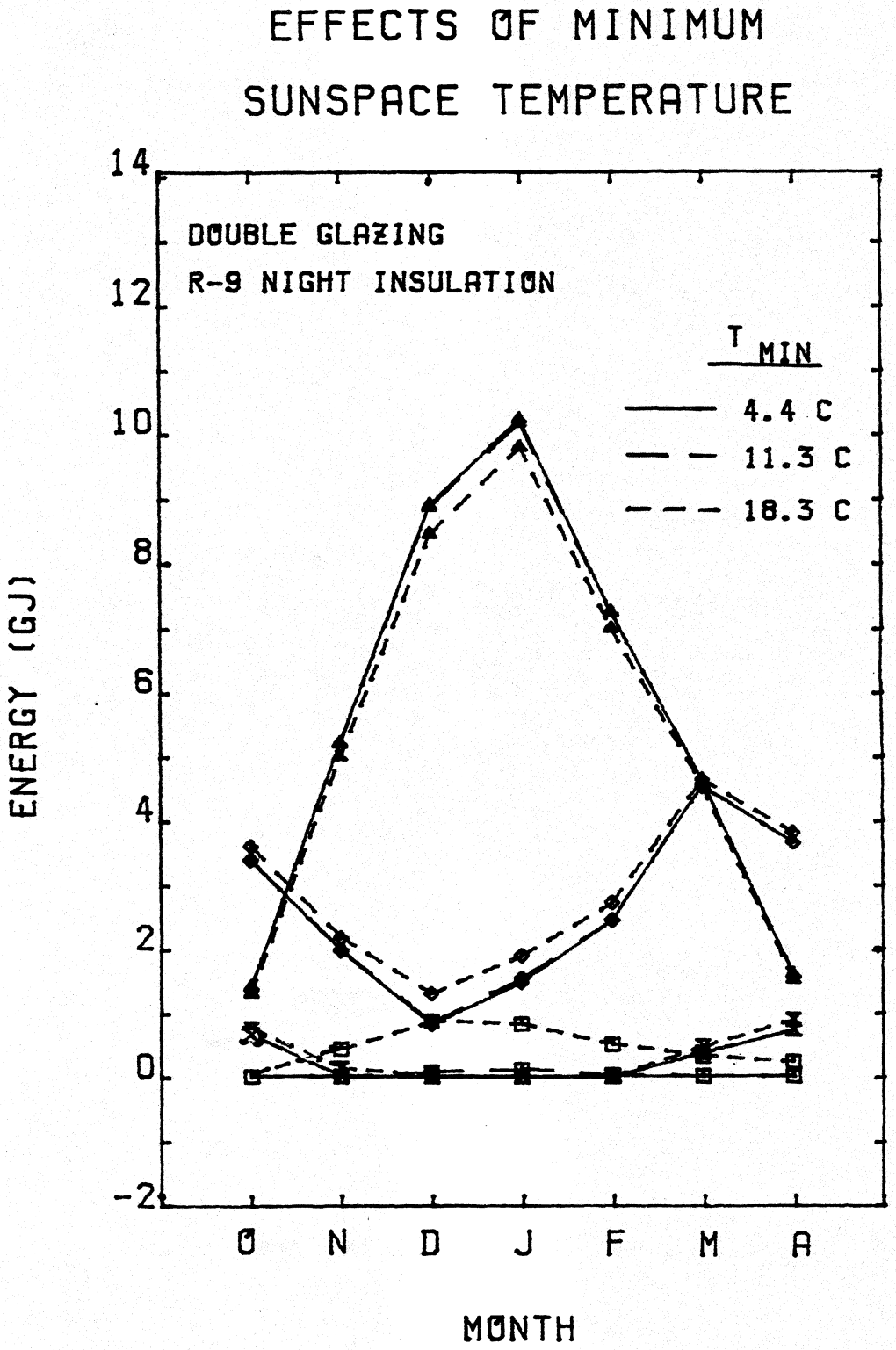
EFFECTS OF MINIMUM
SUNSPACE TEMPERATURE
DOUBLE GLAZING
R-9 NIGHT INSULATION
T MIN
4.4 C
11.3 C
18.3 C
ENERGY (GJ)
14
12
10
8
6
4
2
0
-2
O
N
D
J
F
M
A
MONTH

For the double-glazed sunspaces, some heat must be removed from the sunspace to prevent overheating in October, March and April. One additional fact worth noting is that the performance of the single-glazed system with night insulation is very similar to that of the double-glazed system without night insulation.

These studies show that maintenance of plant compatible temperature levels can significantly add to the overall heat requirements of some building-sunspace systems. Use of additional sunspace thermal storage devices may also be useful in this context, especially for insulated common wall systems.

In some locations, raising the minimum sunspace temperature is not enough to insure plant productivity. Solar radiation intensity and duration can also be limiting factors. Of course, artificial lighting may be provided to make up the difference, but this will not be examined as plant light requirements vary widely. The TRNSYS sunspace component can be used to examine specific situations by including the light power consumption in the sunspace auxiliary heating rate. For most situations, the effect of additional lighting on the thermal performance will be small.

3.3.7 Summer Cooling Considerations

All of the results presented up to this point are for simulations of the building heating season, October to April. Although the primary focus of this thesis is the use of sunspaces to reduce auxiliary heating requirements, the effect on building summer cooling will be briefly examined in this section.

The effect of the sunspace on the building cooling loads is very dependent on the characteristics of the common wall. Systems with insulated common walls should not have a significant effect on building cooling loads, while systems with conductive walls will have a major effect. Venting of the sunspace air to the environment will reduce the sunspace temperatures and cut down on the additional cooling load. Whitewashing the glazings or using shading devices reduces the solar energy entering the sunspace, which also diminishes the additional cooling load.

Simulations to examine summer cooling load effects were performed for two locations, Albuquerque and Nashville. It should be noted the cooling load calculations do not include latent cooling loads and that the cooling degree-hour calculations used may be in error in some cases (for example, see the TRNSYS manual (10)). Simulations were performed for a masonry common wall system with various sunspace-to-ambient venting rates. Simulations with no solar input and 50% shading were also performed for comparison. Two insulated common wall simulations were performed for each location; one with no solar input and one with solar but with no cooling strategy. The characteristics of the simulations are summarized in Table 3.12.

Total energy quantities and the average sunspace air temperature are plotted in Figure 3.18 for the vented masonry wall systems. Results for the other systems are shown on Table 3.13.

Table 3.12

Simulation Characteristics for the Summer Cooling Study

Location: Albuquerque, NM and Nashville, TN

Common wall	masonry	insulated
thickness (m)	0.15	0.15
ρC_p (KJ/m^3 C)	2009	280
conductivity (W/m C)	1.73	0.045

Double glazing, R-value 0.22 m^2-C/W

Venting mass flow rates (kg/hr) 0, 223, 1115, 2230

Building

UA 158 W/C

Capacitance 5000 KJ/C

Internal gains: see Table 3.4

Sunspace venting to ambient set point 32.2 C

Building cooling set point 25.5 C

Figure 3.18

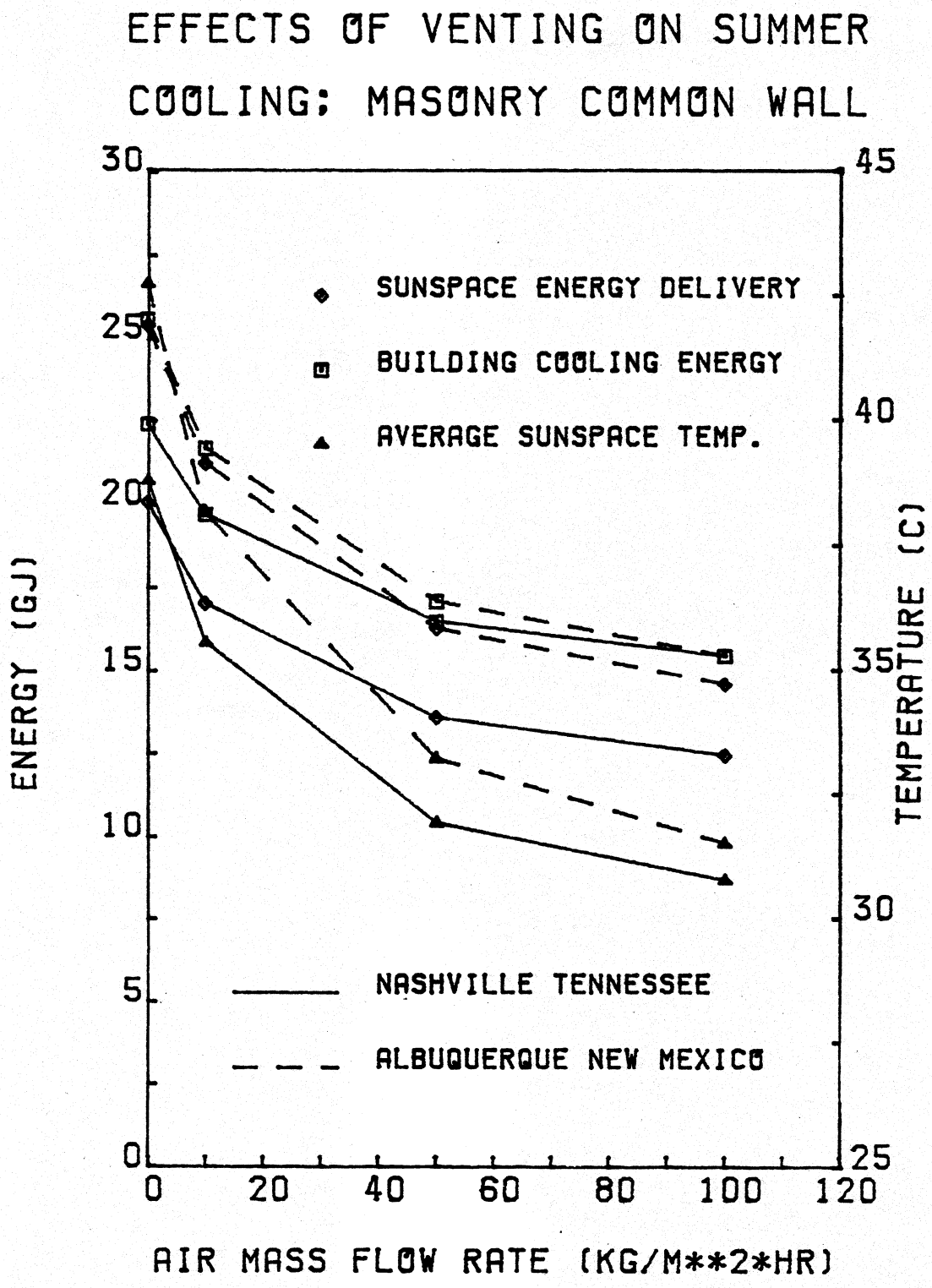
EFFECTS OF VENTING ON SUMMER COOLING: MASONRY COMMON WALL
SUNSPACE ENERGY DELIVERY
BUILDING COOLING ENERGY
AVERAGE SUNSPACE TEMP.
NASHVILLE TENNESSEE
ALBUQUERQUE NEW MEXICO
ENERGY (GJ)
TEMPERATURE (C)
AIR MASS FLOW RATE (KG/M**2*HR)
0
5
10
15
20
25
30
25
30
35
40
45
0
20
40
60
80
100
120

Table 3.13

Results of the Summer Cooling Study

(Nashville/Albuquerque)

	$Q_{Delivery}$(GJ)	Q_{cool}(GJ)	$\overline{T}_{sunspace}$
masonry wall, no solar	-0.22/-0.51	4.94/3.98	23.28/22.31
masonry wall, 50% solar	9.99/12.32	13.33/13.43	31.16/32.83
insulated wall, no solar	-0.03/-0.07	5.02/4.27	23.15/22.03
insulated wall, no cooling strategy	2.43/3.05	6.81/6.61	49.39/55.84

Insulated common wall systems incur only slightly raised building cooling loads, as a result of the sunspace even though the average sunspace air temperature is quite high. If any sunspace cooling strategy is employed, the additional cooling load will be much less.

Masonry common wall systems, however, have a marked effect on the building cooling load. Venting the sunspace air to ambient conditions does lessen the effect, but the additional cooling load is still significant. Decreasing the sunspace-to-ambient venting set point would help, but during mid-summer the sunspace is already being vented fairly continuously during daylight hours. Reducing the solar energy input by 50% has a much greater effect on reducing the building cooling load. In practice, a combination of venting and shading should be employed to reduce the building heat gain from the sunspace as much as possible. Presumably, not all of the additional building cooling load would have to be met by an air conditioner. Venting ambient air to the building when possible could supply some free cooling. It is apparent, however, that summer cooling of masonry common wall systems is a major concern.

3.4 Conclusion

The effects of many variables were quantified in this chapter. Other studies of this type can easily be performed using the TRNSYS sunspace component described in Chapter 2. The main utility of the many studies performed in this chapter is that the important vari-

ables which determine sunspace performance were identified. The next chapter describes a simplified monthly-based design method for sunspace systems, which incorporates these factors.

Chapter 4: A Design Method for Sunspaces

4.1 Introduction

It is desirable to develop a simplified method for predicting the performance of building-attached sunspace systems. Optimization of system design using the TRNSYS model of Chapter 2 would be costly and requires access to a main frame computing system. In addition, hourly weather data is needed. A design method which requires only one set of calculations per month and readily available monthly average weather data is one solution to this problem. Currently available monthly based design methods are discussed in Section 1.3.

A generalized method for predicting the monthly average daily solar radiation absorbed by the sunspace wall and floor is presented in this chapter. The effects of changing the sunspace geometry, optical properties, and the wall and floor solar absorbtivity on the amount of absorbed solar radiation are easily evaluated.

Many sunspace designs incorporate a thermally conductive common wall. This type of sunspace is similar to collector-storage wall systems. By using an approach similar to that developed by Monsen for the prediction of monthly average delivery of collector-storage walls (15), the energy delivery of this class of sunspace may be estimated. By using this method, the effects of altering the sunspace thermal parameters on sunspace energy delivery can be examined.

The limits of conductive common wall sunspace system performance are also similar to those of collector-storage wall systems (15). Equations for both zero and infinite thermal storage building systems are developed, and problems with their solution on a monthly basis are discussed.

An alternative to using the theoretical limits of sunspace system performance to define building auxiliary heating requirements is also discussed. It involves considering the sunspace energy delivery as a distributed energy input which reduces the balance point temperature of the building. Heating loads are then calculated using degree-day calculations with reduced base temperature degree-days.

Design method results are compared with detailed TRNSYS simulation values. In calculating the TRNSYS building heating load, a slightly different method was used for the simulations discussed in this chapter. The studies of Chapter 3 incorporated a temperature level control building load model. A thermostat component monitored the building temperature and directed auxiliary heating and cooling components, which kept the building within the specified temperature bounds. The temperature level control approach closely simulates the performance of actual building components. However, results are somewhat dependent on the specified heating and cooling rates of the auxiliary components. If the load on the building is greater than the sunspace energy delivery, the temperature drops below the low set point. The auxiliary heater is then activated.

If the auxiliary heating rate exceeds the building load, the temperature of the building will rise above the set point.

Energy rate control eliminates the dependence on the auxiliary heating and cooling rate. If a heating or cooling load exists on the building, energy is added or subtracted to exactly maintain the thermostat set point. This is analogous to a system where the furnace or air conditioner is tempered to exactly meet the instantaneous building load. The TRNSYS Type 19 mode 1 room model operates with energy rate control. The building capacitance is modeled as a single lumped capacitance, and no latent loads are considered, as in the simulations of Chapter 3. For a further discussion of energy rate and temperature level control, see the TRNSYS manual (10).

4.2 Simplifying Assumptions of the Design Method

Two assumptions allow the sunspace thermal network (Figure 2.2) and the accompanying differential equations (Equation 2.4.1) to be greatly simplified. The first of these is that air flow between the sunspace and the attached building has little effect on the building auxiliary heating requirements. The venting studies of Chapter 3 and Figures 3.8 through 3.12 show that this is a good approximation for relatively thin (0.1 - 0.3 m) common walls made of a thermally conductive material such as masonry. The reasons for this are thoroughly discussed in Chapter 3. Results from the methods of this chapter will slightly underpredict the energy delivery of vented masonry wall systems.

The second assumption is that the net internal energy change of the sunspace wall and floor over the month is small compared to the other sunspace energy quantities. This is found to be true by examining the monthly integrated energy stored as sensible heat in the floor and wall. Table 4.1 compares several monthly energy quantities for an unvented sunspace with a 0.3 m thick masonry common wall. The implication of this assumption is that the monthly average wall and floor temperature profiles are linear. The monthly average wall temperature profiles for the same system are plotted in Figure 4.1.

The second assumption allows two of the heat flow paths to be simplified to a large degree. The series of resistors and capacitors through the wall can be combined into a single linear resistance from the outside to the inside of the wall. If the heat transfer coefficient from the wall to the attached building is assumed to be constant, a single conductance term describes the monthly average heat transfer from the sunspace wall surface to the building. Similarly, a single conductance describes the monthly average heat transfer from the floor surface to the ground. The floor surface-to-ground conductance includes the thermal conductivity of the floor, the R-value of the floor insulation and the effective ground resistance.

The complicated thermal network of Figure 2.2 can be reduced on a monthly basis to that of Figure 4.2 by using the two assumptions described above and by assuming convection coefficients are con-

Table 4.1

Integrated Monthly Energy Quantities

Location: Madison, WI

	Energy (MJ)			
Month	Sunspace Stored	Sunspace Delivery	Absorbed Solar Radiation	Loss to Ambient
October	0.17	2.22	7.34	4.79
November	-0.28	0.89	5.09	4.34
December	0.01	-0.27	3.93	4.21
January	0.11	0.04	5.91	5.68
February	0.18	0.84	6.91	5.82
March	0.11	2.34	10.28	7.69
April	-0.18	2.46	8.48	5.77

Figure 4.1

MONTHLY AVERAGE WALL TEMPERATURE PROFILE; 0.3 M THICK MASONRY

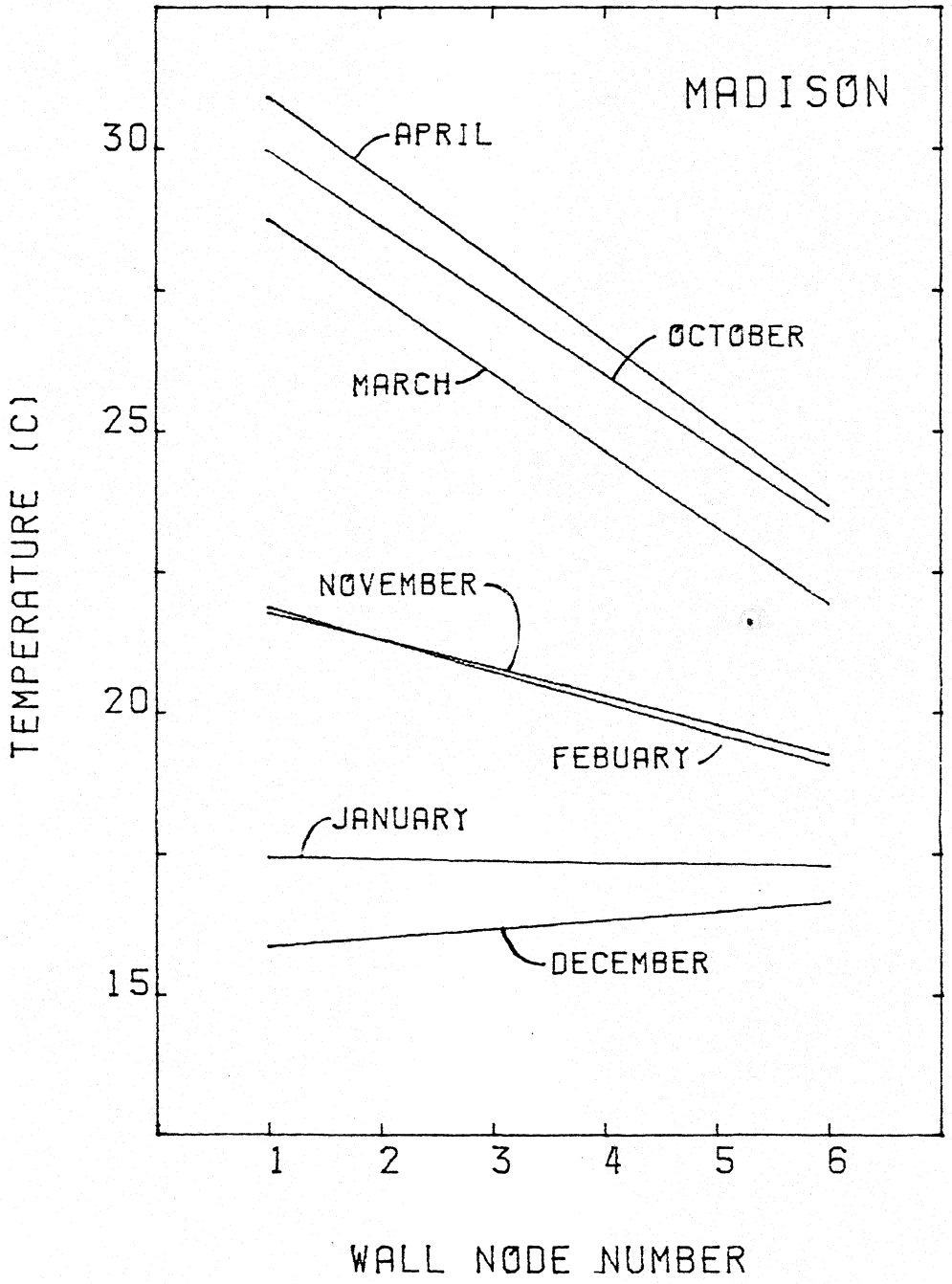

Figure 4.2

MONTHLY AVERAGE SUNSPACE THERMAL NETWORK

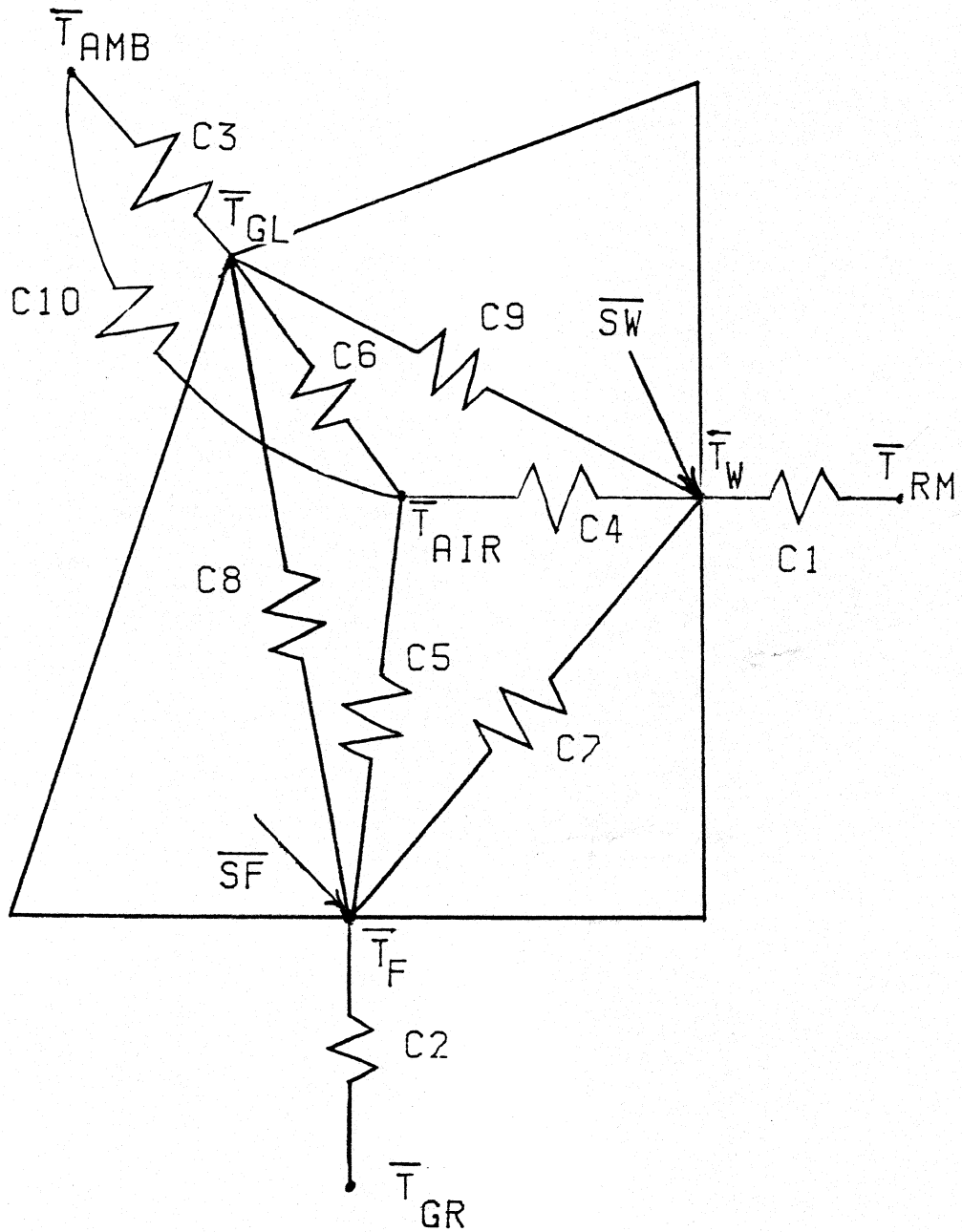

stant. The room, ground, and ambient temperatures are monthly average values, denoted by the bar. Before determining the monthly average sunspace wall, floor, air and glazing temperatures, the absorbed solar radiation on the wall and floor ($\overline{SW}$ and $\overline{SF}$) must be calculated.

4.3 Determination of the Monthly Average Absorbed Radiation

The first step in solving the equations which describe the simplified monthly average thermal network of Figure 4.2 is to calculate the solar radiation absorbed by the wall and floor. The approach described here is similar to that of Klein (32) for determining the monthly average transmittance-absorbtance product of solar collectors. Generally, the daylight hours of the "average" day of the month (16) are divided into 12 equal time intervals, and the beam radiation incident on the sunspace surfaces is determined at the midpoint of each interval. Incident diffuse radiation is calculated on a daily basis, as the transmittance to diffuse radiation is assumed to be constant. After numerically integrating the beam radiation components, multiple radiation reflections within the sunspace are accounted for by using the $\hat{F}$ (F-hat) formulation described in Section 2.3.4.

$\overline{H}$, the monthly average daily horizontal radiation, is available for many locations. A correlation developed by Erbs (33) determines the monthly average diffuse fraction, $\overline{H}_d/\overline{H}$:

$$\overline{H}_d/\overline{H} = 1.317 - 3.023\ \overline{K}_T + 3.372\ \overline{K}_T^2 - 1.769\ \overline{K}_T^3 \qquad 4.3.1$$

where $\bar{K}_T$ is the monthly average daily clearness index. $\bar{K}_T$ is equal to $\bar{H}$ divided by the monthly average daily horizontal extraterrestrial radiation, $\bar{H}_o$. Equations for $\bar{H}_o$ are presented by Duffie and Beckman (16). Equation 4.3.1 assumes the distribution of K_T, the daily clearness index is independent of location.

With this information, the average hourly horizontal beam radiation intensity, I_b, may be estimated by using its long-term average distribution. Equations for long-term distributions of r_T (the hourly-to-daily total radiation ratio) and r_d (the hourly-to-daily diffuse radiation ratio) from Collares-Pereira and Rabl (34) are as follows:

$$r_d = \frac{24}{\pi} \frac{\cos \omega_r - \cos \omega_s}{\sin \omega_s - \omega_s \cos \omega_s} \qquad 4.3.2$$

$$r_T = r_d \, (A + B \cos \omega_r)$$

$$A = 0.409 + 0.5016 \sin (\omega_s - 1.047) \qquad 4.3.3$$

$$B = 0.6609 - 0.4767 \sin (\omega_s - 1.047)$$

ω_r and ω_s are the hour-angle and the sunrise hour-angle, respectively. The average hourly beam radiation on a tilted surface, $G_{b,t}$, can now be defined:

$$G_{b,t} = R_b \, (r_T \, \bar{H} - r_d \, \bar{H}_d) \qquad 4.3.4$$

where R_b is the ratio of beam radiation on the tilted surface to that on the horizontal. Equations for R_b and θ_i, the beam radiation

incidence angle on a tilted surface, are found in (16). The transmittance of the glazing at a particular incidence angle can be determined analytically by using Fresnel's equation or by experiment (32). A FORTRAN subroutine TALF from TRNSYS (10) which calculates glazing transmittance from optical properties is included in the Appendix. Once the intensity of the beam radiation which is transmitted through the two sloped glazings for a particular hour-angle is determined, the energy is apportioned to the wall, floor, and glazing surfaces by geometric calculations described in Section 2.3.3 and Figure 2.4.

The total monthly average daily incident radiation on the sunspace surfaces is the sum of the numerically-integrated beam radiation and the daily diffuse incident radiation. If the ground and sky are assumed to be isotropic sources, the diffuse radiation incident on a glazing surface at a tilt β can be calculated on a daily basis:

$$\bar{H}_{d,t} = \bar{H}_d \left(\frac{1 + \cos\beta}{2}\right) + \rho_g \bar{H} \left(\frac{1 - \cos\beta}{2}\right) \qquad 4.3.5$$

where ρ_g is the ground reflectance. As in the TRNSYS model of Chapter 2, the effective incidence angle of the diffuse radiation is assumed to be 60 degrees. Transmitted diffuse radiation is distributed to the sunspace surfaces by using Hottel's crossed string view factors (see Section 2.3.2).

Incident radiation calculated by the described monthly average daily method is compared with monthly integrated TRNSYS values (divided by the number of days per month) in Figure 4.3. The plotted

Figure 4.3

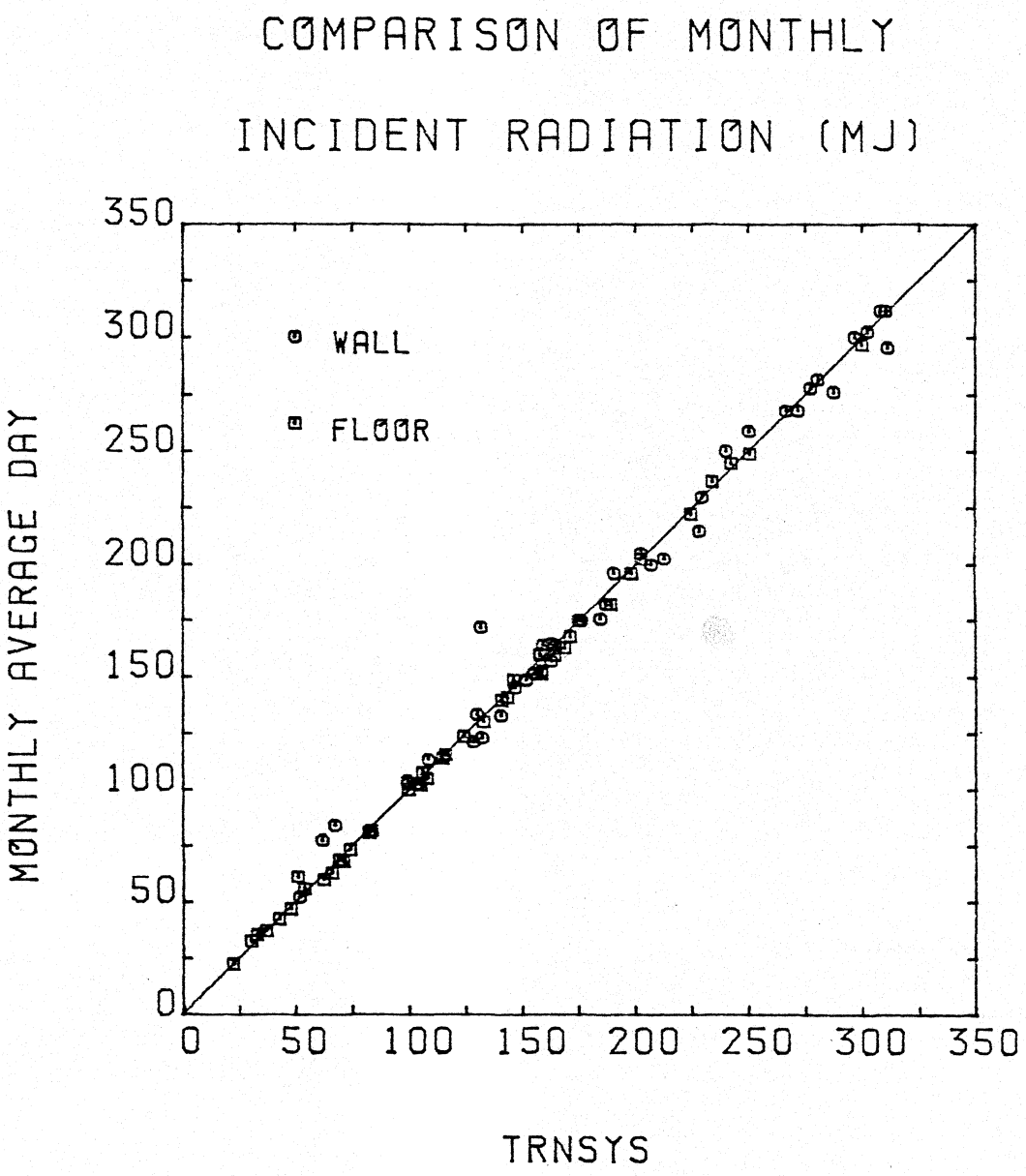
COMPARISON OF MONTHLY
INCIDENT RADIATION (MJ)
MONTHLY AVERAGE DAY
TRNSYS
WALL
FLOOR
0
50
100
150
200
250
300
350

values are for heating season simulations with the geometry of Figure 3.1 using TMY weather data (31) for Madison, Wisconsin; Caribou, Maine; Ely, Nevada; Albuquerque, New Mexico; Seattle, Washington; and Nashville, Tennessee. Generally, the monthly calculations produce results which are very similar to those of TRNSYS simulations. One point, however, lies well off the idea 45-degree line. For the month of January in Caribou, Maine, the result of average day calculations for radiation incident on the wall was 171.9 MJ, but the TRNSYS simulation value was 131.4 MJ. The difference between the two calculation methods lies in the diffuse radiation fraction for the month. Using equation 4.3.1 yields $\overline{H}_d/\overline{H} = 0.453$. Numerically integrating the total horizontal radiation from the TMY data tape and the horizontal diffuse radiation from the TRNSYS radiation processor over the month gives $\Sigma H_d/\Sigma H = 0.583$. The average transmittance for beam radiation is greater than that of diffuse radiation; therefore, more radiation is transmitted through the glazings using the monthly average day calculations. In addition, the distribution to the sunspace surfaces is different for beam and diffuse radiation. These two factors can cause a significant variation in the calculated monthly average incident radiation values. Nearly all the discrepancies between calculated incident radiation in Figure 4.3 can be traced to a difference in diffuse fraction. The largest differences in diffuse fraction and calculated incident radiation occur consistently in two locations--Caribou, Maine and Seattle, Washington.

The hourly radiation values for a given month from the Typical Meteorological Year weather data tape are selected from 23 years of data. Although total horizontal radiation values were a key factor in selecting a "typical" month, radiation distributions were not directly considered (35). It is possible that some of the months selected have distributions of K_T which differ from those assumed in the derivation of Equation 4.3.1.

The deviations of Figure 4.3 are acceptable, and isolated differences arise due to variations in the diffuse radiation fraction. A FORTRAN subroutine, RAD, to calculate the monthly average daily incident radiation for the sunspace surface--given the month, average daily horizontal radiation intensity, ground reflectance and sunspace geometry--is included in the Appendix.

The monthly average daily solar radiation absorbed by the wall and floor ($\overline{SW}$ and $\overline{SF}$) can be calculated by using Equation 2.3.9 and $\hat{F}$ (F-hat) values calculated from the sunspace geometry and optical properties (see Section 2.3.4). A computer algorithm for obtaining $\hat{F}$ values for a three-surface (wall, floor and glazing) sunspace, FHAT, is included in the Appendix. Since subroutine FHAT calculates the $\hat{F}$ matrix in exactly the same manner as the TRNSYS sunspace component, differences between monthly average absorbed solar radiation and values from TRNSYS simulations arise only from discrepancies in incident radiation.

The methods described in this section may be extended for sunspaces with extra thermal mass containers if desired. Agreement be-

tween monthly average calculations and TRNSYS results will be similar to that of Figure 4.3.

4.4 The Monthly Average Sunspace Temperatures and Energy Delivery

Once the monthly absorbed solar radiation has been calculated, the sunspace temperatures and energy flows may be determined. For the monthly design method calculations, the conductances and the temperatures of the ground, room and ambient are assumed to be constant at their monthly average values. Since the thermal storage capacity of the wall and floor is not taken into account, the following four monthly energy balance equations may be written for the network of Figure 4.2:

$$C_3 (\overline{T}_{amb} - \overline{T}_{gl}) + C_6 (\overline{T}_{air} - \overline{T}_{gl}) + C_8 (\overline{T}_f - \overline{T}_{gl}) + C_9 (\overline{T}_w - \overline{T}_{gl}) = 0 \qquad 4.4.1$$

$$C_4 (\overline{T}_w - \overline{T}_{air}) + C_5 (\overline{T}_f - \overline{T}_{air}) + C_6 (\overline{T}_{gl} - \overline{T}_{air}) + C_{10} (\overline{T}_{amb} - \overline{T}_{air}) = 0 \qquad 4.4.2$$

$$C_2 (\overline{T}_{gr} - \overline{T}_f) + C_6 (\overline{T}_{air} - \overline{T}_f) + C_7 (\overline{T}_w - \overline{T}_f) + C_8 (\overline{T}_{gl} - \overline{T}_f) + \overline{SF} = 0 \qquad 4.4.3$$

$$C_1 (\overline{T}_{rm} - \overline{T}_w) + C_4 (\overline{T}_{air} - \overline{T}_w) + C_7 (\overline{T}_f - \overline{T}_w)$$

$$+ C_9 (\overline{T}_{gl} - \overline{T}_w) + \overline{SW} = 0 \qquad 4.4.4$$

All the conductances are calculated in the same manner as their counterparts in Figure 2.2, except that temperatures and convection coefficients assume their monthly average values and the units must be compatible with daily absorbed radiation. It is convenient to use subroutine FHAT, which is also useful in calculating absorbed solar radiation, to help compute infrared radiation conductances between the sunspace surfaces.

The values of C1 and C2 in Figure 4.2 are composites of earlier conductances. Using the same terminology of Section 2.2, they are defined as:

$$C_1 = \left(\frac{t_w}{k_w} + \frac{1}{h_{w-rm}}\right)^{-1} \cdot A_w \qquad 4.4.5$$

$$C_2 = \left(\frac{t_f}{k_f} + R_{insul} + R_{gr,eff}\right)^{-1} \cdot A_f \qquad 4.4.6$$

Use of glazing night insulation may be included in the design method by calculating a time-weighted effective glazing R-value:

$$R_{gl,eff} = \frac{(1 - t)R_{gl} + t(R_{gl} + R_{ni})}{24} \qquad 4.4.7$$

where t is the average number of hours in the day that the night insulation is in place. It is assumed that the night insulation is

removed before dawn and put in place after sunset so no solar radiation is prevented from entering the sunspace. The value of effective glazing resistance is combined with the glazing-to-ambient convection coefficient and infrared conductance as described by equation 2.2.15 to obtain a value for C_3.

The energy balance equations, 4.4.1 to 4.4.4, form a system of equations with four unknowns which can be solved by any suitable technique, such as Gaussian elimination, for the monthly average glazing, air, floor, and wall temperatures. However, the infrared conductances, C_7, C_8, C_9, and a portion of C_3, are dependent on the temperatures of the wall, floor, and glazing. The solution technique is as follows. An initial guess, for all unknown temperatures, of 27 C is used to obtain corrected values of the monthly average wall, floor, glazing, and air temperatures. The new temperatures are then used to re-calculate the temperature dependent conductances. Iterations continue until the temperatures do not differ appreciably from those used to calculate the infrared conductances. Convergence within 0.001 C usually occurs after fewer than four iterations.

With the monthly average inside wall surface temperature, $\overline{T}_w$, the sunspace energy delivery may be calculated from equation 4.4.8:

$$\overline{Q}_{in} = C_1 \, (\overline{T}_w - \overline{T}_{rm}) \qquad 4.4.8$$

Results from monthly average calculations, as described in this

section, are compared with detailed TRNSYS simulation results in Figure 4.4. In order to avoid confusion with discrepancies caused by differences in incident solar radiation values, the energy delivery computed by monthly average temperature methods used TRNSYS simulation incident radiation as an input.

If the monthly energy storage calculated by the TRNSYS simulation is near zero, the predicted energy delivery values are nearly identical. Variations arise mainly due to the assumption of no appreciable energy storage in the wall and floor, implicit in Equations 4.4.3 and 4.4.4. However, over a total heating season, energy storage is negligible. If monthly average temperature calculations under-predict energy delivery for one month, there is a tendency for the predicted energy delivery for the following month to be greater than results from detailed TRNSYS simulations. Over a heating season, the total sunspace energy delivery to the attached building calculated by the simplified method approaches detailed simulation results more closely than Figure 4.4 might suggest. For the six heating season calculations plotted in the figure, the average annual deviation in results was only 1.2 percent.

The annual average deviation between TRNSYS results and calculations employing monthly average incident radiation from subroutine RAD was 4.9 percent. The monthly values are compared in Figure 4.5.

4.5 Theoretical Limits to Sunspace System Performance

The theoretical limits of the auxiliary heating requirements of a sunspace system may be derived analytically. These limits are

Figure 4.4

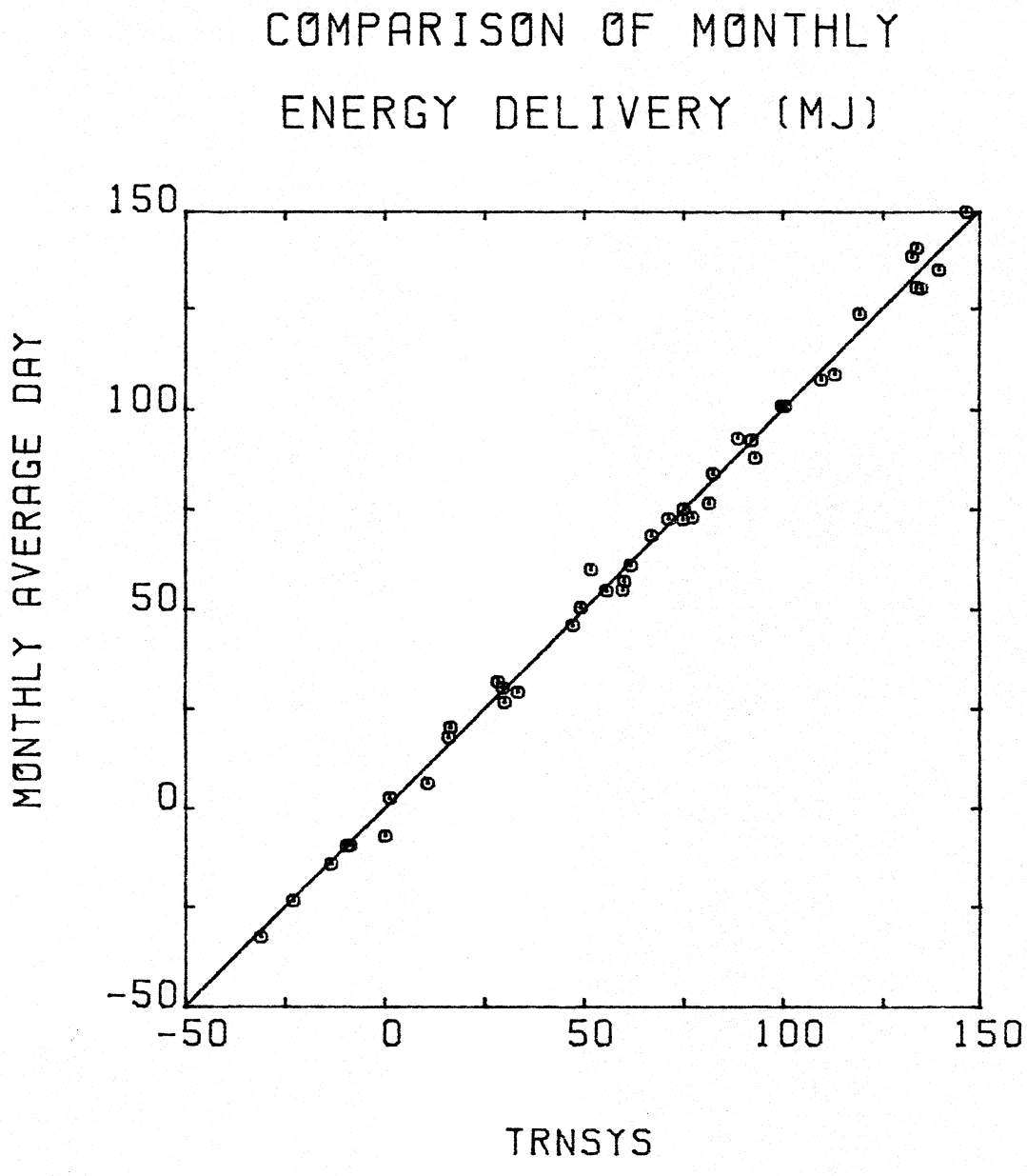
COMPARISON OF MONTHLY
ENERGY DELIVERY (MJ)
MONTHLY AVERAGE DAY
150
100
50
0
-50
-50
0
50
100
150
TRNSYS

Figure 4.5

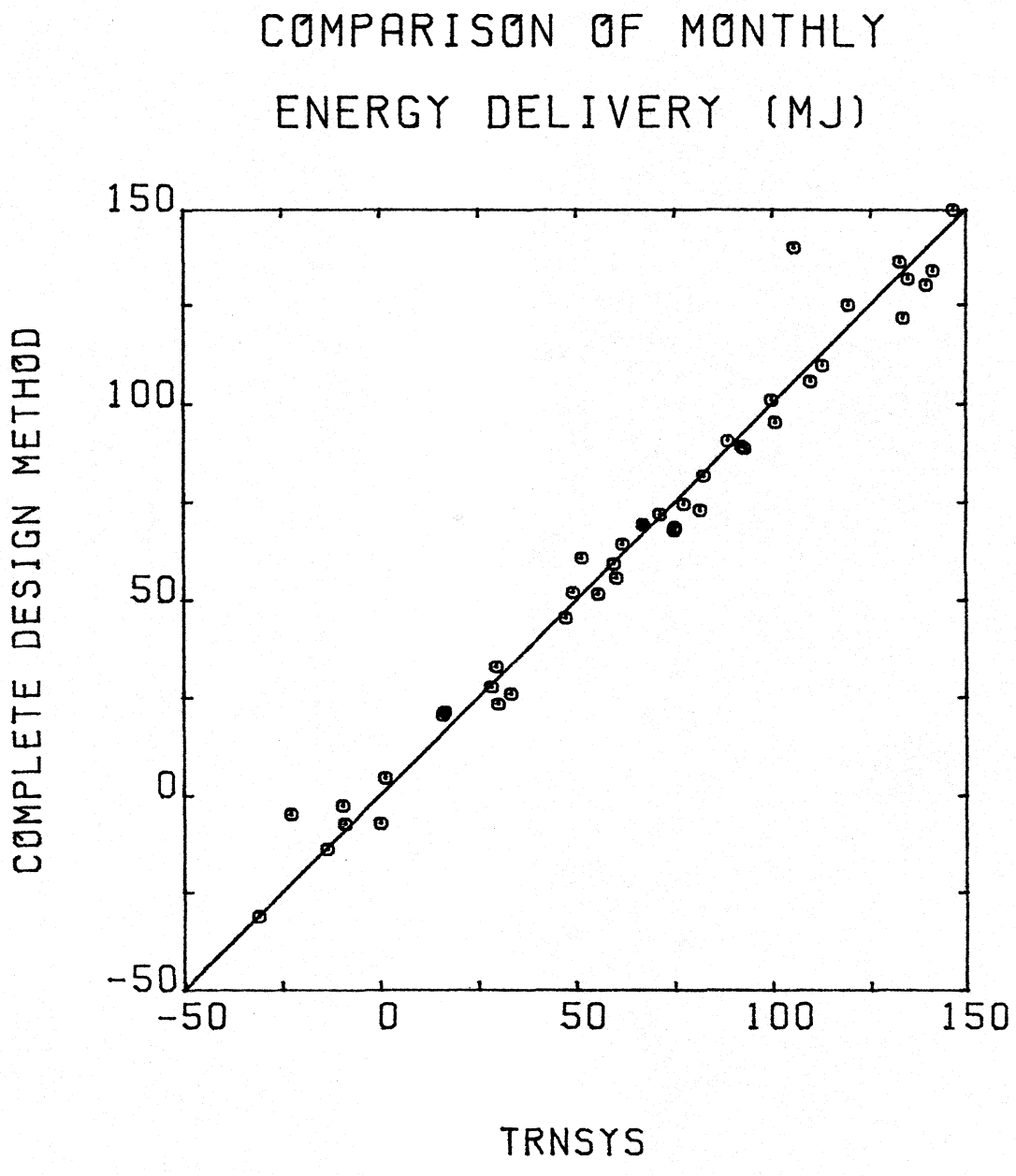
COMPARISON OF MONTHLY
ENERGY DELIVERY (MJ)
COMPLETE DESIGN METHOD
150
100
50
0
-50
-50
0
50
100
150
TRNSYS

similar to those for direct gain and collector storage wall systems (14,15). If the attached building has an infinite thermal storage capacity, auxiliary consumption is minimized, since all of the sunspace energy delivery, up to the building energy requirements, is usable. Zero thermal storage capacity systems, however, must reject any sunspace energy delivery in excess of the instantaneous building load. Therefore, heating requirements are maximized in zero thermal storage systems.

4.5.1 Infinite Building Thermal Capacity

For an infinite thermal capacitance building, all of the sunspace energy delivery which exceeds the building heating load is absorbed by the structure. The temperature of the building is constant and equal to the building auxiliary heating thermostat set point, T_r. Stored excess solar radiation is released to meet the building load whenever instantaneous sunspace gains are not sufficient.

A monthly energy balance on an infinite capacitance building gives the monthly auxiliary heating requirement:

$$Q_{aux,i} = [L_a - Q_{in}]^+ \qquad 4.5.1$$

L_a is the building heating load not including the sunspace, and Q_{in} is the net sunspace energy delivery. The above equation assumes the monthly distribution of Q_{in} is such that the total energy delivery over the month was available to meet the building heating load whenever a load occurred. Only positive values of monthly auxiliary energy are considered, and no month-to-month carryover of stored

energy is allowed.

Calculation of Q_{in} is discussed in Section 4.4. L_a, the heating load through the non-solar building components, may be determined in several ways. One common procedure is the UA degree-day method (19):

$$L_a = (UA)_a \, (DD)_b \qquad 4.5.2$$

In this equation $(UA)_a$ is the loss coefficient of the building if the sunspace is adiabatic, and $(DD)_b$ is the monthly degree-days evaluated at the building balance point temperature, T_b, given by:

$$T_b = T_r - \dot{g}/(UA)_a \qquad 4.5.3$$

The average rate of building internal energy gains, $\dot{g}$, includes heat generation of appliances and people, but not the energy delivery of the sunspace. Degree-days for several base temperatures in 224 locations calculated from a relation developed by Thom (36) are tabulated in (4). Degree days may also be calculated from recently developed equations of Erbs (37).

If the transmittance of the glazing is equal to zero, no solar radiation would be absorbed by the sunspace wall and floor. An additional heating load, L_s, occurs due to heat losses from the building through the sunspace. Computation of L_s involves solving equations 4.4.1 through 4.4.4 with $\overline{SF}$ and $\overline{SW}$ set equal to zero. Subroutine TWBAR, included in the Appendix, calculates L_s and Q_{in} for the monthly average day. After the monthly average wall

temperature for no solar input has been computed, L_s is as follows:

$$L_s = C_1 (\overline{T}_r - \overline{T}_{w,ns}) \qquad 4.5.4$$

Equation 4.5.1 may be re-written as:

$$Q_{aux,i} = (L - Q_s)^+ \qquad 4.5.5$$

where L, the total building load is given by

$$L = L_a + L_s \qquad 4.5.6$$

and Q_s, the solar gain, is

$$Q_s = Q_{in} + L_w \qquad 4.5.9$$

If the transmittance of the sunspace glazing is zero, $Q_{in} = -L_w$ and Q_s is zero. The system auxiliary heating requirement is then simply the total building load, L.

4.5.2 Zero Building Thermal Capacity

For a building with zero thermal storage capacity, sunspace energy delivery in excess of instantaneous load demand cannot be stored for later use. If sunspace instantaneous delivery is less than the load, auxiliary energy must be supplied to maintain the building temperature at the thermostat low set point. Conversely, if the instantaneous sunspace delivery exceeds the load demand, excess energy must be immediately removed from the building to prevent overheating. The building temperature remains at the thermostat heating set point due to auxiliary heat addition and

excess solar gain removal.

The sunspace common wall for the zero thermal capacity system must also have no thermal storage capacity ($\rho C_p = 0$). The wall thermal conductivity presents a resistance to heat flow, but there is no time delay in energy delivery.

A monthly energy balance yields the auxiliary heating requirements of a zero thermal capacitance sunspace system:

$$Q_{aux,z} = [L - Q_s + Q_{dump}]^+ \qquad 4.5.10$$

L and Q_s were defined in the previous section. The monthly energy rejected from the zero thermal storage system, Q_{dump}, is the integral of the rate of instantaneous energy removal required to keep the building at the heating set point. The rate of energy removal can be calculated from an instantaneous energy balance on the building:

$$\dot{Q}_{dump} = [C_1 (T_w - T_r) - (UA)_a (T_b - T_a)]^+ \qquad 4.5.11$$

where C_1 is given by Equation 4.4.5, T_w is the common wall temperature on the sunspace side, T_r is the building heating set point, and T_a is the ambient temperature.

For a massless floor and wall, the monthly average thermal network of Figure 4.2 and Equations 4.4.1 through 4.4.4 may be used on an instantaneous basis. Rearranging these equations yields the following matrix equation:

$$\begin{bmatrix} -C_3-C_6-C_8-C_9 & C_6 & C_8 & C_9 \\ C_6 & -C_4-C_5-C_6-C_{10} & C_5 & C_4 \\ C_8 & C_5 & -C_2-C_5-C_7-C_8 & C_7 \\ C_9 & C_4 & C_7 & -C_1-C_4-C_7-C_9 \end{bmatrix} \begin{bmatrix} T_{gl} \\ T_{air} \\ T_f \\ T_w \end{bmatrix}$$

$$= \begin{bmatrix} -C_3\ T_{amb} \\ -C_{10}\ T_{amb} \\ -S_F - C_2\ T_{gr} \\ -S_w - C_1\ T_{rm} \end{bmatrix} \qquad 4.5.12$$

Solving for T_w yields:

$$T_w = \frac{\begin{bmatrix} X_1\ E\ [S_F\ (AB - DE) + S_w\ (EF - B^2)] + \\ (AB - DE)\ [T_{gr}\ C_2\ X_1\ E - T_a\ (BH - C_3\ C_8\ E)] + \\ (EF - B^2)\ [T_{rm}\ C_1\ X_1\ E - T_a\ (AH - C_3\ C_9\ E)] \end{bmatrix}}{(AB - DE)^2 - (EG - A^2)\ (EF - B^2)}$$

where

$$X_1 = C_3 + C_6 + C_8 + C_9 \qquad 4.5.13$$

$$X = C_4 + C_5 + C_6 + C_{10}$$

$$X_3 = C_2 + C_5 + C_7 + C_8$$

$$X_4 = C_1 + C_4 + C_7 + C_9$$

$$A = C_6\ C_9 + C_4\ X_1$$

$$B = C_6\ C_8 + C_5\ X_1$$

$$D = C_8\ C_9 + C_7\ X_1$$

$$E = C_6^{\,2} - X_1\ X_2$$

$$F = C_8^{\,2} - X_1\ X_3$$

$$G = C_9^{\,2} - X_1\ X_4$$

$$H = C_3\ C_6 + C_{10}\ X_1$$

For the equations which follow, it is convenient to refer to the denominator and the second and third lines in the numerator as single terms, J_1 and J_2, respectively. Equation 4.5.13 can be re-written as:

$$T_w = \frac{X_1\ E\ [S_F\ (AB - DE) + S_w\ (EF - B^2)] + J_2}{J_1} \qquad 4.5.14$$

A transmittance-absorbtance product for the sunspace wall can be defined such that:

$$S_w = A_w\ G_v\ (\tau\alpha)_w \qquad 4.5.15$$

where G_v is the instantaneous radiation incident on a vertical,

south-facing surface. Substituting Equation 4.5.15 into 4.5.14, using the result in Equation 4.5.11 and integrating over the month gives the monthly energy rejected from the zero thermal capacitance system:

$$Q_{dump} = \frac{C_1 X_1 E (EF - B^2)}{J_1} A_w (\overline{\tau\alpha})_w \int_{month} (G_v - G_c)^+ dt \qquad 4.5.16$$

where $(\tau\alpha)_w$ has been replaced by its monthly average equivalent defined by:

$$(\overline{\tau\alpha})_w = \frac{\overline{SW}}{A_w \overline{H}_v} \qquad 4.5.17$$

G_c, the critical radiation level is:

$$G_c = \frac{1}{A_w (\overline{\tau\alpha})_w (EF - B^2) X_1 E} \left\{ \frac{(UA)_a (\overline{T}_b - \overline{T}_a) J_1}{C_1} + \overline{T}_r J_1 - \overline{SF} (AB - DE) X_1 E - J_2 \right\} \qquad 4.5.18$$

The integral in Equation 4.5.16 appears in the defining relation of $\overline{\phi}$, the monthly average daily utilizability:

$$\overline{\phi} = \frac{\int_{month} (G_T - G_c)^+ dt}{\int_{month} G_T dt} \qquad 4.5.19$$

$\overline{\phi}$ is the fraction of the monthly radiation on a tilted surface which lies above the specified critical radiation level, G_c. Since $\overline{\phi}$ is a

measure of the dumped energy for passive solar systems rather than useful energy delivery as in active solar systems, the term "un-utilizability" is used. The dumped solar energy for a zero thermal storage capacity system in terms of $\overline{\phi}$ is:

$$Q_{dump} = \frac{C_1 X_1 E (EF - B^2)}{J_1} A_w (\overline{\tau\alpha})_w \overline{\phi} \overline{H}_v N \qquad 4.5.20$$

N is the number of days in the month. The above relation can be substituted into Equation 4.5.10 for the auxiliary heating requirements of a zero thermal storage capacity sunspace system. The fractional portion of equation 4.5.20, $C_1 X_1 E (EF - B^2)/J_1$, is a dimensionless ratio of conductance terms which describes the heat flow network of Figure 2.5.

Utilizability is a radiation statistic first developed by Whillier (38). ϕ is the fraction of the total solar radiation which lies above a specified critical level. Originally ϕ was developed on an hourly basis. It is a non-linear function of critical radiation level because it is a measure of the variability of solar radiation intensity. Liu and Jordan (39) extended Whillier's work on monthly average hourly utilizability. They found that ϕ is not strongly dependent on values of ground reflectance or view factors from the surface to the sky and ground. In addition, Liu and Jordan (40) found that the monthly variability of solar radiation is a strong function of the monthly clearness index, $\overline{K}_T$. Klein (17) used this to develop a correlation for $\overline{\phi}$, the monthly average daily utilizability. He found that $\overline{\phi}$ is a function of three dimensionless

parameters, $\bar{K}_T$, $\bar{R}/R_n$, and X_c.

$\bar{K}_T$, the monthly clearness index, is simply the ratio of terrestrial monthly average horizontal radiation to extraterrestrial monthly average horizontal radiation. $\bar{R}/R_n$ varies with collector orientation and time of year. $\bar{R}$ is the monthly average ratio of tilted surface radiation to horizontal radiation. R_n is the ratio of the tilted surface radiation to horizontal radiation at noon of the average day of the month. X_c is the critical radiation level, G_c, divided by G_n, the tilted surface radiation intensity at noon of the average day of the month. The relation developed by Klein is as follows:

$$\bar{\phi} = \exp\left((A + B\,(\bar{R}/R_n))\,(X_c + C\,X_c^2)\right)$$

$$A = 2.943 - 9.271\,\bar{K}_T + 4.031\,\bar{K}_T^2 \qquad 4.5.21$$

$$B = -4.345 + 8.853\,\bar{K}_T - 3.602\,\bar{K}_T^2$$

$$C = -0.170 - 0.306\,\bar{K}_T + 2.936\,\bar{K}_T^2.$$

4.5.3 Problems with the Utilizability Approach for Sunspaces

The utilizability concept is useful for describing direct gain (14), collector-storage wall (15), and some active solar heating systems (16). The equations for the critical radiation level are relatively simple for these systems. The physical meaning of the equations is clear, and they lead to an intuitive understanding of the solar components' behavior. In the case of sunspaces, however,

Equation 4.5.18 for critical radiation level is complex, and the physical meaning is not immediately apparent.

In addition, the equations presented in the previous section--which are meant to be used to quantify the variability in sunspace energy delivery--have an inherent flaw. The equation for the monthly critical radiation level (Equation 4.5.18) contains the monthly average daily solar radiation absorbed by the sunspace floor, $\overline{SF}$. By using the monthly average value, the variability of solar radiation for this surface has been ignored. During the spring and fall, when horizontal radiation intensity is relatively large compared to the winter months, using Equation 4.5.18 can lead to an extremely low or even a negative critical radiation level. A low critical radiation level implies that nearly all of the radiation incident on the sunspace common wall causes the building temperature to rise above the heating set point. Building auxiliary heating energy for that month would be zero. This result conflicts with TRNSYS simulation values. For accuracy in the annual results, the variability of horizontal solar radiation must also be taken into consideration. The following equation for the instantaneous energy rejected from a zero thermal storage sunspace system is obtained by substituting Equation 4.5.13 into Equation 4.5.11:

$$\dot{Q}_{dump} = \left[C_1 \left(\frac{X_1 E [S_F (AB - DE) + S_w (EF - B^2)] + J_1}{J_2} - T_r \right) - (UA)_a (T_r - T_a) \right]^+ \qquad 4.5.22$$

Accounting for the variability of solar radiation incident on the floor as well as the wall on a monthly basis is difficult. It is not possible to cast the above equation in a form compatible with Equation 4.5.19. Instead, a function must be developed which simultaneously accounts for the distribution of horizontal and vertical solar radiation, as well as the fact that radiation incident on the floor has a different impact on sunspace energy delivery than the solar radiation incident on the wall. Development of such a relation would be difficult, and its utility would be limited to sunspace systems.

Once the auxiliary energy requirement of a zero thermal storage capacity sunspace system has been quantified--assuming the above problem can be solved--a correlation for finite capacitance systems must be developed. Monsen (14,15) gives relations for finite capacitance direct gain and collector storage wall systems. One of the independent variables in these formulations is the effective building capacitance. This corresponds with the effective building capacitance of the TRNSYS Type 12 and Type 19 building load models. Single node effective capacitance is meant to be a representation of the distributed capacitance of an actual building. Recent studies by Horn (41) cast doubt on the accuracy of methods employing the effective capacitance concept. Horn found that in addition to being difficult to determine, effective building capacitance varied with building temperature and the month.

In light of the above considerations, a design method which includes utilizability concepts will not be pursued further.

4.6 Prediction of Building Auxiliary Heating Requirements

A method for predicting the monthly energy delivery of a sunspace system with a thermally conductive common wall was developed in Section 4.4. The objective of this section is to determine how the sunspace energy delivery reduces the auxiliary heating requirements of the building.

The unutilizability approach to predicting building auxiliary heating requirements calculates the effect of internal energy gains, not including the passive solar component delivery, by using Equations 4.5.2 and 4.5.3. A balance point temperature is computed for the non-solar portion of the building, and L_a (the auxiliary requirement of the building if the solar component was replaced by an adiabatic wall) is computed using balance temperature degree-days. The effect of the solar component on building auxiliary heating is considered separately.

Implicit in the unutilizability formulation is the assumption that the non-solar internal gains never cause the building temperature to rise above the heating set point. For most residences, this assumption is relatively accurate for computing heating loads, yet is not justified for "superinsulated" houses or some commercial buildings.

Treating solar energy delivered to the building differently than other building internal gains is somewhat artificial. One unit of

solar energy has the same effect as one unit of energy from non-solar internal gains, providing that the time distribution of energy is the same. Building temperature may rise above the heating set point due to large non-solar internal gains, as well as from solar energy delivery. This section discusses a design method which treats solar energy delivery in the same fashion as other building internal gains.

The method is based on the same reduced temperature degree-day calculations discussed in Section 4.5.1 for calculating L_a. Relevant equations are repeated here for completeness. First, a reduced base temperature for the month is calculated:

$$T_b = \overline{T}_r - \dot{g}/(UA)_a \qquad 4.6.1$$

The internal gains term, $\dot{g}$, in Equation 4.6.1 now includes a monthly average daily heat generation of appliances, people, etc., as in Equation 4.5.2, and monthly average sunspace energy, Q_{in}. (Note that it is possible for T_b to be greater than T_r.) The monthly auxiliary heating requirement is then calculated by multiplying the non-solar building loss coefficient, $(UA)_a$, by the balance temperature degree days:

$$Q_{aux} = (UA)_a \, (DD)_b \qquad 4.6.2$$

The balance temperature is different for every month since Q_{in} varies widely. It is recommended that variable base temperature degree-days be calculated from the relations of Erbs (37) if actual

data is unavailable.

Use of Equation 4.4.8 for Q_{in} and Equation 4.6.1 for the base temperature, T_b, requires the monthly average building temperature $\overline{T}_r$. If the monthly average building temperature is assumed to be equal to the heating set point, Equation 4.6.2 is equivalent to Equation 4.5.1 for the auxiliary energy requirement of an infinite thermal storage sunspace system. The base temperature of Equations 4.6.1 and 4.6.2 is not the same as that of Equations 4.5.2 and 4.5.3, however, since in this section $\dot{g}$ includes the sunspace gains, Q_{in}. For buildings with large non-solar building loads, L_a, and relatively small <u>total</u> internal gains, $\dot{g}$, the assumption that $\overline{T}_r = T_{set}$ is correct. Auxiliary heating energy must be continuously supplied to maintain the building at the heating set temperature. For months and systems where L_a and $\dot{g}$ approach the same order of magnitude, the average building temperature rises above T_{set}. The error in calculated auxiliary energy arising from assuming $\overline{T}_r = T_{set}$ is dependent on L_a, $\dot{g}$, and the actual building thermal storage capacity. It is possible to approximate the effect of thermal storage capacity in months with relatively large total internal gains (28). But, for most systems, the effect on annual heating loads is small. L_a and Q_{in} are usually similar only in the spring and fall when the heating load is a small fraction of the total load. If the total internal gains are substantial for months with a significant heating load, it is recommended that the effects of building capacitance be considered. In this case an iterative solution is necessary since

Q_{in} depends on the average building temperature (see Equation 4.4.8).

Auxiliary energy requirements using $\overline{T}_r = T_{set} = 17.2$ C were predicted for the sunspace geometry of Figure 2.2 in six locations. Intermediate monthly design method quantities are compared in Figures 4.3 and 4.5. The monthly predicted auxiliary energy requirements are plotted against values from detailed TRNSYS simulations in Figure 4.6. The TRNSYS simulations assumed an effective building capacitance of 5000 KJ/C. This is a typical assumed effective capacitance for the building loss coefficient, $(UA)_a$, of 158 W/C.

The average annual deviation in predicted auxiliary energy consumption was 1.27 GJ for the six locations. The worst comparison occurred in Albuquerque, New Mexico, where the annual difference was 1.92 GJ or 17.6 percent. Table 4.2 contains monthly values for Albuquerque. It is seen that the differences in computed monthly auxiliary energy use arise mainly in months where Q_{in} is greater than or approximately equal to L_a, causing the building temperature to rise above the heating set point. L_a was calculated by multiplying the non-solar building loss coefficient by the degree-days for a base temperature of 17.2 C.

At this point, it is tempting to compute a "solar fraction" for the sunspace system. The ambiguity and hence the inaccuracy of the term lies in defining the base load for the system. If the sunspace is replaced by an adiabatic wall, the base load is simply L_a. However, no practical wall is truly adiabatic, and the most logical base load is the building auxiliary heat requirement if the sunspace

Figure 4.6

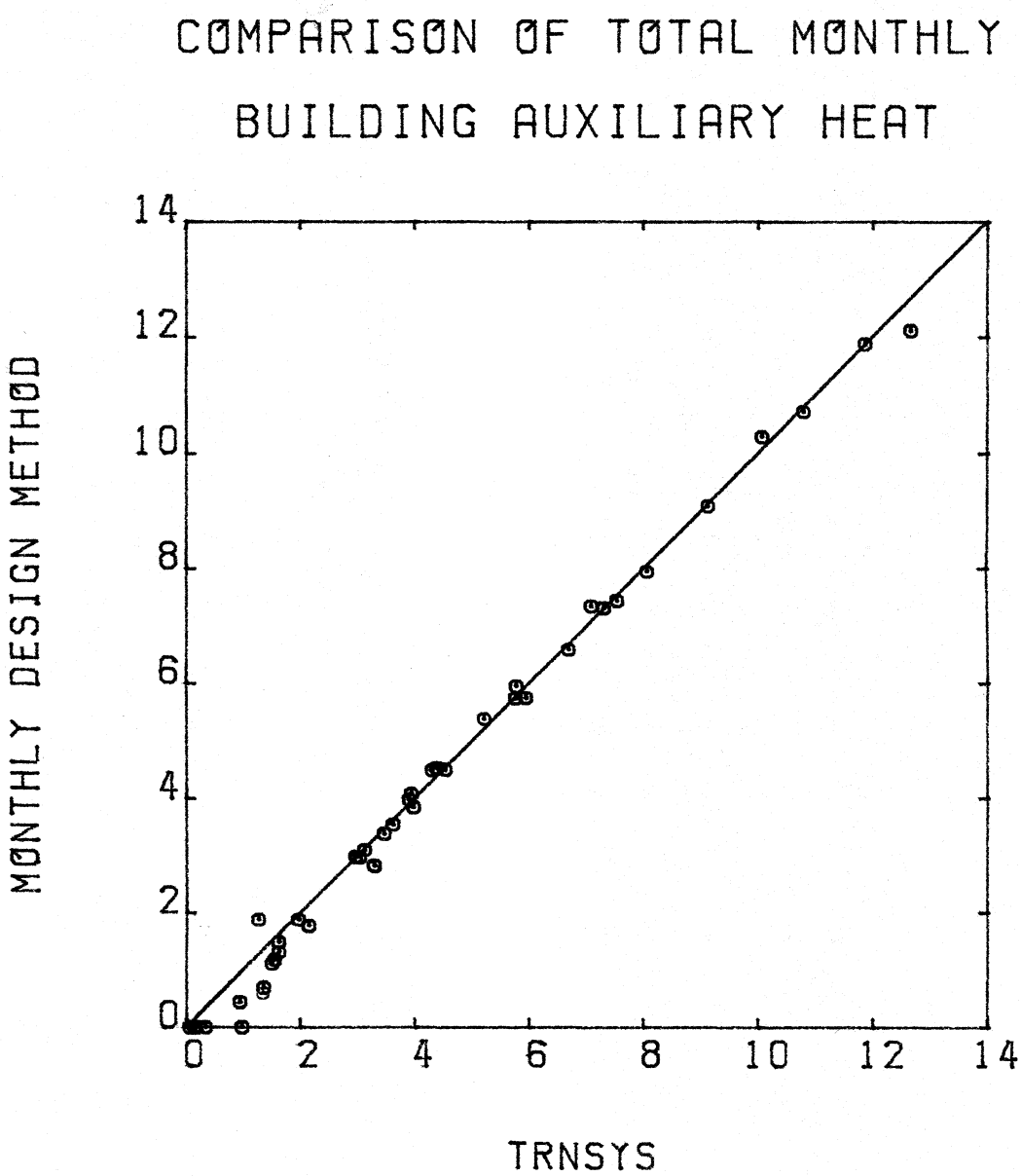
COMPARISON OF TOTAL MONTHLY
BUILDING AUXILIARY HEAT
MONTHLY DESIGN METHOD
TRNSYS
0
2
4
6
8
10
12
14

were replaced by a wall similar to the rest of the building walls. The "solar fraction" would then depend on the building construction. No "solar fraction" is defined in this thesis as the true figure of merit is the life cycle saving (16) or energy use of the sunspace system compared to a building of conventional construction.

However, for the example of Table 4.2, where the worst case comparison of six locations between the design method and TRNSYS results is presented, it is observed that the sunspace provides a large portion of the heating requirement of the building. The design method does an adequate job of predicting the reduction in annual auxiliary heating requirement. More importantly, effects of changing the sunspace design can be evaluated.

Table 4.2

Comparison of Monthly Design Method and TRNSYS Simulation for Albuquerque, New Mexico

	Design Method					TRNSYS	
Month	L_a	Q_{in}	T_b	DD_b	Q_{aux}	Q_{aux}	$\overline{T}_{rm}$
October	1.87 GJ	4.79 GJ	5.88 C	0	0.0 GJ	0.18 GJ	23.16 C
November	4.40	3.95	7.55	33	0.45	0.94	18.74
December	6.40	3.42	9.12	218	2.98	2.96	17.43
January	6.68	3.14	9.78	259	3.54	3.61	17.24
February	5.29	3.42	8.24	137	1.86	1.95	18.30
March	4.45	4.25	7.20	14	0.19	1.25	19.24
April	2.23	3.92	7.63	0	0.00	0.05	22.52
	31.32	26.89		661	9.02	10.94	

Chapter 5: Summary and Recommendations

5.1 Summary

The objectives of this study were to develop a TRNSYS sunspace component, identify important parameters which govern sunspace performance, and develop a simplified design procedure for predicting the auxiliary heating requirements of a building with an attached sunspace.

Chapter 2 describes the TRNSYS sunspace component. The model is versatile and, when coupled with the many other TRNSYS components, a wide variety of systems and configurations may be simulated.

The parametric studies of Chapter 3 identify the important variables in determining sunspace performance. The studies also illustrate the utility of the TRNSYS component and the numerous possibilities for future work. One of the major conclusions of Chapter 3 was: performance of sunspace systems with thermally conductive common walls is not a strong function of venting air mass flow rate.

This conclusion led to the development of a monthly-based design method for sunspace systems with thermally conductive common walls. The results of the design method compare closely to detailed TRNSYS simulation results.

5.2 Recommendations

One of the main limitations of both the sunspace TRNSYS component and subroutine RAD, used for calculating monthly average incident radiation, is that the geometric apportioning of beam radia-

tion to the sunspace surfaces (see Section 2.2.3) assumes the sunspace faces south (or north in the southern hemisphere). Deviations of more than about 15 degrees in the azimuth angle, γ, will significantly affect the actual incident radiation values. If the accurate apportioning of beam radiation to the sunspace surfaces is to be maintained, modifying the computer routines would involve redefining δ, the angle of the solar beam radiation projected on the plane of the sunspace wall (Equation 2.3.1 and Figure 2.4).

In addition, for large values of γ, another assumption is more problematic; namely, that the same amount of radiation which passes into the sunspace through one glazed end surface passes out through the other end glazing. The assumption is never strictly true, since the angle of incidence for beam radiation entering the sunspace is different for radiation passing through an end wall than for the radiation which passes through one of the front glazings. This leads to different transmitted radiation fractions. Yet, for a south-facing sunspace, the largest errors in glazing transmittance occur near sunrise and sunset when the radiation intensity is low, therefore, the overall effect of the assumption is small. This is not true if γ is large. The difference in glazing transmittance should be included in formulating routines for non-south-facing sunspaces. The more complex geometric beam radiation apportioning needed for off-south orientations could easily include an option for sunspace end walls which are opaque to solar radiation.

The greatest limitation of the design method of Chapter 4 is that the calculation of sunspace energy delivery is specific to unvented, thermally-conductive common wall systems. If the conductive common wall is relatively thin (0.1 to 0.4 m), venting of the sunspace air to the building does not have a significant effect on the building auxiliary energy consumption. However, for thicker, thermally massive and insulated common walls, the venting air mass flow rate does effect the system performance. A simplified method of predicting the energy delivery of vented sunspace systems would greatly enhance the utility of the design method, as many retrofit applications employ insulated common walls.

Another possible refinement of the design method is to include the effect of building capacitance. This would enable more accurate prediction of auxiliary energy consumption when the sunspace energy delivery meets a large portion of the building load. Including capacitance effects on a simplified monthly basis would most likely involve use of a lumped "effective" building capacitance. Perhaps relations between $\overline{T}_r - T_{set}$ and Q_{in}/L_a could be developed for different values of building capacitance. Further work on establishing relations which determine the value of effective capacitance would be also helpful in this respect.

Section 3.3.5 touches briefly on the effect of sunspaces on building summer cooling loads. Further work on cooling loads induced by passive solar components, direct gain windows, and collector-storage walls (as well as sunspaces), would enable designers of these

systems to consider the total impact of these components on the building.

Studies of combined passive systems would also be useful. A direct gain window results in building energy gains when the sun is shining. A collector-storage wall or a sunspace with a thermally conductive common wall will delay the energy gains. A properly-designed combined system could provide evenly distributed energy delivery, which would alleviate overheating problems.

Finally, so-called "hybrid" solar energy systems should be investigated. Hybrid systems couple the sunspace or collector-storage wall to some sort of energy storage, such as a rock bed. Heated air (vented from the solar component) can be diverted to storage whenever energy gains exceed building load. The stored energy can then be used to offset building heating loads during periods of little or no sunshine.

Research concerning building-integrated solar energy components should continue. Coupled with energy conservation measures and other renewable energy technologies, passive solar components have a strong potential for reducing our dependence on fossil fuels.

APPENDIX OF COMPUTER ROUTINES

```
PARAMETERS

1.WALL HEIGHT (METERS)
2.WALL THICKNESS (METERS)
3.FLOOR LENGTH (METERS)
4.FLOOR THICKNESS (METERS)
5.SUNSPACE WIDTH (METERS)
6.HORIZONTAL DISTANCE FROM THE INTERSECTION OF GLAZING & GROUND
  TO THE INTERSECTION OF THE GLAZINGS (METERS)
7.VERTICAL DISTANCE FROM THE FLOOR TO THE INTERSECTION
  OF THE GLAZINGS (METERS)
8.NUMBER OF THICKNESS NODES IN THE WALL
9.NUMBER OF THICKNESS NODES IN THE FLOOR
10.CONDUCTIVITY OF THE WALL (W/M-C)
11.CONDUCTIVITY OF THE FLOOR (W/M-C)
12.DENSITY-SPECIFIC HEAT PRODUCT OF THE WALL (KJ/M**3-C)
13.DENSITY-SPECIFIC HEAT PRODUCT OF THE FLOOR (KJ/M**3-C)
14.SOLAR ABSORBTIVITY OF THE WALL
15.INFRARED EMMITTANCE OF THE WALL
16.SOLAR ABSORBTIVITY OF THE FLOOR
17.INFRARED EMMITTANCE OF THE FLOOR
18.NUMBER OF COVERS
19.INFRARED EMMITTANCE OF THE GLAZING
20.EXTINCTION-THICKNESS COEFFICIENT OF THE GLAZING (PER SHEET)
21.REFRACTIVE INDEX OF THE COVER MATERIAL
22.R-VALUE OF THE COVER(S) (M**2-C/W)
23.R-VALUE OF THE GLAZING NIGHT INSULATION (M**2-C/W)
24.R-VALUE OF THE FLOOR INSULATION (M**2-C/W)
25.AIR CHANGE RATE (CHANGES/HOUR)
26.FRACTION OF GLAZING SURFACE WHICH IS OPAQUE TO SOLAR RADIATION
27.INITIAL TEMPERATURE OF MASS NODES
28.EFFECTIVE R-VALUE OF THE GROUND (M**2-C/W)
29.AVERAGE HEIGHT OF THE EXTRA THERMAL MASS CONTAINERS (METERS)
30.AVERAGE WIDTH OF THE EXTRA THERMAL MASS CONTAINERS (METERS)
31.THERMAL MASS-SPECIFIC HEAT PRODUCT OF ADDITIONAL MASS (KJ/C)
32.SURFACE AREA OF ADDITIONAL THERMAL MASS (M**2)
33.SOLAR ABSORBTIVITY OF THE ADDITIONAL THERMAL MASS CONTAINERS
34.INFRARED EMMITTANCE OF THE ADDITIONAL THERMAL MASS CONTAINERS

INPUTS

1.CONTROL FUNCTION FOR VENTING MASS FLOW, 1:TO ROOM   0:NO VENTING
  -1:TO AMBIENT
2.CONTROL FUNCTION FOR GLAZING NIGHT INSULATION, 0:NOT USED 1:IN PLACE
```

3.GROUND TEMPERATURE (C)
4.AMBIENT TEMPERATURE (C)
5.ROOM TEMPERATURE (C)
6.OUTSIDE GLAZING TO AMBIENT CONVECTION COEFFICIENT (W/M**2-C)
7.HEAT TRANSFER COEFFICIENT BETWEEN WALL AND ROOM INCLUDING RADIATION
(W/M**2-C)
8.CONVECTION COEFFICIENT BETWEEN FLOOR AND SUNSPACE AIR (W/M**2-C)
9.CONVECTION COEFFICIENT BETWEEN WALL AND SUNSPACE AIR (W/M**2-C)
10.CONVECTION COEFFICIENT BETWEEN GLASS AND SUNSPACE AIR (W/M**2-C)
11.BEAM RADIATION INCIDENT ON UPPER GLAZING (KJ/M**2-HR)
12.DIFFUSE RADIATION INCIDENT ON UPPER GLAZING (KJ/M**2-HR)
13.BEAM RADIATION INCIDENT ON LOWER GLAZING (KJ/M**2-HR)
14.DIFFUSE RADIATION INCIDENT ON LOWER GLAZING (KJ/M**2-HR)
15.ANGLE OF INCIDENCE FOR UPPER GLAZING (DEGREES)
16.ANGLE OF INCIDENCE FOR LOWER GLAZING (DEGREES)
17.SOLAR ZENITH ANGLE (DEGREES)
18.SOLAR AZIMUTH ANGLE (DEGREES)
19.VENTING AIR MASS FLOW RATE FROM ROOM OR AMBIENT (KG/HR)
20.RATE OF ADDING AUXILARY ENERGY TO SUNSPACE AIR (KJ/HR)
21.CONVECTION COEFFICIENT FROM EXTRA MASS TO SUNSPACE AIR (W/M**2-C)

OUTPUTS

1.RATE OF ENERGY DELIVERY TO THE ADJOINING ROOM (KJ/HR)
2.RATE OF INTERNAL ENERGY STORED IN THE SUNSPACE (KJ/HR)
3.RATE OF SOLAR ENERGY PASSING THROUGH THE GLAZING (KJ/HR)
4.RATE OF SOLAR ENERGY ABSORBED BY THE WALL, FLOOR AND ADDITIONAL
THERMAL MASS (KJ/HR)
5.RATE OF HEAT LOSS TO AMBIENT (KJ/HR)
6.RATE OF ENERGY DELIVERY TO THE ROOM BY CONDUCTION (KJ/HR)
7.RATE OF ENERGY LOSS TO AMBIENT BY CONDUCTION THROUGH GLAZING (KJ/HR)
8.RATE OF ENERGY LOSS TO THE GROUND (KJ/HR)
9.TEMPERATURE OF THE SUNSPACE AIR (C)
10.INSIDE GLAZING TEMPERATURE (C)
11.TEMPERATURE OF THE WALL SURFACE ON THE SUNSPACE SIDE (C)
12.TEMPERATURE OF FIRST INTERIOR WALL NODE (C)
10+I.TEMPERATURE OF WALL OR FLOOR NODE I (C)
10+NMN. TEMPERATURE OF BOTTOM FLOOR NODE (C)
11+NMN.TEMPERATURE OF EXTRA MASS NODE (C)
12+NMN.INTERNAL TIMESTEP (HR)
13+NMN.VENTING MASS FLOW RATE (KG/HR)

```
C   THIS TRNSYS SUBROUTINE CALCULATES THE ENERGY FLOWS AND TEMPERATURES
C   FOR AN ATTACHED SUNSPACE.  FOR A LIST OF PARAMETERS, INPUTS, AND
C   OUTPUTS OR A DETAILED DISCUSSION OF THE COMPONENT SEE B.
C   PARSONS MASTERS THESIS; UNIVERSITY OF WISCONSIN-MADISON, 1983.
      SUBROUTINE TYPE37(TIME,XIN,OUT,T,DTDT,PAR,INFO)
      COMMON /SIM/ TIMEO,TIMEF,DELT
      DIMENSION XIN(21),OUT(20),PAR(50),INFO(10),
     2F(4,4),EIR(4),ES(4),RSR(4,4),RIR(4,4),T(20)
     2 ,FHAT(4,4),FHATS(4,4),FDL(4),FDU(4),
     2 BU(4),BL(4),RAD(4),COND(4,4),QSRAD(4),TM(21),QDTDT(21),TI(21),
     2 ROH(4),DTDT(21),DUMMY(4)
      DATA SIGMA/.20411E-06/RHO/1.204/
      DATA CP/1.012/AB/273.3/
      IF(INFO(7).GT.-1)GOTO 55
C     SET PARAMETERS
      XLW=PAR(1)
      THW=PAR(2)
      XLFL=PAR(3)
      THF=PAR(4)
      WTH=PAR(5)
      HC=PAR(6)
      VG=PAR(7)
      NWL=PAR(8)
      NFL=PAR(9)
      WK=PAR(10)
      FK=PAR(11)
      RCPW=PAR(12)
      RCPF=PAR(13)
      ES(1)=PAR(14)
      EIR(1)=PAR(15)
      ES(2)=PAR(16)
      EIR(2)=PAR(17)
      NCOV=IFIX(PAR(18)+.1)
      EIR(3)=PAR(19)
      XKL=PAR(20)
      RI=PAR(21)
      RGL=PAR(22)
      RNI=PAR(23)
      RFI=PAR(24)
      RATE=PAR(25)
      SFRAC=PAR(26)
      NFI=NWL+1
      NMN=NWL+NFL
      TIN=PAR(27)
      RGR=PAR(28)
      NSUR=3
```

```
      EIR(4)=0.
      ES(4)=0.
      NEM=NMN
      IF(INFO(4).LT.29) GOTO 5
      NEM=NMN+1
      HTM=PAR(29)
      WDM=PAR(30)
      CAPX=PAR(31)
      XSA=PAR(32)
      EIR(4)=PAR(34)
      ES(4)=PAR(33)
      NSUR=4
5     CONTINUE
       INFO(6)=NEM+12
C  INITIALIZE AIR AND GLAZING TEMPS
      DO 10 I=1,NEM
10    TM(I)=TIN
      XNC=FLOAT(NCOV)
      TGLI=(TM(1)*XNC+XIN(4))/(XNC+1.)
      TSS=(TM(1)+TGLI)/2.
      TGLO=TGLI
C       CALCULATION OF SUNSPACE GEOMETRY
      AFL=XLFL*WTH
      AWL=XLW*WTH
      VC=XLW-VG
      HG=XLFL-HC
      XUG=SQRT(VC**2+HC**2)
      AUG=XUG*WTH
      XLG=SQRT(HG**2+VG**2)
      ALG=XLG*WTH
      XAR=VG*HC+(HG*VG+HC*VC)/2.
      AGL=2.*XAR+AUG+ALG
      BETA=0.0
      PHI=1.5707963
      IF(HC.GT.0.)BETA=ATAN(VC/HC)
      IF(HG.GT.0.)PHI=ATAN(VG/HG)
      NPAR=28
      NINP=20
      IF(NSUR.LE.3)GOTO 15
      NPAR=34
      NINP=21
      A1=ATAN(VA/WDM)
      A2=ATAN(VG/HA)
      A3=ATAN(HC/VA)
15      CALL TYPECK(1,INFO,NINP,NPAR,0)
C   SET CONSTANT HEAT TRANSFER COEFF.
      DXW=THW/(NWL-1)
```

```
      DXF=THF/(NFL-1)
      H1=3.6*WK/DXW*AWL
      H3=3.6*FK/DXF*AFL
      IF(RFI.LE.0.AND.RGR.LE.0.) WRITE(*,20)
20    FORMAT(' ERROR CHECK GROUND R-VALUE')
      H4=3.6*AFL/(RFI+RGR)
      CAPW=DXW*RCPW*AWL
      CAPF=DXF*RCPF*AFL
      H12=RATE*XAR*WTH*RHO*CP
C      CALCULATE VIEW FACTORS
      DIAG1=SQRT(XLFL**2+XLW**2)
      IF(NSUR.EQ.3) GOTO 25
      HA=XLFL-WDM-HG
      VA=XLW-HTM-VC
      D2=SQRT(HA**2+VA**2)
      D3=SQRT(HA**2+(VA+HTM)**2)
      D4=SQRT(VA**2+HC**2)
      D5=SQRT((HG+HA)**2+HTM**2)
      D6=SQRT(WDM**2+(VA+VC)**2)
      F(1,1)=0.
      F(2,2)=0.
      F(4,4)=0.
      F(1,2)=(WDM+D5+D6+HTM-DIAG1-WDM-HTM)/((VA+VC)*2.)
      F(2,1)=F(1,2)*(VA+VC)/(HG+HA)
      F(1,3)=(VA+VC+DIAG1-WDM-D5)/(2.*(VA+VC))
      F(3,1)=F(1,3)*(VA+VC)/(XLG+XUG)
      F(1,4)=1.-F(1,2)-F(1,3)
      F(4,1)=F(1,4)*(VA+VC)/(WDM+HTM)
      F(2,3)=(D3+DIAG1-HTM-D6)/(2.*(HG+HA))
      F(3,2)=F(2,3)*(HG+HA)/(XLG+XUG)
      F(2,4)=1.-F(2,1)-F(2,3)
      F(3,4)=(D6+HTM+D5+WDM-HG-HA-VA-VC)/(2.*(XLG+XUG))
      F(4,3)=F(3,4)*(XUG+XLG)/(WDM+HTM)
      F(3,3)=1.-F(3,1)-F(3,2)-F(3,4)
      F(4,2)=F(2,4)*(HG+HA)/(HTM+WDM)
      FDU(1)=(XUG+VA+VC-D4)/(2.*XUG)
      FDU(2)=(DIAG1+D3-D6-HTM-XLG)/(2.*XUG)
      FDU(4)=(D6+HTM+D4-VA-VC-D3)/(2.*XUG)
      FDU(3)=1.-FDU(1)-FDU(2)-FDU(4)
      FDL(1)=(DIAG1+D4-D5-WDM-XUG)/(2.*XLG)
      FDL(2)=(XLG+HG+HA-D3)/(2.*XLG)
      FDL(4)=(D3+D5+WDM-D4-HG-HA)/(2.*XLG)
      FDL(3)=1.-FDL(1)-FDL(2)-FDL(4)
      GOTO 30
25    DIAG2=SQRT(HC**2+VG**2)
      F(1,1)=0.0
      F(2,2)=0.0
```

```
      F(1,2)=(XLW+XLFL-DIAG1)/(2.*XLW)
      F(2,1)=F(1,2)*XLW/XLFL
      F(1,3)=1.-F(1,2)
      F(3,1)=F(1,3)*XLW/(XUG+XLG)
      F(2,3)=1.-F(2,1)
      F(3,2)=F(2,3)*XLFL/(XUG+XLG)
      F(3,3)=1.-F(3,1)-F(3,2)
      FDU(1)=(XUG+XLW-DIAG2)/(XUG*2.)
      FDU(2)=(DIAG1+DIAG2-XLW-XLG)/(2.*XUG)
      FDU(3)=1.-FDU(1)-FDU(2)
      FDL(1)=(DIAG1+DIAG2-XUG-XLFL)/(2.*XLG)
      FDL(2)=(XLFL+XLG-DIAG2)/(2.*XLG)
      FDL(3)=1.-FDL(1)-FDL(2)
C  COMPUTE TRANSMITTANCE TO DIFFUSE & REFLECTIVITY TO SOLAR
30    ROHD=-1.
      TAUD=TALF(NCOV,60.,XKL,RI,1.,ROHD)
      ES(3)=1.-ROHD
C     COMPUTE REFLECTIVITY MATRICIES
      DO 35 I=1,NSUR
      DO 35 J=1,NSUR
      RIR(I,J)=(EIR(J)-1.)*F(I,J)
      FHAT(I,J)=0.0
      RSR(I,J)=(ES(J)-1.)*F(I,J)
      FHATS(I,J)=0.0
      IF(I.EQ.J) RIR(I,J)=RIR(I,J)+1.
35    IF(I.EQ.J) RSR(I,J)=RSR(I,J)+1.
C     CALCULATE FHATS & CONDUCTANCES
      D11=SIMUL(NSUR,RIR,DUMMY,1.0E-06,-1,4)
      D22=SIMUL(NSUR,RSR,DUMMY,1.0E-06,-1,4)
      DO 45 I=1,NSUR
      DO 45 K=1,NSUR
      DO 40 J=1,NSUR
      FHAT(I,K)=FHAT(I,K)+RIR(I,J)*F(J,K)
40    FHATS(I,K)=FHATS(I,K)+RSR(I,J)*F(J,K)
45    COND(I,K)=EIR(I)*EIR(K)*FHAT(I,K)*SIGMA
      ROH(1)=1.-ES(1)
      ROH(2)=1-ES(2)
      ROH(3)=ROHD
C  SET INITIAL VALUES OF CONDUCTANCES FOR TIMESTEP CHECK
      TGLIA=TGLI+AB
      TGLOA=TGLO+AB
      TWA=TM(1)+AB
      TAMBA=TAMB+AB
      TFA=TM(NFI)+AB
C     SET VARIABLE CONDUCTANCES
      H14=0.
      H15=0.
```

```
      H16=0.
      H17=0.
      IF(NSUR.LE.3) GOTO 50
      TMA=TM(NEM)+AB
      ROH(4)=1.-ES(4)
      AWL=(VA+VC)*WTH
      AFL=(HG+HA)*WTH
      H14=XSA*3.6*XIN(21)
      H15=COND(2,4)*AFL*(TFA**2+TMA**2)*(TFA+TMA)
      H16=COND(1,4)*AWL*(TWA**2+TMA**2)*(TWA+TMA)
      H17=COND(3,4)*(AUG+ALG)*(TGLIA**2+TMA**2)*(TGLIA+TMA)
50    H5A=SIGMA*EIR(3)*(TGLOA**2+TAMBA**2)*(TGLOA+TAMBA)*AGL
      H5B=3.6*XIN(6)*AGL
      H5=H5A+H5B
      IF(RGL.GT.0) H5=1./(1./H5+RGL/(AGL*3.6))
      H9=COND(1,3)*AWL*(TWA**2+TGLIA**2)*(TWA+TGLIA)
      H10=COND(1,2)*AWL*(TWA**2+TFA**2)*(TWA+TFA)
      H11=COND(2,3)*AFL*(TFA**2+TGLIA**2)*(TFA+TGLIA)
      IF(RNI.NE.0.AND.XIN(2).EQ.1)H5=1./(1./H5+RNI/(AGL*3.6))
55    IF(INFO(7).GT.0)GOTO 140
C     BEAM RADIATION CALCULATIONS
      DO 60 I=1,NSUR
      BU(I)=0.0
60    BL(I)=0.0
      TRAD=XIN(11)+XIN(12)+XIN(13)+XIN(14)
      IF(TRAD.GT.0.0001.AND.XIN(2).LT.0.5)GOTO 70
      DO 65 I=1,NSUR
65    RAD(I)=0.0
      GOTO 125
70    CONTINUE
      TSE=ATAN(TAN(XIN(17)/57.29578)*COS(XIN(18)/57.29578))
      IF (NSUR.LE.3) GOTO 100
      IF(TSE.NE.90.) GOTO 75
      BU(1)=1.
      BL(1)=VA/VG
      BL(4)=1.-BL(1)
      GOTO 115
75    IF(TSE.GT.0.) GOTO 85
      ANGCK=TSE+1.5707693
      BL(2)=1.
      BP1=XLW/TAN(ANGCK)
      BP2=VG/TAN(ANGCK)+HC
      IF(ANGCK.GT.A1) GOTO 80
      IF(BP1.LT.XLFL) THEN
      BU(3)=(BP2-XLFL)/(BP2-BP1)
      BU(2)=1.-BU(3)
      ELSE
```

```
      BU(3)=1
      ENDIF
      GOTO 115
80    BP3=HTM/TAN(ANGCK)+WDM
      BU(4)=(BP3-BP1)/(BP2-BP1)
      BU(3)=(BP2-XLFL)/(BP2-BP1)
      BU(2)=1.-BU(4)-BU(3)
      GOTO 115
85    CONTINUE
      ANGCK=1.5707963-TSE
      BP1=TAN(ANGCK)*HC
      BP2=TAN(ANGCK)*WDM+VG
      BP3=TAN(ANGCK)*XLFL+VG
      IF(TSE.LT.A3) GOTO 90
      BU(1)=1.
      BL(1)=(VA-BP1)/(BP3-BP1)
      BL(2)=(BP3-BP2)/(BP3-BP1)
      BL(4)=1.-BL(1)-BL(2)
      GOTO 115
90    IF(TSE.GT.A2) GOTO 95
      BL(2)=1
      BU(2)=(BP1-BP2)/(BP1+VC)
      BU(1)=(VA+VC)/(BP1+VC)
      BU(4)=1.-BU(1)-BU(2)
      GOTO 115
95    BL(2)=(BP3-BP2)/(BP3-BP1)
      BL(4)=1.-BL(2)
      BU(1)=(VA+VC)/(BP1+VC)
      BU(4)=1.-BU(1)
      GOTO 115
100   IF(XIN(17).NE.90.0) GOTO 105
      BU(1)=1
      BL(1)=1
      GOTO 115
105   IF(TSE.GE.0.0) GOTO 110
      ANGCK=TSE+1.5707963
      IF(ANGCK.GE.PHI)THEN
      BU(2)=1
      BL(2)=1
      ELSE
      WP=XLW/TAN(ANGCK)
      IF(WP.GE.XLFL) THEN
      BU(3)=1.
      ELSE
      CP=VG/TAN(ANGCK)
      OS=CP-HG
      SIS=XLFL-WP
```

```
      BU(2)=SIS/(SIS+OS)
      BU(3)=OS/(SIS+OS)
      ENDIF
      ENDIF
      GOTO 115
110   FP=HC-VG*TAN(TSE)
      IF(FP.LT.0.0) THEN
      FP=-FP
      BU(1)=1
      BL(1)=FP/(FP+XLFL)
      BL(2)=1-BL(1)
      ELSE
      BL(2)=1
      WP=FP/TAN(TSE)
      BU(2)=WP/(WP+XLW)
      BU(1)=1-BU(2)
      ENDIF
C   CALCULATE TRANSMITTANCE OF THE GLASS TO SOLAR
115   TALFU=TALF(NCOV,XIN(15),XKL,RI,1.0,ROHD)
      TALFL=TALF(NCOV,XIN(16),XKL,RI,1.0,ROHD)
C  COMPUTE TOTAL INCIDENT SOLAR
      DO 120 I=1,NSUR
120   RAD(I)=((FDU(I)*XIN(12)*AUG+FDL(I)*XIN(14)*ALG)*TAUD
     2 +BU(I)*AUG*XIN(11)*TALFU+BL(I)*ALG*XIN(13)*TALFL)*(1.-SFRAC)
125   CONTINUE
      TRADI=0.
      TRADAB=0.
      QSRAD(4)=0.
C TOTAL RAD INCIDENT & REFLECTED
      ES(3)=0.0
      DO 135 I=1,NSUR
      TRADI=TRADI+RAD(I)
      SQSFHR=0.0
      DO 130 J=1,NSUR
130   SQSFHR=SQSFHR +RAD(J)*ROH(J)*FHATS(J,I)
      QSRAD(I)=ES(I)*(RAD(I)+SQSFHR)
135   TRADAB=TRADAB+QSRAD(I)
C   SET INPUT TEMPERATURES
140   TGR=XIN(3)
      TAMB=XIN(4)
      TRM=XIN(5)
      QV=0.
      QAMB=0.
      QRMC=0.
      QRMT=0.
      QGR=0.
      QSTORE=0.
```

```
      QGL=0.
C  CHECK FOR EXTERNAL ITERATIONS
      IF(INFO(7).GT.0)THEN
      DO 145 I=1,NEM
145   TM(I)=TI(I)
      ELSE
      DO 150 I=1,NEM
150   TI(I)=TM(I)
      ENDIF
      H2=3.6*XIN(7)*AWL
      H5B=3.6*XIN(6)*AGL
      H6=XIN(10)*3.6*AGL
      H7=XIN(9)*3.6*AWL
      H8=XIN(8)*3.6*AFL
      IF(NSUR.GT.3) H14=XSA*3.6*XIN(21)
C  TIME STEP CHECK
      CK1=CAPW/2./(H1+H7+H9+H11+H16)
      CK2=CAPW/2./(H1+H2)
      CK3=CAPF/2./(H3+H8+H10+H11+H15)
      CK4=CAPF/2./(H3+H4)
      CK5=1.
      IF(NSUR.GT.3) CK5=CAPX/(H15+H14+H16+H17)
      DTMAX=MIN(CK1,CK2,CK3,CK4,CK5)
      NTS=IFIX(DELT/DTMAX+1)
      DTMAX=DELT/FLOAT(NTS)
      DO 225 ITS=1,NTS
      NCHECK=0
155   IF(NCHECK.GT.20)GOTO 185
      TSSOLD=TSS
      TGLIA=TGLI+AB
      TGLOA=TGLO+AB
      TWA=TM(1)+AB
      TAMBA=TAMB+AB
      TFA=TM(NFI)+AB
C     SET VARIABLE CONDUCTANCES
      H5A=SIGMA*EIR(3)*(TGLOA**2+TAMBA**2)*(TGLOA+TAMBA)*AGL
      H5=H5A+H5B
      IF(RGL.GT.0) H5=1./(1./H5+RGL/(AGL*3.6))
      H9=COND(1,3)*AWL*(TWA**2+TGLIA**2)*(TWA+TGLIA)
      H10=COND(1,2)*AWL*(TWA**2+TFA**2)*(TWA+TFA)
      H11=COND(2,3)*AFL*(TFA**2+TGLIA**2)*(TFA+TGLIA)
      IF(RNI.NE.0.AND.XIN(2).EQ.1)H5=1./(1./H5+RNI/(AGL*3.6))
      IF(NSUR.EQ.3) GOTO 160
      TMA=TM(NEM)+AB
      H15=COND(2,4)*AFL*(TFA**2+TMA**2)*(TFA+TMA)
      H16=COND(1,4)*AWL*(TWA**2+TMA**2)*(TWA+TMA)
      H17=COND(3,4)*(AUG+ALG)*(TGLIA**2+TMA**2)*(TGLIA+TMA)
```

```
160   AMDOT=XIN(19)
      H13=AMDOT*CP
      IF(XIN(1)) 165,175,170
165   TS=TAMB
      EA=1.
      RM=0
      GOTO 180
170   TS=TRM
      RM=1
      EA=0
      GOTO 180
175   TS=TSS
      EA=0
      RM=0
      AMDOT=0.
180   CONTINUE
C  FIND GLASS &MEAN AIR TEMP
      F1=(H6+H7+H8+H12+H13+H14)/H6
      F2=H5+H6+H9+H11+H17
      F3=H6-F1*F2
      F4=H12+H5*F1
      F5=H7+H9*F1
      F6=H8+H11*F1
      F7=H14+H17*F1
      TGLI=-(TAMB*F4+TM(1)*F5+TM(NFI)*F6+TM(NEM)*F7+TS*H13+XIN(20))/F3
      TSS=(TGLI*F2-H5*TAMB-H9*TM(1)-H11*TM(NFI)-H17*TM(NEM))/H6
      QGLI=H5*(TGLI-TAMB)
      TGLO=TGLI-QGLI*RGL/(3.6*AGL)
      NCHECK=NCHECK+1
      DTAIR=TSSOLD-TSS
      IF(ABS(DTAIR).GT.0.01)GOTO 155
185   TO=TSS
C     CALCULATE HEAT FLUXES
      QV=H13*(TSS-TS)
      QAMB=(QGLI+H12*(TSS-TAMB)+QV*EA)/NTS+QAMB
      QRMC=H2*(TM(NWL)-TRM)/NTS+QRMC
      QRMT=(H2*(TM(NWL)-TRM)+QV*RM)/NTS+QRMT
      QGR=H4*(TM(NMN)-TGR)/NTS+QGR
      QGL=H5*(TGLI-TAMB)/NTS+QGL
      QDTDT(1)=(QSRAD(1)+(TM(2)-TM(1))*H1+(TGLI-TM(1))*H9+(TM(NF1)-TM(1)
     2 )*H10 +(TSS-TM(1))*H7+H16*(TM(NEM)-TM(1)))
      IF(NSUR.GT.3) QDTDT(NEM)=H14*(TSS-TM(NEM))+H15*
     2 (TM(NFI)-TM(NEM))+H16*(TM(1)-TM(NEM))+QSRAD(4)+H17*(TGLI-TM(NEM))
      NM1=NWL-1
      DO 190 I=2,NM1
190   QDTDT(I)=(TM(I-1)+TM(I+1)-2.*TM(I))*H1
      QDTDT(NWL)=((TRM-TM(NWL))*H2+(TM(NM1)-TM(NWL))*H1)
```

```
      QDTDT(NFI)=((TM(1)-TM(NFI))*H10+(TSS-TM(NFI))*H8+(TGLI-TM(NFI))
     2 *H11+(TM(NFI+1)-TM(NFI))*H3+QSRAD(2)+H15*(TM(NEM)-TM(NFI)))
      NFF=NMN-1
      DO 195 I=NFI+1,NFF
195   QDTDT(I)=(TM(I-1)+TM(I+1)-2.*TM(I))*H3
      QDTDT(NMN)=((TGR-TM(NMN))*H4+(TM(NFF)-TM(NMN))*H3)
C  CALC NEW TEMPERATURES OF MASS NODES
      IF(TIME.EQ.TIME0) GOTO 210
      TM(1)=TM(1)+QDTDT(1)*DTMAX*2./CAPW
      DO 200 I=2,NWL-1
200   TM(I)=TM(I)+QDTDT(I)*DTMAX/CAPW
      TM(NWL)=TM(NWL)+QDTDT(NWL)*DTMAX*2./CAPW
      TM(NFI)=TM(NFI)+QDTDT(NFI)*DTMAX*2./CAPF
      DO 205 I=NFI+1,NMN-1
205   TM(I)=TM(I)+QDTDT(I)*DTMAX/CAPF
      TM(NMN)=TM(NMN)+QDTDT(NMN)*DTMAX*2./CAPF
      IF(NSUR.GT.3) TM(NEM)=TM(NEM)+QDTDT(NEM)*DTMAX/CAPX
210   QST=0.
      DO 220 I=1,NEM
220   QST=QST+QDTDT(I)
      QSTORE=QSTORE+QST/NTS
225   CONTINUE
C  SET OUTPUTS
      OUT(1)=QRMT
      OUT(2)=QSTORE
      OUT(3)=TRADI
      OUT(4)=TRADAB
      OUT(5)=QAMB
      OUT(6)=QRMC
      OUT(7)=QGL
      OUT(8)=QGR
      OUT(9)=TO
      OUT(10)=TGLI
      DO 230 I=1,NEM
230   OUT(10+I)=TM(I)
      OUT(11+NEM)=DTMAX
      OUT(12+NEM)=AMDOT
      RETURN
      END
```

Function SIMUL

Call statement

D = SIMUL (N,A,X,EPS,INDIC,NRC)

Passed Arguments

N: number of rows in matrix A

A: coefficient matrix

X: solution vector

EPS: tolerance for a singular matrix

INDIC: control function

< 0 compute inverse of A in place

0 solve augmented matrix of N x N + 1

> 0 solve the system but don't invert A

NRC: dimension of matrix A

Returned Arguments

D: determinant of the matrix

Program is taken from Applied Numerical Methods by Carnahan, Luther and Wilkes, Wiley, New York (1969).

```
      FUNCTION SIMUL(N,A,X,EPS,INDIC,NRC)
      DIMENSION IROW(50),JCOL(50),JORD(50),Y(50),A(NRC,NRC),X(N)
      MAX=N
      IF(INDIC.GE.0) MAX=N+1
      IF(N.LE.50) GO TO 5
      WRITE(*,200)
      SIMUL=0.
      RETURN
5     DETER=1.
      DO 18 K=1,N
      KM1=K-1
      PIVOT=0.
      DO 11 I=1,N
      DO 11 J=1,N
      IF(K.EQ.1) GO TO 9
      DO 8 ISCAN=1,KM1
      DO 8 JSCAN=1,KM1
      IF(I.EQ.IROW(ISCAN) ) GO TO 11
      IF(J.EQ.JCOL(JSCAN) ) GO TO 11
8     CONTINUE
9     IF (ABS(A(I,J)).LE.ABS(PIVOT) ) GO TO 11
      PIVOT=A(I,J)
      IROW(K)=I
      JCOL(K)=J
11    CONTINUE
      IF(ABS(PIVOT).GT.EPS) GO TO 13
      SIMUL=0.
      RETURN
13    IROWK=IROW(K)
      JCOLK=JCOL(K)
      DETER=DETER*PIVOT
      DO 14 J=1,MAX
14    A(IROWK,J)=A(IROWK,J)/PIVOT
      A(IROWK,JCOLK)=1./PIVOT
      DO 18 I=1,N
      AIJCK=A(I,JCOLK)
      IF(I.EQ.IROWK) GO TO 18
      A(I,JCOLK)= -AIJCK/PIVOT
      DO 17 J=1,MAX
17    IF(J.NE.JCOLK) A(I,J)=A(I,J)-AIJCK*A(IROWK,J)
18    CONTINUE
      DO 20 I=1,N
      IROWI=IROW(I)
      JCOLI=JCOL(I)
      JORD(IROWI)=JCOLI
20    IF(INDIC.GE.0) X(JCOLI)=A(IROWI,MAX)
```

```
      INTCH=0
      NM1=N-1
      DO 22 I=1,NM1
      IP1=I+1
      DO 22 J=IP1,N
      IF(JORD(J).GE.JORD(I)) GO TO 22
      JTEMP=JORD(J)
      JORD(J)=JORD(I)
      JORD(I)=JTEMP
      INTCH=INTCH+1
22    CONTINUE
      IF (INTCH/2*2.NE.INTCH) DETER=-DETER
      IF(INDIC.LE.0) GO TO 26
      SIMUL=DETER
      RETURN
26    DO 28 J=1,N
      DO 27 I=1,N
      IROWI=IROW(I)
      JCOLI=JCOL(I)
27    Y(JCOLI)=A(IROWI,J)
      DO 28 I=1,N
28    A(I,J)=Y(I)
      DO 30 I=1,N
      DO 29 J=1,N
      IROWJ=IROW(J)
      JCOLJ=JCOL(J)
29    Y(IROWJ)=A(I,JCOLJ)
      DO 30 J=1,N
30    A(I,J)=Y(J)
      SIMUL=DETER
      RETURN
200   FORMAT('N TOO BIG')
      END
```

Subroutine RAD

Call Statement:

Call RAD (MN,H,ALAT,AZMTH,RHO,NG,RI,XKL,HGT,WD,HOR,VER,
XLN,RADI,XKT,RBARV,RN,GN)

Passed Arguments:

MN: month

H: monthly average daily horizontal radiation (KJ/m^2)

ALAT: latitude (degrees)

AZMTH: Azimuth, as written must be zero

RHO: ground reflectance

NG: number of glazing sheets

RI: refractive index of the glazing

XKL: extinction coefficient of the glazing (per sheet)

HGT: sunspace wall height (m)

WD: sunspace floor width (m)

HOR: horizontal distance from the wall to the intersection of the glazing planes (m)

VER: vertical distance from the floor to the intersection of the glazing planes (m)

XLN: sunspace width (m)

Returned Arguments:

RADI: matrix with incident radiation values for the monthly average day (KJ)

1: wall 2: floor 3: glazing

XKT: monthly average daily clearness index

RBARV: ratio of daily incident radiation on a vertical surface to that on a horizontal surface

Subroutine RAD (continued)

RN: ratio of incident radiation on a vertical surface to that on a horizontal surface at noon of the average day

GN: intensity of radiation on a vertical surface at noon of the average day (KJ/m^2)

Uses subroutine TALF

```
C    THIS SUBROUTINE CALCULATES THE MONTHLY AVERAGE RADIATION ON THE TWO
C    SUNSPACE GLAZING SURFACES AND THE AMOUNT OF THIS RADIATION THAT
C    STRICKS THE WALL AND THE FLOOR OF THE SUNSPACE.  THE RADIATION IS
C    BROKEN INTO BEAM AND DIFFUSE COMPONENTS AND SEPERATE GLAZING TRANS-
C    MITTANCES ARE USED.  FOR INFORMATION ON THE TILTED RADIATION AND THE
C    MONTHLY AVERAGE TRANSMITTANCES, SEE KLIEN, 'AN ALGORYTHM FOR
C    CALCULATING MONTHLY-AVERAGE RADIATION ON INCLINED SURFACES' AND
C    'CALCULATION OF THE MONTHLY-AVERAGE TRANSMITTANCE-ABSORBTANCE
C    PRODUCT RATIO', SOLAR ENERGY
      SUBROUTINE RAD(MN,H,ALAT,AZMTH,RHO,NG,RI,XKL
     2 ,HGT,WD,HOR,VER,XLN,RADI,XKT,RBAR3,RN,GN)
      DIMENSION DAY(12),FDU(3),FDL(3),BU(3),BL(3),
     . GBRAD(3),HBRAD(3),HDRAD(3),RADI(3)
      DATA DAY/17.,47.,75.,105.,135.,162.,198.,228.,258.,288.,
     1   318.,344./
      DATA RDCONV/0.0174533/,PI/3.1415927/
      DATA IDELT/12/,SC/4871./
C.
      AFL=WD*XLN
      AW=HGT*XLN
      VC=HGT-VER
      HC=WD-(WD-HOR)
      XUG=SQRT(VC**2+HC**2)
      AUG=XUG*XLN
      XLG=SQRT((WD-HOR)**2+VER**2)
      ALG=XLG*XLN
      XAR=VER*HC+((WD-HOR)*VER+HC*VC)/2.
      AGL=2.*XAR+AUG+ALG
      BETA=0.0
      PHI=1.570796
      IF(HC.GT.0.)BETA=ATAN(VC/HC)
      IF(HOR.LT.WD)PHI=ATAN(VER/(WD-HOR))
      SLOPE1=0.0
       SLOPE2=1.570796/RDCONV
      IF(HC.GT.0.0) SLOPE1=ATAN(VC/HC)/RDCONV
      IF((WD-HOR).GT.0.0) SLOPE2=ATAN(VER/(WD-HOR))/RDCONV
      SLOPE3=90.
      DECL = 23.45*SIN((284.+DAY(MN))/365.*2.0*PI)
      DECL = SIGN(AMIN1(ABS(DECL),89.0-ABS(ALAT)),DECL)
      COSLP1 = COS(SLOPE1*RDCONV)
      SINSL1 = SIN(SLOPE1*RDCONV)
      COSLP2 = COS(SLOPE2*RDCONV)
      SINSL2 = SIN(SLOPE2*RDCONV)
      COSLP3 = COS(SLOPE3*RDCONV)
      SINSL3 = SIN(SLOPE3*RDCONV)
      IF(ABS(AMOD(AZMTH,90.0)) .LT. 0.001) AZMTH = AZMTH + 0.001
      COSAZM = COS(AZMTH*RDCONV)
      SINAZM = SIN(AZMTH*RDCONV)
```

```
      TANAZM = SINAZM/COSAZM
      SINLAT = SIN(ALAT*RDCONV)
      COSLAT = COS(ALAT*RDCONV)
      TANLAT = SINLAT/COSLAT
      SINDEC = SIN(DECL*RDCONV)
      COSDEC = COS(DECL*RDCONV)
      TANDEC = SINDEC/COSDEC
      COSWS = -TANDEC*TANLAT
      WS = ACOS(COSWS)
      SINWS = SIN(WS)
      ECC = 1.0+0.033*COS(2.0*PI*DAY(MN)/365.)
      HO = 24.0/PI*ECC*SC*(COSLAT*COSDEC*SINWS+WS*SINLAT*SINDEC)
      H = AMIN1(H,HO)
      XKT = H/HO
C  ERBS MONTHLY-AVERAGE NON-SEASONAL DIFFUSE CORRELATION
      DRF=1.317-3.023*XKT+3.372*XKT*XKT-1.769*XKT*XKT*XKT
      A = 0.409+0.5016*SIN(WS-1.047)
      B = 0.6609-0.4767*SIN(WS-1.047)
      DIAG1=SQRT(WD**2+HGT**2)
      DIAG2=SQRT(HC**2+VER**2)
C      VIEW FACTORS FOR DIFFUSE RADIATION -OLD DFRACT
      FDU(1)=(XUG+HGT-DIAG2)/(XUG*2.)
      FDU(2)=(DIAG1+DIAG2-HGT-XLG)/(2.*XUG)
      FDU(3)=1.-FDU(1)-FDU(2)
      FDL(1)=(DIAG1+DIAG2-XUG-WD)/(2.*XLG)
      FDL(2)=(WD+XLG-DIAG2)/(2.*XLG)
      FDL(3)=1.-FDL(1)-FDL(2)
C.  THE A AND B COEFFICIENTS ARE FOR A CURVE FIT TO THE HOURLY
C.  TO DAILY TOTAL RADIATION GIVEN BY COLLARES-PEREIRA AND RABL.
C.  DETERMINE RECIEVER VIEW FACTORS AND TRANSMITTANCE-ABSORPTANCE
C.  PRODUCT RATIOS FOR DIFFUSE AND GROUND REFLECTED RADIATION
C  FLAT PLATES
      FSKY1 = (1.+COSLP1)/2.
      FGND1 = (1.-COSLP1)/2.
      ROHD=-1.
      TADR = TALF(NG,60.,XKL,RI,1.,ROHD)
      FSKY2 = (1.+COSLP2)/2.
      FGND2 = (1.-COSLP2)/2.
      FSKY3 = (1.+COSLP3)/3.
      FGND3 = (1.-COSLP3)/3.
8     DELT = 2.*WS/FLOAT(IDELT)
      HRSTP=DELT*12./PI
      HB = 0.
      HD = 0.
      HBTT1 = 0.
      HBT1 = 0.
      HBTT3 = 0.
      HBT3 = 0.
      HBTTA1 = 0.
```

```
      RBBAR1 = 0.
      TABAR1 = 0.
      HBTT2 = 0.
      HBT2 = 0.
      HBTTA2 = 0.
      RBBAR2 = 0.
      TABAR2 = 0.
      IFLAG=0
      DO 73 I=1,3
73    HBRAD(I)=0.0
      IF(WS .LT. 0.0001) GO TO 110
      OMEGA = WS + DELT/2.
C.  DETERMINE BEAM RADIATION COMPONENTS USING NUMERICAL
C.  INTEGRATION OVER AN AVERAGE DAY
      DO 75 J = 1,IDELT
      OMEGA = OMEGA - DELT
74    IF(IFLAG.EQ.1) OMEGA=0.
      COSHR = COS(OMEGA)
      SINHR = SIN(OMEGA)
      COSTZ = COSLAT*COSDEC*COSHR+SINLAT*SINDEC
      IF(COSTZ .LT. 0.0001) GO TO 75
C.  COSTZ IS THE COSINE OF THE ANGLE OF BEAM RADIATION INCIDENT
C.  ON A HORIZONTAL SURFACE
C.
      SINTZ = SIN(ACOS(COSTZ))
      SAZM = 0.0
      IF(SINTZ .LT. 0.0001) GO TO 10
      SINSZM = COSDEC*SINHR/SINTZ
      SAZM = ASIN(SINSZM)/RDCONV
C  DETERMINE IF THE ABSOLUTE VALUE OF THE SOLAR AZIMUTH
C  IS GREATER THAN 90 DEGREES BY COMPARING THE HOUR
C  ANGLE WITH THE HOUR ANGLE AT WHICH THE SOLAR AZIMUTH IS
C  +/- 90 DEGREES
      CWEW = TANDEC/TANLAT
      CWEW = SIGN(AMIN1(ABS(CWEW),1.),CWEW)
      WEW = PI
      IF(ALAT*(DECL-ALAT) .LE. 0.0) WEW = ACOS(CWEW)
      IF((ABS(OMEGA)-ABS(WEW))*ALAT*(DECL-ALAT) .LE. 0.)
     .        SAZM = SIGN(180.,SAZM) - SAZM
C  FLAT PLATES
10    COSTT1 = COSTZ*COSLP1+SINTZ*SINSL1*COS((SAZM-AZMTH)*RDCONV)
      COSTT2 = COSTZ*COSLP2+SINTZ*SINSL2*COS((SAZM-AZMTH)*RDCONV)
      COSTT3 = COSTZ*COSLP3+SINTZ*SINSL3*COS((SAZM-AZMTH)*RDCONV)
      IF(COSTT1 .LT. 0.0001) GO TO 70
      THETA1 = ACOS(COSTT1)/RDCONV
      TABR1 = TALF(NG,THETA1,XKL,RI,1.,ROHD)
70    RB1 = AMAX1(COSTT1/COSTZ,0.0)
      IF(COSTT2 .LT. 0.0001) GO TO 71
      THETA2 = ACOS(COSTT2)/RDCONV
```

```
      TABR2 = TALF(NG,THETA2,XKL,RI,1.,ROHD)
71    RB2 = AMAX1(COSTT2/COSTZ,0.0)
       RB3 = AMAX1(COSTT3/COSTZ,0.0)
      RDIF = PI/24.0*(COSHR-COSWS)/(SINWS-WS*COSWS)
      IF (RDIF.LT.0.0) RDIF = 0.0
      RT = RDIF*(A+B*COSHR)
      IF (RT.LT.0.0) RT = 0.
      GD = RDIF*DRF
      GB = (RT-GD)
C.  RDIF IS THE AVERAGE HOURLY TO DAILY DIFFUSE RADIATION RATIO.
C.  RT IS THE AVERAGE HOURLY TO DAILY TOTAL RADIATION RATIO
      GBT1 = GB*RB1
      GBTTA1 = GBT1*TABR1
      HBTT1 = HBTT1+GBT1
      HBT1 =HBT1+GBT1
      HBTTA1 = HBTTA1+GBTTA1
      GBT2 = GB*RB2
      GBTTA2 = GBT2*TABR2
      HBTT2 = HBTT2+GBT2
      HBT2 =HBT2+GBT2
      HBTTA2 = HBTTA2+GBTTA2
      GBT3 = GB*RB3
      HBTT3 = HBTT3+GBT3
      HBT3 =HBT3+GBT3
      HB = HB + GB
      HD = HD + GD
      TSE=ATAN((SINTZ/COSTZ)*COS(SAZM*RDCONV))
      DO 1950 I=1,3
      BU(I)=0.0
1950   BL(I)=0.0
      IF(TSE.GE.0.0) GOTO 2100
      ANGCK=TSE+1.5707963
      IF(ANGCK.GE.PHI)THEN
      BU(2)=1.
      BL(2)=1.
      ELSE
      WP=HGT/TAN(ANGCK)
      IF(WP.GE.WD) THEN
      BU(3)=1.
      ELSE
      CP=VER/TAN(ANGCK)
      OS=CP-(WD-HOR)
      SIS=WD-WP
      BU(2)=SIS/(SIS+OS)
      BU(3)=OS/(SIS+OS)
      ENDIF
      ENDIF
      GOTO 2200
2100   FP=HC-VER*TAN(TSE)
```

```
      IF(FP.LT.0.0) THEN
      FP=-FP
      BU(1)=1.
      BL(1)=FP/(FP+WD)
      BL(2)=1.-BL(1)
      ELSE
      BL(2)=1.
      WP=FP/TAN(TSE)
      BU(2)=WP/(WP+HGT)
      BU(1)=1.-BU(2)
      ENDIF
2200  DO 72 I=1,3
      GBRAD(I)=GBTTA1*BU(I)*AUG+GBTTA2*BL(I)*ALG
72    HBRAD(I)=HBRAD(I)+GBRAD(I)
      IF(IFLAG.EQ.1) GOTO 130
75    CONTINUE
C.
110   IF(HB .GT. 0.) RBBAR1 = HBTT1/HB
      RBAR1 = (1.0-DRF)*RBBAR1+DRF*(1.+COSLP1)/2.+RHO*(1.-COSLP1)/2.
      HT1 = H*RBAR1
      IF(HT1 .GT. 0.) TABAR1 = (HBTTA1 + HD*FSKY1*TADR
     .  + RHO*(HB+HD)*FGND1*TADR)/(HBT1+HD*FSKY1+RHO*(HB+HD)*FGND1)
      IF(HB .GT. 0.) RBBAR2 = HBTT2/HB
      RBAR2 = (1.0-DRF)*RBBAR2+DRF*(1.+COSLP2)/2.+RHO*(1.-COSLP2)/2.
      IF(HB .GT. 0.) RBBAR3 = HBTT3/HB
      RBAR3 = (1.0-DRF)*RBBAR3+DRF*(1.+COSLP3)/2.+RHO*(1.-COSLP3)/2.
      HT2 = H*RBAR2
      IF(HT2 .GT. 0.) TABAR2 = (HBTTA2 + HD*FSKY2*TADR
     .  + RHO*(HB+HD)*FGND2*TADR)/(HBT2+HD*FSKY2+RHO*(HB+HD)*FGND2)
      HDS1=DRF*FSKY1+RHO*FGND1
      HDS2=DRF*FSKY2+RHO*FGND2
      DO 120 I=1,3
      HBRAD(I)=HBRAD(I)*HRSTP
      HDRAD(I)=TADR*(HDS1*FDU(I)*AUG+HDS2*FDL(I)*ALG)
120   RADI(I)=(HBRAD(I)+HDRAD(I))*H
      IFLAG=1
      GOTO 74
130   CONTINUE
      RN=(GBT3+GD*FSKY3+RT*RHO*FGND3)/RT
      GN=RN*RT*H
      RETURN
      END
```

Function TALF

Call Statement

TAUALF = TALF (N,THETA,XKL,REFRIN,ALPHA,RHOD)

Arguments

N: number of glazing covers

THETA: angle of incidence

XKL: extinction coefficient of the glazing (per sheet)

REFRIN: refractive index of the glazing

ALPHA: surface solar absortance, for computation of the transmittance only; set equal to 1

RHOD: reflectivity of the glazing to diffuse radiation. If RHOD $\leq$ 0 the function will compute RHOD using an angle of incidence of 60 degrees.

Function TALF is taken from TRNSYS (10).

```
      FUNCTION TALF(N,THETA,XKL,REFRIN,ALPHA,RHOD)
      DIMENSION R(2),T(2),RHO(2),TAU(2),REF(2)
C.  THIS FUNCTION SUBPROGRAM CALCULATES THE TRANSMITTANCE-ABSOPRTANCE
C.  PRODUCT FOR A SOLAR COLLECTOR WITH N COVERS, A REFRACTIVE INDEX
C.  REFRIN, A KL VALUE OF XKL, AND A FLAT BLACK ABSORBER SURFACE.  THE
C.  INCIDENT RADIATION IS AT AN ANGLE THETA.  FOR THE FIRST CALL TO THIS
C.  FUNCTION BY EACH UNIT, RHOD MUST BE LESS THAN ZERO.
      DATA PI/3.1415927/
      IF(N.GE.1) GO TO 5
      TAUALF=ALPHA
      RETURN
5     IF(RHOD.GT.0.) GO TO 40
      THETA1=PI/3.
10    THETA2=ASIN(SIN(THETA1)/REFRIN)
      R(1)=SIN(THETA2-THETA1)
      R(2)=SIN(THETA2+THETA1)
      T(1)=R(1)/COS(THETA2-THETA1)
      T(2)=R(2)/COS(THETA2+THETA1)
      RHO(1)=R(1)*R(1)/R(2)/R(2)
      RHO(2)=T(1)*T(1)/T(2)/T(2)
      TABS=EXP(-XKL/COS(THETA2))
      DO 30 J=1,2
      T(J)=TABS*(1.-RHO(J))**2/(1.-TABS*TABS*RHO(J)*RHO(J))
      R(J)=RHO(J)*(1.+TABS*T(J))
      TAU(J)=T(J)
      REF(J)=R(J)
      IF(N.EQ.1) GO TO 30
      DO 20 I=2,N
      TAU(J)=TAU(J)*T(J)/(1.-REF(J)*R(J))
      REF(J)=REF(J)+TAU(J)*TAU(J)*R(J)/(1.-REF(J)*R(J))
20    CONTINUE
30    CONTINUE
      IF(RHOD.GT.0.) GO TO 50
C..INITIALIZE RHOD.
      RHOD=(REF(1)+REF(2))/2.
40    THETA1=THETA*PI/180.
      IF(THETA1.LT.0.001) THETA1=0.001
      GO TO 10
50    TALF=(TAU(1)+TAU(2))/2.*ALPHA/(1.-(1.-ALPHA)*RHOD)
       RETURN
       END
```

Subroutine TWBAR

Call Statement:

```
Call TWBAR (HGT,WD,HOR,VER,XLN,NG,RI,XKL,RGL,SFRAC,EGL,
     EWL,EFL,THW,THF,CNW,CNF,RGR,ESW,ESF,HS,HR,HA,AIRCH,
     RADI,TABAR,TGRBAR,TRMBAR,TWNS,XLS,TWLBAR,QIN,ABWL,
     ABFL)
```

Passed Arguments:

HGT: sunspace wall height (m)

WD: sunspace floor width (m)

HOR: horizontal distance from the wall to the intersection of the glazing planes (m)

VER: vertical distance from the floor to the intersection of the glazing planes (m)

XLN: length of the sunspace (m)

NG: number of glazing sheets

RI: refractive index of the glazing

XKL: extinction coefficient of the glazing (per sheet)

RGL: R-value of the glazing system (M^2-C/W)

SFRAC: fraction of the glazing planes which is opaque to solar radiation

EGL: infrared emittance of the glazing system

EWL: infrared emittance of the wall

EFL: infrared emittance of the floor

THW: wall thickness (m)

THF: floor thickness (m)

CNW: wall thermal conductivity (W/m-C)

CNF: floor thermal conductivity (W/m-C)

Subroutine TWBAR (continued)

RGR: R-value from the bottom of the floor to the ground (m^2-C/W)

ESW: wall solar absorbtance

ESF: floor solar absorbtance

HS: convection coefficient from the glazing, wall and floor to the sunspace air (W/m^2-C)

HR: heat transfer coefficient from the wall to the building (W/m^2-C)

HA: convection coefficient from the glazing to ambient (W/m^2-C)

AIRCH: sunspace infiltration air changes per hour

RADI: matrix with incident radiation values for the monthly average day (KJ)

1: wall 2: floor 3: glazing

TABAR: monthly average ambient temperature (C)

TGRBAR: monthly average ground temperature (C)

TRMBAR: monthly average building temperature (C)

Returned Arguments:

TWNS: monthly average wall temperature if solar radiation equals zero (C)

XLS: heating load on the building due to the sunspace if solar radiation equals zero (KJ/day)

TWLBAR: monthly average wall temperature (C)

QIN: monthly average sunspace energy delivery (KJ/day)

ABWL: monthly average solar radiation absorbed by the wall (KJ/day)

Subroutine TWBAR (continued)

ABFL: monthly average solar radiation absorbed by the floor (KJ/day)

TWBAR uses subroutines: TALF, FHAT, GAUSS.

```
      SUBROUTINE TWBAR(HGT,WD,HOR,VER,XLN,NG,RI,XKL,RGL,SFRAC,EGL
     . ,EWL,EFL,THW,THF,CNW,CNF,RGR,ESW,ESF,HS,HR,HA,AIRCH,RADI
     . ,TABAR,TGRBAR,TRMBAR,TWNS,XLS,TWLBAR,QIN,ABWL,ABFL)
      DIMENSION FHATS(3,3),RADI(3),QSRAD(3),ES(3),ROH(3),EI(3)
     2 ,FHATI(3,3),A(20,20)
      DATA WKJDCV/86.4/,SIG/5.67E-08/
      AZMTH=0.0
      ES(1)=ESW
      ES(2)=ESF
      ROHD=-1
      TAUD=TALF(NG,60.,XKL,RI,1.,ROHD)
      ES(3)=1.-ROHD
      DO 15 I=1,3
15    ROH(I)=1.-ES(I)
      GLLOW=SQRT(VER**2+(WD-HOR)**2)
      GLUP=SQRT((HGT-VER)**2+HOR**2)
      END=HOR*VER+0.5*HOR*(HGT-VER)+0.5*VER*(WD-HOR)
      AGL=(GLLOW+GLUP)*XLN+2.*END
      CALL FHAT(HGT,WD,GLLOW,GLUP,ES,FHATS)
      EI(1)=EWL
      EI(2)=EFL
      EI(3)=EGL
C   INITIALIZE 4TBAR**3 FOR ALL IR C'S
      TB8=1.08E08
      TB9=TB8
      TB7=TB8
      TB3=TB8
      TGL=300.
      TAIR=TGL
      TFL=TGL
      TWL=TGL
      C6=HS*WKJDCV*AGL
      C5=HS*WKJDCV*WD*XLN
      C4=HS*WKJDCV*HGT*XLN
      C1=WKJDCV/(1./(HR*HGT*XLN)+THW/(CNW*HGT*XLN))
      C10=AIRCH*END*XLN*1.204*1.012*24
      C2=WKJDCV/(THF/(CNF*WD*XLN)+RGR/(WD*XLN))
      CALL FHAT(HGT,WD,GLLOW,GLUP,EI,FHATI)
      TA=TABAR+273.
      TRM=TRMBAR+273.
      TGR=TGRBAR+273.
```

```
      DO 76 I=1,3
76    QSRAD(I)=0.0
78    DO 80 II=1,11
C   TEMP DEPENDENT C'S
      C8=EI(3)*EI(2)*(GLLOW+GLUP)*XLN*FHATI(3,2)*TB8*SIG*WKJDCV
      C9=EI(3)*EI(1)*(GLLOW+GLUP)*XLN*FHATI(3,1)*TB9*SIG*WKJDCV
      HIR=EI(3)*SIG*TB3
      HTOT=HA+HIR
      C3=AGL/(RGL+1./HTOT)*WKJDCV
      C7=EI(1)*EI(2)*WD*XLN*FHATI(2,1)*TB7*SIG*WKJDCV
      A(1,1)=-(C3+C6+C8+C9)
      A(1,2)=C6
      A(1,3)=C8
      A(1,4)=C9
      A(1,5)=-C3*TA
      A(2,1)=C6
      A(2,2)=-(C4+C5+C6+C10)
      A(2,3)=C5
      A(2,4)=C4
      A(2,5)=-C10*TA
      A(3,1)=C8
      A(3,2)=C5
      A(3,3)=-(C2+C5+C7+C8)
      A(3,4)=C7
      A(3,5)=-QSRAD(2)-C2*TGR
      A(4,1)=C9
      A(4,2)=C4
      A(4,3)=C7
      A(4,4)=-(C1+C4+C7+C9)
      A(4,5)=-QSRAD(1)-C1*TRM
      CALL GAUSS(4,5,A)
      TGL=A(1,5)
      TAIR=A(2,5)
      TFL=A(3,5)
      TWLN=A(4,5)
      TGLO=TGL-C1*RGL/(AGL*WKJDCV)*(TGL-TA)
      TB3=(TGLO**2+TA**2)*(TGLO+TA)
      TB8=(TGL**2+TFL**2)*(TGL+TFL)
      TB9=(TGL**2+TWLN**2)*(TGL+TWLN)
      TB7=(TWLN**2+TFL**2)*(TWLN+TFL)
      IF(ABS(TWLN-TWL).LT.0.001)GOTO 85
80    TWL=TWLN
```

```
85    QIN=C1*(TWL-TRM)
      TGLBAR=TGL-273.
      TSSBAR=TAIR-273.
      TFLBAR=TFL-273.
      TWLBAR=TWL-273.
      ABWL=QSRAD(1)
      ABFL=QSRAD(2)
      IF(QSRAD(1).GT.0.0)RETURN
      XLS=C1*(TRM-TWL)
      TWNS=TWLBAR
      DO 35 I=1,3
35    RADI(I)=RADI(I)*(1.-SFRAC)
      ES(3)=0.0
      DO 75 I=1,3
      SQSFHR=0.0
      DO 70 J=1,3
70    SQSFHR=SQSFHR+RADI(J)*ROH(J)*FHATS(J,I)
75    QSRAD(I)=ES(I)*(RADI(I)+SQSFHR)
      GOTO 78
      END
```

Subroutine FHAT

Call Statement:

Call FHAT (XLW,XLFL,XLG,XUG,ES,FHATS)

Passed Arguments:

XLW: height of the wall (m)

XLFL: width of the floor (m)

XLG: length of the lower glazing (m)

XUG: length of the upper glazing (m)

ES: a matrix containing the emittance (or absorbtance) of the surfaces

1: wall 2: floor 3: glazing

Returned Arguments:

FHATS: a 3x3 matrix containing the $\hat{F}$ values

```
      SUBROUTINE FHAT(XLW,XLFL,XLG,XUG,ES,FHATS)
      DIMENSION ES(3),FHATS(3,3),F(3,3),RSR(3,3),RSRIV(3,3)
      DIAG1=SQRT(XLFL**2+XLW**2)
      F(1,1)=0.0
      F(2,2)=0.0
      F(1,2)=(XLW+XLFL-DIAG1)/(2.*XLW)
      F(2,1)=F(1,2)*XLW/XLFL
      F(1,3)=1.-F(1,2)
      F(3,1)=F(1,3)*XLW/(XUG+XLG)
      F(2,3)=1.-F(2,1)
      F(3,2)=F(2,3)*XLFL/(XUG+XLG)
      F(3,3)=1.-F(3,1)-F(3,2)
      DO 1400 I=1,3
      DO 1400 J=1,3
      RSR(I,J)=(ES(J)-1.)*F(I,J)
      FHATS(I,J)=0.0
1400    IF(I.EQ.J) RSR(I,J)=RSR(I,J)+1.
      PTRSR=RSR(1,1)*RSR(2,2)*RSR(3,3)+RSR(1,2)*RSR(2,3)*RSR(3,1)+RSR
     2 (1,3)*RSR(2,1)*RSR(3,2)
      QTRSR=RSR(1,3)*RSR(2,2)*RSR(3,1)+RSR(1,2)*RSR(2,1)*RSR(3,3)+RSR
     2 (1,1)*RSR(2,3)*RSR(3,2)
      DETSR=PTRSR-QTRSR
      RSRIV(1,1)=RSR(2,2)*RSR(3,3)-RSR(2,3)*RSR(3,2)
      RSRIV(1,2)=RSR(1,3)*RSR(3,2)-RSR(1,2)*RSR(3,3)
      RSRIV(1,3)=RSR(1,2)*RSR(2,3)-RSR(1,3)*RSR(2,2)
      RSRIV(2,1)=RSR(2,3)*RSR(3,1)-RSR(2,1)*RSR(3,3)
      RSRIV(2,2)=RSR(1,1)*RSR(3,3)-RSR(1,3)*RSR(3,1)
      RSRIV(2,3)=RSR(1,3)*RSR(2,1)-RSR(1,1)*RSR(2,3)
      RSRIV(3,1)=RSR(2,1)*RSR(3,2)-RSR(2,2)*RSR(3,1)
      RSRIV(3,2)=RSR(1,2)*RSR(3,1)-RSR(1,1)*RSR(3,2)
      RSRIV(3,3)=RSR(1,1)*RSR(2,2)-RSR(1,2)*RSR(2,1)
      DO 1500 I=1,3
      DO 1500 J=1,3
1500   RSRIV(I,J)=RSRIV(I,J)/DETSR
      DO 1600 I=1,3
      DO 1600 K=1,3
      DO 1600 J=1,3
1600  FHATS(I,K)=FHATS(I,K)+RSRIV(I,J)*F(J,K)
      RETURN
      END
```

Subroutine GAUSS

Call Statement:

Call GAUSS (K,L,A)

Passed Arguments:

K: number of rows in the coefficient matrix

L: number of columns in the coefficient matrix

A: a KxL augmented coefficient matrix containing the coefficients of the linear equations, see the example below.

Example: to solve the following system of equations

5A + 2B + 3C = 1

2A + B + 8C = 10

3A + 4B + C = 3

the augmented A matrix is

5 2 3 1

2 1 8 10

3 4 1 3

the solution is returned in the last column

A = (1,4) B = (2,4) C = (3,4)

```
      SUBROUTINE GAUSS(K,L,A)
      DIMENSION M(20),N(20),A(20,20)
      IP=0
      DO 60 I=1,K
      DO 10 J=1,L
10    IF(A(I,J).NE.0.0) GOTO 20
      IF(A(I,L+1).EQ.0.0) GOTO 60
      WRITE(*,15)
15    FORMAT(' EQUATIONS ARE INCONSISTANT')
      RETURN
20    IP=IP+1
      M(IP)=I
      N(IP)=J
      DO 30 JJ=J+1,L+1
30    A(I,JJ)=A(I,JJ)/A(I,J)
      A(I,J)=1.
      IF(I.EQ.K) GOTO 60
      DO 50 II=1+1,K
      DO 40 JJ=J+1,L+1
      A(II,JJ)=A(II,JJ)-A(I,JJ)*A(II,J)
40    IF(ABS(A(II,JJ)).LT.0.00000001) A(II,JJ)=0.0
50    A(II,J)=0.0
60    CONTINUE
69    DO 80 II=1,M(IP)-1
      DO 70 JJ=N(IP)+1,L+1
      A(II,JJ)=A(II,JJ)-A(II,N(IP))*A(M(IP),JJ)
70    IF(ABS(A(II,JJ)).LT.0.00000001) A(II,JJ)=0.0
80    A(II,N(IP))=0.0
      IP=IP-1
      IF(IP.EQ.1) RETURN
      GOTO 69
      END
```

BIBLIOGRAPHY

1. Mitchell, John W., Energy Utilization Technology. To be published, John Wiley and Sons: New York (1983).

2. Utzinger, D.M., Klein, S.A., and Mitchell, J.W., "The Effect of Air Flow Rate in Collector-Storage Walls," Solar Energy, 25, pp. 511-519, 1980.

3. Mazria, E., The Passive Solar Energy Book: A Complete Guide to Solar Home, Greenhouse, and Building Design, Rodale Press: Emmaus, PA (1979).

4. Balcomb, J.D., et al., Passive Solar Design Handbook--Volume Two: Passive Solar Design Analysis, United States Department of Energy (1980).

5. Yanda, B., and Fisher, R., The Food and Heat Producing Solar Greenhouse, John Muir Publications: Santa Fe, NM (1976).

6. Schwedler, M.C.A., "The Simulation of Passive Solar Energy Systems," M.S. Thesis, University of Wisconsin-Madison (1981).

7. Dirienzo, R., and McGowan, J.G., "Thermal Performance Model and Design Sensitivity for Attached Sunspaces," Proceedings of the Fifth National Passive Solar Conference, Amherst, MA (1980), pp. 262-266.

8. Palmiter, L., and Wheeling, T., "A Passive Solar Computer Simulation Model," Proceedings of the Fourth National Passive Solar Conference, Kansas City, MO (1979), pp. 200-201.

9. McFarland, R.D., "PASOLE: A General Simulation Program for Passive Solar Energy," Los Alamos Scientific Laboratory Report LA-7433-MS (October 1979).

10. Klein, S.A., et al., "TRNSYS--A Transient Simulation Program," Engineering Experiment Station Report 38, Version 11.0, University of Wisconsin-Madison (1981).

11. Balcomb, J.D., et al., "Performance Analysis of Passive Solar Heated Buildings by the Solar Load Ratio Method," Passive Solar Journal, Volume 1, Number 2 (1982).

12. R.W. Jones, et al., Passive Solar Design Handbook--Volume III: Passive Solar Design Analysis (Addendum). United States Department of Energy (1982).

13. Cinquemani, V., et al., "Input Data for Solar Systems," United States Department of Energy (1978).

14. Monsen, W.A., Klein, S.A., and Beckman, W.A., "Prediction of Direct Gain Solar Heating System Performance." Solar Energy, 2, p. 143 (1981).

15. Monsen, W.A., Klein, S.A. and Beckman, W.A., "The Unutilizability Design Method for Collector-Storage Walls," Solar Energy, Vol. 0 (1982).

16. Duffie, J.A., and Beckman, W.A., Solar Engineering of Thermal Processes, John Wiley and Sons: New York (1980).

17. Klein, S.A., "Calculation of Flat-Plate Collector Utilizability," Solar Energy, Vol. 2, pp. 393-402 (1978).

18. McFarland, R.D., Jones, R.W., and Lazarus, G.S., "Annual Thermal Performance of Sunspace-Type Passive Solar Collectors for Residence Heating--Attached and Semi-Enclosed Geometries." Los Alamos Scientific Laboratory Report LA-9424-MS (September 1982).

19. ASHRAE Handbook of Fundamentals. New York, Am. Soc. of Heating, Refrigerating and Air-Conditioning Engineers, Inc., (1982).

20. Beckman, W.A., Personal Communication (1982).

21. Siegel, R., and Howell, J.R., Thermal Radiation Heat Transfer, Second Edition, McGraw-Hill: New York (1981).

22. Feingold, A., "Radiant-Interchange Configuration Factors Between Various Selected Plane Surfaces." Proceedings, Royal Society (London), Series A, Vol. 292, #1428, pp. 51-60 (1965).

23. Nawrocki, A.D., and Kammerad, R., "Description of an Exact Recursive Method to Simplify Shading Calculations," Lawrence Berkeley Laboratory Report LBL-11390 (April 1981).

24. ASHRAE, 'Procedure for Determining Heating and Cooling Loads for Computerized Energy Calculations.' New York, Am. Soc. of Heating Refrigerating and Air-Conditioning Engineers, Inc., (1971).

25. Welty, J.R., Engineering Heat Transfer, SI Version, John Wiley and Sons: New York (1978).

26. Box, G.E.P., Hunter, W.G., and Hunter, J.S., Statistics for Experimenters, John Wiley and Sons: New York (1978).

27. Watmuff, J.H., et al., "Solar and Wind Induced External Coefficients for Solar Collectors," Comples, 2 (1977).

28. Beckman, W.A., et al., "F-Load, a Building Heating-Load Calculation Program." ASRAE Transactions, V. 88, (1982).

29. Ohanessian, P. and Charters, W.W.S., "Thermal Simulation of a Passive Solar House Using a Trombe-Michel Wall Structure," Solar Energy, Vol. 20, No. 3, (1978), pp. 275-281.

30. Ellwood, C., How To Build and Operate Your Greenhouse, H.P. Books: Tucson, Arizona (1977).

31. SOLMET Typical Meteorological Year, Tape Deck 9734, National Oceanic and Atmospheric Administration. Environmental Data Service, National Climatic Center, Asheville, North Carolina.

32. Klein, S.A., "Calculation of the Monthly-Average Transmittance-Absorbtance Product," Solar Energy, 23, pp. 547-551, 1979.

33. Erbs, D.G., Klein, S.A., and Duffie, J.A., "Estimation of the Diffuse Radiation Fraction for Hourly, Daily and Monthly Average Global Radiation," Solar Energy, 28, pp. 293-302, 1982.

34. Collares-Pereira, M., and Rabl, A., "The Average Distribution of Solar Radiation-Correlations between Diffuse and Hemispherical and between Daily and Hourly Insolation Values," Solar Energy, 22, p. 155, 1979.

35. Hall, I.J., et al., "Generation of a Typical Meteorological Year," Sandia National Laboratory Report; SAND 78-1601, 1978.

36. Thom, H.C.S., "Normal Degree-Days Below Any Base," Monthly Weather Review, Vol. 82, No. 5 (1954).

37. Erbs, D.G., Klein, S.A., and Beckman, W.A., "The Estimation of Degree-Days and Ambient Temperature Bin Data from Monthly-Average Temperatures," To be published, ASHRAE Journal.

38. Whillier, A., "Solar Energy Collection and Its Utilization for House Heating," Ph.D. Thesis, M.I.T., Cambridge, MA (1953).

39. Liu, B.Y.H., and Jordan, R.C., "The Long-Term Average Performance of Flat-Plate Solar Energy Collectors," Solar Energy, 7, 53 (1963).

40. Liu, B.Y.H., and Jordan, R.C., "The Interrelationship and Characteristic Distribution of Direct Diffuse, and Total Solar Radiation," Solar Energy, 4, 3 (1960).

41. Horn, J.C., "Investigation of Various Thermal Capacitance Models," M.S. Thesis, University of Wisconsin-Madison, Madison, WI, (1982).